Man muss lachen und weinen,
lieben, arbeiten, genießen und leiden,
soviel wie mögliche […].
Das ist das wahrhaft Menschliche.

Gustave Flaubert

Geochemische Charakterisierung von Mikrobenmatten aus der Gezeitenzone der Vereinigten Arabischen Emirate und Inkubationsexperiment zur Untersuchung der Mikrobenvergesellschaftung

Geochemical characterization of microbial mats from the intertidal area of the United Arab Emirates and incubation experiment for investigating the microbial community

Von der Fakultät für Mathematik und Naturwissenschaft
der
Carl von Ossietzky Universität Oldenburg

zur Erlangung des Grades und Titels eines

Doktors der Naturwissenschaften
- Dr. rer. nat. -

angenommene Dissertation

von

Ann-Kathrin Scherf

geboren am 23. April 1981 in Perleberg

Gutachter: Prof. Dr. Jürgen Rullkötter

Zweitgutachter: Prof. Dr. Hans-Jürgen Brumsack

Tag der Disputation: 17. Dezember 2008

Inhaltsverzeichnis

Vorwort ..... **V**

Publikationen und Tagungsbeiträge ..... **VII**

Kurzfassung ..... **VIII**

Abstract ..... **X**

Abbildungsverzeichnis ..... **XII**

Tabellenverzeichnis ..... **XIV**

Liste der verwendeten Abkürzungen ..... **XV**

1 Einleitung **1**

1.1 Zielsetzung und Gliederung der vorliegenden Arbeit 3

2 Stand des Wissens **5**

2.1 Mikrobenmatten 5

2.1.1 Stromatolithe 6

2.1.2 Mattenaufbau 6

2.1.3 Stoffwechselprozesse der dominanten Gruppen 8

2.2 Biomarkeruntersuchungen an Mikrobenmatten 9

2.2.1 Aliphatische Kohlenwasserstoffe 10

2.2.2 Isoprenoide 11

2.2.3 Steroide und Hopanoide 12

2.2.4 Fettsäuren 13

2.3 Stabile Isotope 15

2.4 Das Probennahmegebiet 17

2.4.1 Die Gezeitenzone der Vereinigten Arabischen Emirate 19

2.4.2 Die Entstehung der Gezeitenzone 19

2.4.3 Die Sabkha 20

3 Biogeochemistry of high-salinity microbial mats **21**

3.1 Biogeochemistry of high-salinity microbial mats – Part 1: Lipid composition of microbial mats across intertidal flats of Abu Dhabi, United Arab Emirates 21

3.1.1 Abstract 21

3.1.2 Introduction 21

3.1.3 Materials and methods 23

3.1.3.1 Site and sample description 23

3.1.3.2 Gross composition 24

3.1.3.3 Extraction 25

3.1.3.4 Separation of lipid classes 25

3.1.3.5 Derivatization 25

3.1.3.6 Gas chromatography, gas chromatography-mass spectrometry 26

3.1.4 Results and discussion 26
3.1.4.1 Gross composition 26
3.1.4.2 Lipid class composition 28
3.1.4.3 Alkanes and alkenes 28
3.1.4.4 Isoprenoids 30
3.1.4.5 Steroids and hopanoids 31
3.1.4.6 Free fatty acids and phospholipid fatty acids 34
3.1.4.7 Evidence of contribution of selected groups of organisms 38
3.1.4.8 Environmental effects on lipids distribution 39
3.1.5 Conclusions 40
3.2 Biogeochemistry of high-salinity microbial mats – Part 2: Vertical distribution of lipids in a microbial mat from Abu Dhabi, United Arab Emirates 42
3.2.1 Abstract 42
3.2.2 Introduction 42
3.2.3 Materials and Methods 43
3.2.3.1 Site, sample and layer description 43
3.2.3.2 Extraction 45
3.2.3.3 Stable carbon isotope analysis of total organic extracts 45
3.2.3.4 Separation of lipid classes 45
3.2.3.5 Derivatization 46
3.2.3.6 Gas chromatography, gas chromatography-mass spectrometry 46
3.2.4 Results and discussion 46
3.2.4.1 Stable carbon isotope ratios of total lipid extracts 46
3.2.4.2 Alkanes and alkenes 46
3.2.4.3 Isoprenoids 49
3.2.4.4 Steroids and hopanoids 50
3.2.4.5 Phospholipid fatty acids 52
3.2.4.6 Vertical distribution of lipids 55
3.2.4.7 Correlations of lipid biomarkers with the community and trophic structure in the mat 57
3.2.5 Conclusions 59
3.2.6 Acknowledgements 59
4 Lipid biomarkers, pigments and cyanobacterial diversity of microbial mats across intertidal flats of the arid coast of the Arabian Gulf (Abu Dhabi, UAE) 60
4.1 Abstract 60
4.2 Introduction 61
4.3 Materials and Methods 62
4.3.1 Mat samples and their environmental settings 62

4.3.2 Fatty acid analysis 63
4.3.3 Pigment analysis 63
4.3.4 Light microscopy and enrichment cultivation 64
4.3.5 Molecular analysis 64
4.3.6 Phylogenetic analysis 65
4.3.7 Nucleotide sequence accession numbers 66
4.4 Results 66
4.4.1 Intertidal mat landscape 66
4.4.2 Polyphasic characterization of the cyanobacterial communities 67
4.4.2.1 Fatty acid fingerprints 67
4.4.2.2 Pigment analysis 68
4.4.2.3 Light microscopy 69
4.4.2.4 DGGE patterns and molecular diversity 72
4.5 Discussion 74
4.5.1 Effect of the multiply extreme environmental conditions on the effect on the macro- and microstructure of microbial mats 74
4.5.2 Fatty acids and environmental adaption 75
4.5.3 Cyanobacteria and solar radiation 75
4.5.4 Cyanobacterial diversity and resistance to desiccation 76
5 ^{13}C-Labelling of an intact microbial mat from the high-salinity intertidal area of Abu Dhabi, United Arab Emirates - a molecular isotopic study 78
5.1 Abstract 78
5.2 Introduction 78
5.3 Methods 80
5.3.1 Site and sample description 80
5.3.2 Labelling experiment 81
5.3.3 Extraction 82
5.3.4 Separation of lipid classes 82
5.3.5 Derivatization 82
5.3.6 Gas chromatography, gas chromatography-mass spectrometry 82
5.3.7 Total extractable organic matter stable carbon isotope analysis 83
5.3.8 Compound-specific stable carbon isotope analysis 83
5.3.9 Data treatment 84
5.4 Results and discussion 84
5.4.1 Stable carbon isotope ratios of total organic extracts 84
5.4.2 Stable carbon isotope ratios of major hydrocarbons 87
5.4.3 Stable carbon isotope ratios of major phospholipid fatty acids 90
5.5 Conclusions 93

5.6 Acknowledgements 94
6 Gesamtbetrachtung 96
6.1 Biomarkerzusammensetzung der Mikrobenmatten 96
6.2 Anpassung an die extremen Umweltbedingungen 97
6.3 Cyanobakterien als dominante Primärproduzenten 98
6.4 Abschließende Zusammenfassung und Ausblick 98
7 Literatur 100
8 Anhang 125
8.1 Zusätzliche Daten 125
8.2 Photographische Dokumentation 139
Lebenslauf 142
Eidesstattliche Erklärung 143

Vorwort

Die vorliegende Arbeit entstand im Zeitraum von Dezember 2004 bis September 2008 in der Arbeitsgruppe Organische Geochemie unter der Leitung von Prof. Dr. Jürgen Rullkötter am Institut für Chemie und Biologie des Meeres (ICBM) der Carl von Ossietzky Universität Oldenburg.

Mein besonderer Dank gilt Prof. Dr. Jürgen Rullkötter für die Möglichkeit, als Marine Umweltwissenschaftlerin eine Arbeit mit interdisziplinärer Themenstellung bearbeiten zu dürfen. Insbesondere möchte ich mich für die Ermöglichung der Probennahmereisen in die Vereinigten Arabischen Emirate bedanken, die in vielerlei Hinsicht meinen Horizont erweitert haben. Zusätzlich zu diesen Reisen wurde mir die Möglichkeit gegeben, an internationalen Fachtagungen teilzunehmen und dort meine Ergebnisse zu präsentieren. Darüber hinaus bin ich für die fortwährende Unterstützung und die Gespräche dankbar, die wesentlich zum Gelingen der Arbeit beigetragen haben.

Herrn Prof. Dr. Hans-Jürgen Brumsack danke ich ganz herzlich für die Übernahme des Korreferats.

Dr. Dirk de Beer, Dr. Raeid Abed und Katharina Kohls vom Max-Planck-Institut für marine Mikrobiologie möchte ich für die Kooperation danken und für die Einblicke, die sie mir in ihre Arbeit gewährt haben. Raeid danke ich besonders für die gemeinsamen Probennahmen verbunden mit dem Kennenlernen der arabischen Kultur. Shukran djazilan! Katharina danke ich für das Aufmuntern, Durchhalten und gemeinsame Leiden bei der Probennahme 2006 sowie dem anschließenden Experiment.

Dr. Waleed Hamza und Huda Al-Hassani vom College of Sciences der Universität der Vereinigten Arabischen Emirate möchte ich für ihre Gastfreundschaft und die vielseitige Unterstützung bei den Probennahmen danken.

Des Weiteren danke ich Frau Dr. Barbara Scholz-Böttcher, Bernd Kopke und Kerstin Adolph für die Hilfestellungen im Bereich der instrumentellen Analytik an der Vielzahl unserer Massenspektrometer. Stellvertretend für alle, die mich bei meinen Laborarbeiten unterstützt haben, danke ich Swantje Enge und Steffen Schüler, ohne die die Bearbeitung des Inkubationsexperimentes nicht denkbar gewesen wäre.

Bei allen, die seit meiner „HiWi-Zeit“ in der Arbeitsgruppe Organische Geochemie tätig waren, bedanke ich mich für die schöne Zeit in der Arbeitsgruppe und die vielseitige Unterstützung. Besonders möchte ich Dr. Jürgen Köster dafür danken, dass er immer mit seinem Wissen für alle meine Fragen zur Verfügung stand. Außerdem möchte ich allen Mitgliedern des ICBM danken, die mir meine vielfältigen Fragen beantwortet haben und hilfreich waren.

Katja, Jörg, Michael, Verena, Swantje und Caroline danke ich besonders - alle „Wofürs“ aufzuzählen würde jedoch den Rahmen sprengen.

Björn Klein danke ich ganz herzlich für die Hilfe bei der Anfertigung dieser Arbeit. Ohne das Korrekturlesen, die Anmerkungen, manchmal hitzigen Diskussionen sowie die Aufmunterungen und Zwangspausen abseits des Schreibtisches wäre ich sicherlich manchmal verzweifelter und überarbeiteter gewesen.

Schließlich gilt das größte Dankeschön meinen Eltern, die mich in allen Lebenslagen unterstützt und immer Motivation und Trost gespendet haben.

Diese Arbeit wurde von der Deutschen Forschungsgemeinschaft (DFG) gefördert.

Publikationen

Einzelne Kapitel dieser Arbeit wurden in Fachzeitschriften publiziert bzw. vorbereitet, um eingereicht zu werden:

Scherf, A.-K., Rullkötter, J.. Biogeochemistry of high-salinity microbial mats – Part 1: Lipid composition of microbial mats across intertidal flats of Abu Dhabi, United Arab Emirates.

In Vorbereitung für Organic Geochemistry

Scherf, A.-K., Rullkötter, J.. Biogeochemistry of high-salinity microbial mats – Part 2: Vertical distribution of lipids in a microbial mat from Abu Dhabi, United Arab Emirates.

In Vorbereitung für Organic Geochemistry

Abed, R.M.M., Kohls, K., Schoon, R., Scherf, A.-K., Schacht, M., Palinska, K.A., Al-Hassani, H., Hamza, W., Rullkötter, J., Golubic, S., 2008. Lipid biomarkers, pigments and cyanobacterial diversity of microbial mats across intertidal flats of the arid coast of the Arabian Gulf (Abu Dhabi, UAE). FEMS Microbiology Ecology 9, 449-462.

Scherf, A.-K., Rullkötter, J.. ^{13}C-Labelling of an intact microbial mat from the high-salinity intertidal area of Abu Dhabi, United Arab Emirates - a molecular isotopic study.

In Vorbereitung für Organic Geochemistry

Tagungsbeiträge

Scherf, A.-K., Rullkötter, J., 2007. Lipid biomarkers and carbon flow in high-salinity microbial mats. 23rd International Meeting on Organic Geochemistry (9th to 14th September), Torquay, England. (Poster)

Scherf, A.-K., Abed, R.M.M., Rullkötter, J., 2007. Lipid biomarkers as indicators for environmental stress in cyanobacterial mats of Abu Dhabi, U.A.E.. 17th V.M. Goldschmidt Conference (19th to 24th August), Cologne, Germany. (Poster)

Kurzfassung

Mikrobenmatten stellen eines der kleinsten Ökosysteme der Erde dar und sind aufgrund ihrer internen, nahezu geschlossenen Stoffkreisläufe besonders interessante Mikroorganismengemeinschaften. In den vergangenen Jahrzehnten gab es viele organisch-geochemische Untersuchungen an verschiedenen Arten lebender und fossiler Mikrobenmatten aus einer Vielzahl unterschiedlichster Ökosysteme.

In der vorliegenden Arbeit wurden Mikrobenmatten aus der Gezeitenzone südwestlich der Halbinsel Al Dhabaiya (Vereinigte Arabische Emirate) untersucht. Die Gezeitenzone des Arabischen Golfes bietet räumlich unterschiedliche, meist sehr extreme Wachstumsbedingungen mit Wassersalinitäten bis zu 200. Innerhalb des Untersuchungsgebietes finden sich auf engstem Raum morphologisch unterscheidbare Mikrobenmatten. Diese Diversität der Mattentypen ist vor allem durch die Position innerhalb der Gezeitenzone und daraus resultierende unterschiedliche Überflutung, Salinität, Verdunstung und Sedimentation bestimmt.

Anhand von Biomarkeruntersuchungen sollten Gemeinsamkeiten und Unterschiede hinsichtlich der mattenbildenden Organismen, des möglichen Eintrags allochthonen organischen Materials und eventueller diagenetischer Effekte in den einzelnen Matten aufgezeigt werden. Es wurde ermittelt, dass alle Matten nahezu ausschließlich prokaryontischen Ursprungs sind und wechselnde Anteile aerosolisch eingetragenen Landpflanzenmaterials enthalten. Cyanobakterien sind in allen Matten die Hauptprimärproduzenten.

Eine der Matten, die sogenannte Gelatinöse Matte, die unter den lokal extremsten Bedingungen in der oberen Gezeitenzone gefunden wurde, zeigte eine besonders stark ausgeprägte Schichtung im Millimeterbereich. Diese wurde unter der Annahme, dass die einzelnen Schichten unterschiedliche Artengemeinschaften beinhalten, zur Analyse der Vertikalverteilung von Biomarkern über das gesamte Tiefenprofil verwendet. Die Untersuchungen bestätigten die angenommene Verteilung der mattenbildenden Organismen entlang der Tiefenprofile von Licht und Sauerstoff, wobei bereits direkt unterhalb der Mattenoberfläche erste mikrobielle Überarbeitungsprozesse festgestellt wurden. In der tiefsten Lage, unterhalb der aktiven Matte, akkumuliert das teilweise abgebaute organische Material.

Aufgrund der extremen Umweltbedingungen ist der Kohlenstoffmetabolismus innerhalb der Matten von besonderem Interesse, zumal die gemessenen Kohlenstoffisotopenverhältnisse des organischen Gesamtextraktes auf eine Nährstofflimitierung aufgrund der hohen Salinität hinzuweisen scheinen. Für diesen Zweck wurde eine Inkubation mit ^{13}C-markiertem Substrat durchgeführt. Die Inkubation wurde als Zeitreihenexperiment geplant. Kleine Kerne wurden aus der

Gelatinösen Matte entnommen und in künstlichem Meerwasser, das mit ^{13}C-markiertem Natriumbicarbonat versetzt war, inkubiert. Die Messung der Kohlenstoffisotopenverhältnisse erfolgte für die einzelnen Schichten der Matte sowohl am organischen Gesamtextrakt als auch an den dominierenden Kohlenwasserstoffen und Phospholipidfettsäuren. Die Analyse ergab die größte messbare Anreicherung an ^{13}C in *n*-Heptadecan und in einem doppelt ungesättigten *n*-Alken unbekannten Ursprungs. Dies beweist, dass Cyanobakterien und der Quellorganismus des *n*-Alkens die Hauptprimärproduzenten darstellen.

Alle Untersuchungen ergaben die Dominanz des *n*-Alkens unbekannten Ursprungs in der Oberflächenschicht der Gelatinösen Matte, die in diesem Umfang bisher nicht publiziert worden war. Die Untersuchungen lassen einigen Raum für Vermutungen bezüglich des eintragenden Organismus. Die Dominanz in der Oberflächenschicht, die Korrelation in der Vertikalanalyse mit Phytol und die Ähnlichkeit mit der Bildung des markierten *n*-Heptadecans deuten auf einen aeroben phototrophen Quellorganismus hin. Jedoch konnte diese Vermutung in Ermangelung von Kultivierungsdaten weder konkretisiert noch endgültig belegt werden.

Abstract

Microbial mats are one of the smallest ecosystems on planet Earth and are, due to their internal metabolic activities, which result in almost closed nutrient loops, microbial communities of special interest. In the last decades many organic geochemical studies were already performed on various types of living and fossil microbial mats from a variety of habitats.

In the present work microbial mats from the intertidal flat south-west of the Al Dhabaiya peninsula (United Arab Emirates) were analysed. The intertidal flat exhibits locally different, mostly very extreme growth conditions with water salinities reaching 200 caused by shadowless sunshine exposure for nearly twelve hours per day. The study area harbours a variety of morphologically different microbial mats in closest proximity. This diversity of the microbial mats mainly depends on the intertidal position and corresponding differences in inundation with tidal waters, salinity, evaporation and sedimentation.

The biomarker analyses were intended to reveal similarities and differences concerning the mat building organisms, the possible input of allochthonous organic matter and diagenetic effects within each particular mat. In the course of the study nearly exclusively prokaryotic origin were identified in all microbial mats, which contained differing amounts of terrestrial organic matter from aeolian transport. Cyanobacteria are the major primary producers in all mats.

One of the mats, the so called Gelatinous Mat, which thrives under the locally most extreme environmental conditions in the upper intertidal area, shows a distinct lamination on the millimetre scale. This mat was chosen to investigate the vertical distribution of biomarkers, suggesting that the single layers represent different microbial consortia. The results confirmed the assumed zonation of mat building organisms along the vertical gradients of light and oxygen, whereas directly beneath the mat surface microbial degradation was already observed. In the deepest layer, below the active mat, the partially degraded organic matter accumulates.

Due to the very extreme environmental conditions the carbon metabolism within the microbial mats is of special interest, because the measured stable carbon isotope ratios of the total extractable organic matter appear to indicate nutrient limitation caused by the high salinity. For this purpose an incubation experiment with ^{13}C-labelled substrate was carried out. The incubation was planned as time series experiment. Small cores taken from the Gelatinous mat were incubated in artificial seawater which was spiked with ^{13}C-labelled sodium bicarbonate. The measurements of the stable carbon isotope ratios were performed on the distinct layers of the mat as well on the total extractable organic matter and the dominant hydrocarbons and

phospholipid fatty acids. The analyses show the strongest enrichment of ^{13}C in both *n*-heptadecane and in a diunsaturated *n*-alkene of unknown origin. This proves that cyanobacteria and the *n*-alkene producing organism are the major primary producers.

All investigations revealed the predominance of the *n*-alkene of unknown origin in the top layer of the Gelatinous mat, which has not been reported before to this extent. The analysis leaves some space for speculation concerning the source organism. The predominance in the surface layer and both the correlation with phytol throughout the depth profile and the similarity in the uptake of labelled substrate during the biosynthesis of *n*-heptadecane hint to an aerobic phototrophic organism, although this assumption could neither be substantiated nor proven because of lacking cultivation data.

Abbildungsverzeichnis

1.1 Photographien morphologisch unterschiedlicher Mikrobenmatten in der Gezeitenzone südwestlich von Al Dhabaiya, Vereinigte Arabische Emirate .. 2

2.1 Typischer Aufbau einer Mikrobenmatte. Dargestellt sind auch die vertikalen Profile der relativen Sauerstoff- und Schwefelwasserstoffkonzentrationen in der Matte am Tag und in der Nacht 7

2.2 Strukturformeln von a – Phytol, b – Squalen und c- einem C_{25}-HBI ohne Doppelbindungen 11

2.3 Strukturformeln von a – Cholest-5-en-3β-ol, b – Cholestan-3β-ol und c-Cholest-2-en 12

2.4 Strukturformeln von a – Bakteriohopantetrol, b – Diplopterol und c-Diplopten 13

2.5 Strukturformeln der verschiedenen Alkylketten in Lipiden..... 15

2.6 Lokation des Probennahmegebiets an der Küste des Arabischen Golfs 18

2.7 Politische Karte der Arabischen Halbinsel 18

3.1 Map showing the location (south-west corner of the Al Dhabaiya peninsula) of the studied microbial mats along the Arabian Gulf coast of Abu Dhabi and a satellite image of the sampling site. 23

3.2 Concentrations of *n*-alkanes and major hydrocarbons in the Abu Dhabi microbial mats..... 29

3.3 Partial total ion current chromatogram of hydroxyl compounds in the Pink mat 32

3.4 Concentrations of sterols and hopanols in the microbial mats from Abu Dhabi..... 33

3.5 Partial total ion current chromatograms of (a) TMS derivatives of the free fatty acids and (b) phospholipid fatty acid methyl esters from the top layer of the Gelatinous mat. 35

3.6 Relative amounts of summed PLFA groups in the Abu Dhabi microbial mats 36

3.7 Map showing the location (south-west corner of the Al Dhabaiya peninsula) of the studied microbial mats along the Arabian Gulf coast of Abu Dhabi and a satellite image of the sampling site. 44

3.8 Simplified vertical profile of the Gelatinous mat with stable carbon isotope ratios of the total extractable organic carbon 44

3.9 Concentrations of *n*-alkanes and major hydrocarbons 47

3.10 Relative amounts of summed PLFA groups 53

3.11 Vertical distribution of selected lipid biomarkers 56

4.1 Map showing the location of the studied cyanobacterial mats on the Arabian Gulf coast near Abu Dhabi and satellite images of the sampling site modified from Google Earth 62

4.2 Photographs showing the landscape of the microbial mats in the intertidal flat of Abu Dhabi 63

4.3 Distribution of fatty acids in the intertidal microbial mats of Abu Dhabi. (a) Total ion current chromatograms of the studied microbial mats. (b) Relative abundances and distribution of different fatty acid groups in the mats. 68

4.4 Distribution of intracellular and extracellular pigments among the studied microbial mats 69

4.5 Photomicrographs of identified filamentous and unicellular morphotypes of cyanobacteria in the studied mat samples 70

4.6 DGGE fingerprints of PCR-amplified 16S rRNA gene fragments obtained from the studied microbial mats using cyanobacteria-specific primers 72

4.7 16S rRNA gene-based phylogenetic reconstruction based on maximum likelihood methods, showing the affiliation of cyanobacterial sequences retrieved from DGGE and cultures obtained from the studied microbial mats 73

5.1 Map showing the location (south-west corner of the Al Dhabaiya peninsula) of the studied microbial mats along the Arabian Gulf coastal area of Abu Dhabi and a satellite image of the sampling site. 80

5.2 Simplified vertical profile of the photosynthetic zone of the Gelatinous mat. 81

5.3 Set–up of the labelling experiment. 81

5.4 Stable carbon isotope ratios of the total extractable organic carbon of the individual layers over time 85

5.5 Enrichment plots of ^{13}C in total extractable organic matter from individual layers as a function of time 86

5.6 Compound specific enrichment plots of major hydrocarbons from layer 1 as a function of time 88

5.7 Compound specific enrichment plots of major hydrocarbons from layer 2 as a function of time 89

5.8 Compound specific enrichment plots of major PLFAs from layer 1 as a function of time 91

5.9 Compound specific enrichment plots of major PLFAs from layer 2 as a function of time 92

8.1 Oberfläche und Seitenansicht der Roten Matte 139

8.2 Nahaufnahme der „Pinnacles“ 139

8.3 Großflächig ausgebreitet die Pinnacle Matte (schwarz) und von Wasser überflutet die Gelatinöse Matte 140

8.4 Ohne die Reflektion des Lichtes gut erkennbar: Die rote Oberfläche der Gelatinösen Matte 140

8.5 Seitenansicht der Gelatinösen Matte 141

8.6 Aufbau des Inkubationsexperimentes 141

Tabellenverzeichnis

2.1 Relevante autotrophe Organismen in einer Mikrobenmatte mit Angabe des Stoffwechselweges, der jeweiligen Energiequelle und des Elektronendonors 8

3.1 Macroscopic characteristics, environmental settings at the time of sampling and dominant microorganisms of the studied mats 24

3.2 Gross composition of microbial mats 27

3.3 Relative abundances (%) of compound classes among the total hydrocarbons . 28

3.4 Hydroxyl compounds annotated in Figs. 3.4 and 3.5 34

3.5 Relative abundances (%) of the phospholipid fatty acid groups and major PLFAs 38

3.6 Relative abundances of compound classes in total hydrocarbon fractions 47

3.7 Concentrations of *n*-alkanes in µg/g organic extract (n.d. - not determined) 48

3.8 Concentrations of hydroxy compounds in µg/g organic extract 51

3.9 Relative abundances of the phospholipid fatty groups and major PLFAs 54

4.1 Comparison of the cyanobacterial community among the studied microbial mats as determined by light epifluorescence microscopy and morphological traits of identified morphotypes. 71

5.1 $\delta^{13}C$ values of the total extractable organic carbon for layers 1 to 3 with unlabelled and 1%, 10% and 30% ^{13}C-bicarbonate 86

5.2 $\delta^{13}C$ values of the major hydrocarbons for layers 1 and 2 with unlabelled, 10% and 30% ^{13}C-bicarbonate. 89

5.3 $\delta^{13}C$ of the major PLFAs for layers 1 and 2 with unlabelled and 10% ^{13}C-bicarbonate 93

8.1 Konzentrationen der *n*-Alkane, Methylalkane, *n*-Alkene und Isoprenoide in µg/g organischer Gesamtextrakt in den Mikrobenmatten und der Oberflächenschicht der Roten Matte 125

8.2 Konzentrationen der *n*-Alkane, Methylalkane, *n*-Alkene und Isoprenoide in µg/g organischer Gesamtextrakt in den Schichten der Gelatinösen Matte 127

8.3 Relative Anteile aller Phospholipidfettsäuremethylester in % in den Mikrobenmatten und der Oberflächenschicht der Roten Matte 129

8.4 Relative Anteile aller Phospholipidfettsäuremethylester in % in den Schichten der Gelatinösen Matte 131

8.5 Doppelbestimmungen der Kohlenstoffisotopenverhältnisse des organischen Gesamtextraktes der Proben aus dem Inkubationsexperiment 133

8.6 Doppelbestimmungen der Kohlenstoffisotopenverhältnisse ausgewählter Kohlenwasserstoffe in Schicht 1 aus dem Inkubationsexperiment 134

8.7 Doppelbestimmungen der Kohlenstoffisotopenverhältnisse ausgewählter Kohlenwasserstoffe in Schicht 2 aus dem Inkubationsexperiment 135

8.8 Doppelbestimmungen der Kohlenstoffisotopenverhältnisse ausgewählter PLFAs in Schicht 1 aus dem Inkubationsexperiment 136

8.9 Doppelbestimmungen der Kohlenstoffisotopenverhältnisse ausgewählter PLFAs in Schicht 2 aus dem Inkubationsexperiment 137

Liste der verwendeten Abkürzungen

Abb.	Abbildung
b.d.	*below detection*
BSFA	*branched saturated fatty acid*
CFA	*cyclopropyl fatty acid*
CFB	*Cytophaga*/*Flavobacteria*/*Bacteroidetes*-Gruppe
eV	Elektronenvolt
Fig.	*Figure*
GC	Gaschromatographie
ir	*isotope ratio*
KAS	Kaltaufgabesystem
MS	Massenspektrometrie
MUFA	*monounsaturated fatty acid*
m/z	Verhältnis von Masse zu Ladung
n.d.	*not determined*
PLFA	Phospholipidfettsäure / *phospholipid fatty acid*
PUFA	*polyunsaturated fatty acid*
rRNA	*ribosomal ribonucleic acid*
sp.	Species
SFA	*saturated straight-chain fatty acid*
TIC	*total inorganic carbon*
TMS	Trimethylsilyl
TN	*total nitrogen*
TOC	*total organic carbon*
TS	*total sulphur*
VPDB	Vienna Pee Dee Belemnite

1 Einleitung

Photosynthetische Mikrobenmatten sind selbsterhaltende Ökosysteme im Millimeterbereich (z.B. Park, 1977; Revsbech et al., 1983; Golubic, 1991; van Gemerden, 1993; Kendall et al., 2002). Die Arbeit an Mikrobenmatten hat eine lange Tradition in der biogeochemischen und mikrobiologischen Forschung (z.B. Cardoso et al., 1976; Philp et al., 1978; Ward et al., 1980; Zeng et al., 1992a, b; Kenig et al., 1995; Wieland et al., 2003; Fourçans et al., 2004), da rezente Mikrobenmatten wegen ihrer morphologischen Ähnlichkeiten als moderne Analoga fossiler Stromatolithen gelten (z.B. Awramik, 1984; Boudou et al., 1986; van Gemerden, 1993). Folglich sah man schon in den 1970er Jahren die Möglichkeit, rezente Mikrobenmatten als Modellsysteme für mikrobielle Gemeinschaften zu untersuchen, die fähig sind, stromatolith-ähnliche Strukturen aufzubauen. Die Ergebnisse sollten dazu beitragen, fossile Aufzeichnungen zu interpretieren und eventuell die Entstehung des frühen Lebens auf der Erde genauer zu entschlüsseln.

In den 1990er Jahren traten Cyanobakterienmatten erneut in den Fokus, da sie als erste Lebewesen wieder auf ölverschmutzten Flächen am Arabischen Golf siedelten (Höpner et al., 1996; Hoffmann, 1996). Da allerdings gezeigt wurde, dass Cyanobakterienreinkulturen nicht allein in der Lage sind, die Erdölkohlenwasserstoffe abzubauen (Abed und Köster, 2005), trat die Gesamtvergesellschaftung der Matten in den Vordergrund der Forschung. Auf der Suche nach metabolisch dominanten und vor allem auch gesamtbiomasse-relevanten Mikroorganismen wurden in den letzten Jahrzehnten viele Mikrobenmatten untersucht, insbesondere solche aus extremen Milieus. Sie sind exzellente natürliche „Labore“, die dabei helfen, die Stoffwechselinteraktionen und sich daraus ergebende biogeochemische Gradienten zu verstehen (Karsten und Kühl, 1996). Mikrobenmatten weisen abhängig von ihrem Standort häufig unterschiedliche Morphologien sowie Mikroorganismen-gemeinschaften und biogeochemische Zusammensetzungen auf (Kendall und Skipwith, 1968; Golubic, 1991). Die photische und aerobe Zone ist meistens durch Cyanobakterien, aerobe heterotrophe sowie photosynthetische Bakterien dominiert; mit zunehmender Tiefe folgen anaerobe phototrophe Bakterien (van Gemerden, 1993).

Der Arabische Golf war vor allem in den 1960er und 1970er Jahren für zahlreiche Geologen ein Untersuchungsgebiet von großem Interesse (z.B. Evans et al., 1969; Purser und Evans, 1973; Kinsman und Park, 1976). Der Küstenbereich der Vereinigten Arabischen Emirate ist allein durch seinen über 90%-igen Carbonatanteil einzigartig (Sanford und Wood, 2001). Aufgrund der Halbinseln, die in den Golf hineinragen, wird die Küstenlinie unterbrochen, und so entstanden unterschiedliche Lebensräume in den dazwischen liegenden Abschnitten (Purser und Evans, 1973;

Kenig, 1990). Es ist schon seit den 1960er Jahren bekannt, dass es eine intensive Besiedlung der Gezeitenzone der Vereinigten Arabischen Emirate mit Mikrobenmatten gibt (Evans et al., 1969). Bereits in den 1980er und 1990er Jahren waren diese Gegenstand organisch-geochemischer Analysen. Kenig et al. (1990, 1991, 1995, 2000) untersuchten sowohl das rezente Sediment als auch das kerogengebundene organische Material sowie Mangroven- und Mikrobenmattenproben in den Abschnitten nordöstlich und südwestlich der Abu-Dhabi-Halbinsel.

In der vorliegenden Arbeit wurden zum ersten Mal rezente Mikrobenmatten aus dem Gebiet südwestlich der Halbinsel Al Dhabaiya, ca. 50 km südlich von Abu Dhabi, mit organisch-geochemischen Methoden untersucht. Der südliche Küstenstreifen des Arabischen Golfs stellt einen besonders interessanten und vielseitigen Lebensraum dar. Es handelt sich um eine Gezeitenzone, die durch Barriereinseln vor dem auflaufenden Wasser geschützt ist (Alsharhan und Kendall, 2003). Durch die geologischen Bedingungen im Laufe der Entstehung dieses Gebietes hat sich eine Salzwüste (Sabkha) als Verbindung zwischen Festland und Gezeitenzone ausgebildet (Evans et al., 1969; Bush, 1973; Glennie, 2001). Diese bietet zusammen mit den vorherrschenden Klimabedingungen einen für alle höheren Organismen unwirtlichen Lebensraum (Revsbech et al., 1983; Cohen, 1989). Bei früheren Untersuchungen der dort siedelnden Mikrobenmatten bezüglich Morphologie und dominanter mattenbildender Arten wurde eine hohe Diversität festgestellt (Kendall und Skipwith, 1968; Golubic, 1991), die unter anderem auf die sehr unterschiedlichen Umweltbedingungen innerhalb der Gezeitenzone zurückzuführen sind, wenn man die Kleinskaligkeit des Gesamthabitats betrachtet.

Abb. 1.1: Photographien morphologisch unterschiedlicher Mikrobenmatten in der Gezeitenzone südwestlich von Al Dhabaiya, Vereinigte Arabische Emirate.

1.1 Zielsetzung und Gliederung der vorliegenden Arbeit

Ziel der vorliegenden Arbeit war die geochemische Charakterisierung morphologisch unterscheidbarer Mikrobenmatten aus der Gezeitenzone der Vereinigten Arabischen Emirate. Diese wurde sowohl zwischen den einzelnen Typen vergleichend als auch im Vertikalprofil durchgeführt, um einen genauen Einblick in die Biomarkerverteilung der einzelnen Schichten zu erhalten. Um nicht nur anhand von Biomarkern Rückschlüsse auf die mikrobielle Zusammensetzung sowie die metabolisch dominierenden Arten ziehen zu können, wurde zusätzlich ein Inkubationsexperiment durchgeführt. Mit Hilfe eines isotopenmarkiertem Substrats, das durch die Primärproduzenten aufgenommen und in das organische Material eingebunden wird, und anschließende Biomarkeranalyse sollten die dominanten autotrophen Organismen identifiziert werden.

Kapitel 3 umfasst zwei Manuskripte, die die geochemische Charakterisierung der Mikrobenmatten beinhalten. In Kapitel 3.1 werden fünf morphologisch verschiedene Mikrobenmatten hinsichtlich ihrer Biomarkerzusammensetzung vergleichend betrachtet. Zusätzlich werden von zwei der Matten die Oberflächenschichten untersucht und ebenfalls in die Interpretation im Hinblick auf die besiedelnde mikrobielle Gemeinschaft, den Eintrag terrestrischen organischen Materials und etwaige diagenetische Effekte mit einbezogen. Kapitel 3.2. stellt den zweiten Teil der geochemischen Charakterisierung der Mikrobenmatten vom Arabischen Golf dar. In diesem Manuskript wird eine aufgrund ihrer ausgeprägten Schichtung im Millimeterbereich sowie der extremen Bedingungen des Habitats ausgewählte Mikrobenmatte im Vertikalprofil analysiert, um von der Biomarkerverteilung in den einzelnen Schichten Rückschlüsse auf die Organismengemeinschaften innerhalb der einzelnen Schichten und auf diagenetische Effekte ziehen zu können. Mikrobenmatten bestehen aus oft farblich unterschiedlichen Schichten unterschiedlicher Dichte, die jeweils Gruppen von metabolisch ähnlichen Mikroorganismen enthalten. Diese können dann anhand der für sie spezifischen Biomarker identifiziert werden.

Kapitel 4 ist eine Gemeinschaftsarbeit aller Kooperationspartner im Rahmen des Projektes „Diversität und Rolle aerober heterotropher Arten im autochthonen und allochthonen Kohlenstoffkreislauf“. In dieser Publikation wird insbesondere die Anpassung der Mikrobenmatten an die extremen Umweltbedingungen in der Gezeitenzone des Arabischen Golfes beschrieben. Permanente Sonneneinstrahlung von ca. zwölf Stunden am Tag, damit verbundene Austrocknung und Salzgehalte bis zu 200 stellen einen extremen Lebensraum dar. Im Manuskript werden phylogenetische Analysen der mattenbildenden Cyanobakterien sowie die Analyse der

Phospholipidfettsäuren und Pigmente der einzelnen Matten in Bezug auf Stressanpassung untersucht und ausgewertet. Der eigene Anteil an dieser Publikation ist die geochemische Aufarbeitung der Mikrobenmatten und die Analyse, Auswertung und Interpretation der Phospholipidfettsäuredaten.

In Kapitel 5 sind die Ergebnisse eines Inkubationsexperimentes zusammengefasst. Teilstücke einer Mikrobenmatte wurden in Aquarien mit künstlichem Meerwasser, das mit isotopisch markiertem Natriumbikarbonat versetzt war, über einen Tag/Nacht/Tag-Zyklus inkubiert. Insgesamt gab es vier Ansätze mit unterschiedlichen Anteilen an ^{13}C-markiertem Substrat. Anhand eines Zeitplans wurde aus allen Parallelansätzen beprobt. Die Mikrobenmatten wurden gemäß ihrer optisch erkennbaren Schichtung aufgearbeitet und analysiert. Mittels Isotopenverhältnismassenspektrometrie am gesamten extrahierbaren organischen Material sowie auf komponentenspezifischer Ebene konnte die Aufnahme des ^{13}C in die Biomasse verfolgt werden. Dies ermöglicht in erster Linie die Identifizierung der dominanten Primärproduzenten, gewährt aber auch im weiteren Verlauf Einblicke in Stoffwechselprozesse zwischen verschiedenen Organismengruppen. Die Probennahme erfolgte mit Hilfe der Kooperationspartner Dr. Raeid Abed, Katharina Kohls (beide MPI Bremen) und Dr. Waleed Hamza (Universität der Vereinigten Arabischen Emirate). Das Inkubationsexperiment konnte mit freundlicher Unterstützung auf dem Campus des College of Sciences der Universität der Vereinigten Arabischen Emirate in Al Ain (V.A.E.) durchgeführt werden. Versuchsplanung und –durchführung sowie die geochemische Aufarbeitung, Analyse und Auswertung der Daten und das Erstellen des Manuskripts erfolgten selbstständig durch die Autorin.

2 Stand des Wissens

2.1 Mikrobenmatten

Mikrobenmatten sind flächige, vertikal geschichtete organosedimentäre Strukturen, welche aus millimeterfeinen Lagen bestehen (z.B. Park, 1977; Revsbech et al., 1983; Golubic, 1991; van Gemerden, 1993; Kendall et al., 2002) und durch benthische mikrobielle Gemeinschaften gebildet werden (Margulis et al. 1980). Sie stellen eines der kleinsten und ältesten Ökosysteme der Erde dar (z.B. Awramik, 1984; Boudou et al., 1986; van Gemerden, 1993; Schouten et al., 2001). Diese kleinskaligen Ökosysteme, welche oft nur 5 bis 10 mm dick sind, bestehen meistens aus einigen funktionellen Gruppen von Mikroorganismen, welche durch ihre metabolischen Prozesse interagieren (z.B. Boudou et al., 1986; Dobson et al., 1988). Der Ausdruck "Matte" bezieht sich dabei auf ein zusammenhängendes geschichtetes System, das die Lebensgemeinschaften auf der Oberfläche von aquatischen Sedimenten bilden. Dabei wachsen die Mikroorganismen nicht nur auf ihrer Unterlage, sondern beeinflussen und verändern durch ihre Stoffwechselaktivitäten nachhaltig die Eigenschaften der Oberflächen (Karsten und Kühl, 1996).

Die wichtigsten Mikroorganismengruppen in mikrobiellen Matten sind Cyanobakterien, farblose Schwefelbakterien, Purpurschwefelbakterien und sulfatreduzierende Bakterien. Die Arten verteilen sich entlang der Mirkogradienten von Licht, Sulfid und Sauerstoff (z.B. Revsbech et al., 1983; Boudou et al., 1986; van Gemerden, 1993).

Das organische Material wird vor allem an der Sediment-Wasser-Grenzschicht durch autotrophe Organismen wie z.B. Cyanobakterien, anoxygene photosynthetische Bakterien und je nach Saison auch Diatomeen gebildet. Unterhalb der Mattenoberfläche ist das Sediment dunkel, sulfatreduzierende Bakterien und andere anaerobe heterotrophe Mikroorganismen überwiegen. Das organische Material ist folglich hauptsächlich prokaryontischen Ursprungs (z.B. van Gemerden, 1993 als Übersichtartikel), da die häufig sehr extremen Umweltbedingungen das Auftreten und Überleben höherer Organismen (sowohl Pflanzen als auch Tiere) ausschließen (Revsbech et al., 1983; Cohen, 1989). Solch extreme Umweltbedingungen gibt es unter anderem in hypersalinen Gewässern, heißen Quellen, trockenen Wüsten, antarktischen Seen und in marinen Gezeitenzonen (z.B. Cohen, 1984, 1989; Jørgensen und Cohen, 1977; Javor und Castenholz, 1981; Bauld, 1984; Stal et al., 1985; de Wit und van Gemerden, 1988; Ward et al., 1998). Dort siedeln sich meist anspruchslose beziehungsweise besonders tolerante Mikrobenarten an und bilden Biofilme. Diese entziehen dem Medium Nährstoffe, welche sie durch ihr Zellwachstum im Biofilm

fixieren und lokal akkumulieren. Damit stellen sie wiederum ökologische Nischen für andere Bakterien dar, die unter dem ursprünglichen Nährstoffangebot nicht leben könnten (Margulis et al., 1980; Karsten und Kühl, 1996). In diesen mikrobiologisch aktiven Sedimenten spielen auch diagenetische Prozesse eine Rolle (Edmunds und Eglinton, 1984).

2.1.1 Stromatolithe

Stromatolithe sind als „laminierte Steine“ definiert, deren Ursprung eindeutig der Aktivität mikrobieller Gemeinschaften zugeordnet werden kann (Krumbein, 1983). Sie bestehen aus wechselnden organisch-reichen und mineralreichen Schichten (Park, 1976). Die frühesten bekannten Lebensformen auf der Erde sind in Form von Stromatolithen aus dem Präkambrium erhalten, wobei die ältesten Funde auf 3,5 Milliarden Jahre datiert wurden (z.B. Park, 1977). Mikrofossilien, die in präkambrischen Stromatolithen gefunden wurden, zeigen eine erstaunliche Analogie zu rezenten Cyanobakterien. Also waren Cyanobakterien damals die dominanten Primärproduzenten für organisches Material auf dem Planeten (Awramik, 1984). Allerdings wuchsen die Organismen im Präkambrium im Gegensatz zu modernen Mikrobenmatten unter anoxischen Bedingungen (Walter et al., 1992).

Das Maximum der Verbreitung von Stromatolithen war vor ca. 2 Milliarden Jahren. Zu dieser Zeit etwa begann auch die durch Endosymbiose verschiedener Bakteriengruppen gesteuerte Entwicklung der Eukaryonten. Sie ist nach heutigem Stand der Wissenschaft ein unmittelbares Produkt der Evolution von Biofilmen. Diese hatten einen erheblichen Einfluss auf geologische Vorgänge in globalen Dimensionen, da sie massive Veränderungen in biogenen und sedimentären Stoffkreisläufen bewirkten. So sind photosynthetische mikrobielle Gemeinschaften für die Umstellung der Erdatmosphäre von anaeroben zu aeroben Verhältnissen im Paläoproterozoikum verantwortlich und spielen auch heute noch eine entscheidende Rolle bei der Fixierung von atmosphärischem CO_2 (Cohen und Rosenberg, 1989).

2.1.2 Mattenaufbau

Mikrobenmatten sind Gemeinschaften aus phototrophen, chemotrophen und heterotrophen Organismen, welche vertikal definierte Schichten bilden (van Gemerden, 1993). Schematisch ist diese Schichtung in Abb. 2.1 dargestellt.

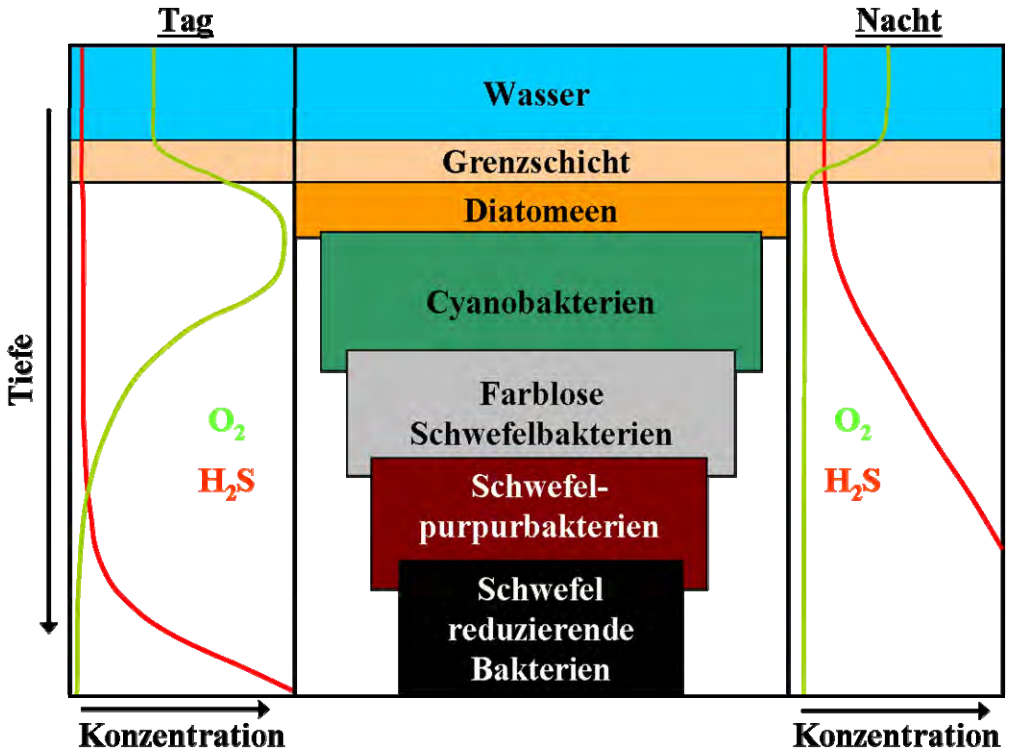

Abb. 2.1: Typischer Aufbau einer Mikrobenmatte. Dargestellt sind auch die vertikalen Profile der relativen Sauerstoff- und Schwefelwasserstoffkonzentrationen in der Matte am Tag und in der Nacht (verändert nach van Gemerden, 1993).

An der Oberfläche der Mikrobenmatte finden sich häufig Diatomeen, gefolgt von Cyanobakterien, wobei typischerweise ein bis zwei Cyanobakterienarten die dominierenden phototrophen Organismen (Dobson, 1988) und somit auch die Hauptprimärproduzenten von organischem Material und Sauerstoff sind. Wegen der sehr engen Kopplung von autotrophen und heterotrophen Prozessen wird das meiste organische Material innerhalb der aktiven Zone der Mikrobenmatte „recycelt“ (Karsten und Kühl, 1996). Unterhalb der Schicht der Cyanobakterien befindet sich häufig eine Schicht farbloser Schwefelbakterien, gefolgt von Schwefelpurpurbakterien. Die tiefste aktive Schicht wird dominiert von sulfatreduzierenden Bakterien (van Gemerden, 1993).

Vor allem in Mikrobenmatten aus heißen Quellen (zum Beispiel Yellowstone National Park, USA) wird häufig eine weitere Gruppe autotropher Bakterien gefunden. Hierbei handelt es sich um die grünen Nicht-Schwefelbakterien der *Chloroflexus*-Gruppe (z.B. Ward et al., 1997; Zeng et al., 1992a). Das sind filamentöse anoxygene phototrophe Organismen, welche in den jeweiligen Mikrobenmatten als Hauptprimärproduzenten bzw. gemeinsam mit Cyanobakterien vorkommen (z.B. Zeng et al., 1992a; van der Meer et al., 2008).

Die gemeinsame metabolische Aktivität der verschiedenen Mikroorganismen resultiert in steilen chemischen Mikrogradienten innerhalb der Matte, insbesondere

von Sauerstoff und Sulfid (siehe Abb. 2.1; Revsbech et al., 1983; des Marais, 1995; Stal, 1995). Während des Tages, also unter Lichteinstrahlung, ist die photosynthetische Oberflächenschicht der Mikrobenmatte an Sauerstoff übersättigt, während die CO_2-Konzentration sehr niedrig ist (Canfield und des Marais, 1994; Wieland und Kühl, 2000). Bei Dunkelheit breitet sich die anoxische Zone bis direkt unterhalb der Mattenoberfläche aus. Die Tiefenprofile von Sauerstoff, Schwefelwasserstoff etc. können durch sogenannte Mikrosensoren gemessen werden. Dabei handelt es sich um mikrometerdünne Sensoren, die hochauflösend verschiedene Parameter innerhalb von kleinskaligen Ökosystemen messen können. Mikrosensormessungen von Sauerstoff werden beispielsweise benutzt, um die Bruttophotosynthese zu bestimmen (Revsbech und Jørgensen, 1983; Jørgensen und des Marais, 1986; Jensen und Revsbech, 1989).

2.1.3 Stoffwechselprozesse der dominanten Gruppen

Wie im vorangegangenen Kapitel beschrieben, besteht eine benthische Mikrobenmatte aus einer Reihe von Mikroorganismen, welche unterschiedliche Stoffwechselwege aufweisen und die Stoffwechselinteraktionen innerhalb der Matte bestimmen (van Gemerden, 1993). Eine Zusammenfassung der autotrophen Stoffwechselprozesse in einer Mikrobenmatte findet sich in Tabelle 2.1.

Tabelle 2.1: Relevante autotrophe Organismen in einer Mikrobenmatte mit Angabe des Stoffwechselweges, der jeweiligen Energiequelle und des Elektronendonors (verändert nach van Gemerden, 1993)

	Energiequelle	Elektronendonor
Cyanobakterien		
Oxygene Photosynthese	Licht	H_2O
Anoxygene Photosynthese	Licht	H_2S
Grüne Nicht-Schwefelbakterien		
Anoxygene Photosynthese	Licht	H_2 bzw. H_2S
Farblose Schwefelbakterien		
Chemosynthese	H_2S bzw. O_2	H_2S
Purpurschwefelbakterien		
Anoxygene Photosynthese	Licht	H_2S
Chemosynthese	H_2S bzw. O_2	H_2S

Die Grundlage für das Wachstum von Mikrobenmatten stellt die Photosynthese von Cyanobakterien und Diatomeen (falls vorhanden) dar. Da Cyanobakterien in den meisten Fällen die dominierenden Primärproduzenten sind, hängt das Wachstum und Überleben der anderen Organismen in den tieferen Mattenlagen von ihren Ausscheidungen und Zersetzungsprodukten ab (Bateson und Ward, 1988). Das

organische Material, das durch die Cyanobakterien bereitgestellt wird, steht den aeroben heterotrophen Bakterien zur Atmung zur Verfügung, wobei Sauerstoff verbraucht und neues CO_2 gebildet wird, welches wiederum von den autotrophen Organismen genutzt werden kann. Außerdem wird es zu reduzierten Verbindungen umgesetzt, die den sulfatreduzierenden Mikroorganismen als Nahrungsquelle dienen (z.B. van Gemerden, 1993). Hierbei entsteht Schwefelwasserstoff, welcher als Eisensulfid ausfällt und/oder in der photischen Zone durch farblose Schwefelbakterien oder Schwefelpurpurbakterien oxidiert wird (Kühl et al., 2003).

Die aeroben farblosen Schwefelbakterien sind chemotrophe Organismen, die vor allem den freigesetzten Schwefelwasserstoff, aber auch andere reduzierte Formen des Schwefels mit Hilfe von Sauerstoff oxidieren, um auf diesem Wege Energie zu gewinnen. Dabei wird neben Sulfat auch elementarer Schwefel freigesetzt. Im Gegensatz zu den aeroben farblosen Schwefelbakterien sind die Schwefelpurpurbakterien anaerobe phototrophe Mikroorganismen. Schwefelpurpurbakterien können Schwefelwasserstoff und andere reduzierte Schwefelverbindungen mit Hilfe des Lichts oxidieren und als Elektronendonatoren zur Reduktion von CO_2 nutzen. Diese zwei Gruppen von Organismen sind dafür verantwortlich, dass weniger als 1% des Schwefelwasserstoffs, welcher durch dissimilatorische Sulfatreduktion produziert wurde, die Atmosphäre erreicht (z.B. Karsten und Kühl, 1996).

Die Sulfatreduktion wird als wichtigster anaerober Mineralisationsprozess betrachtet (Canfield und des Marais, 1993). Der von den sulfatreduzierenden Bakterien freigesetzte Schwefelwasserstoff beeinträchtigt die Physiologie der Cyanobakterien erheblich (Cohen et al., 1986). Wird viel H_2S in der Matte produziert und unterhalb der Cyanobakterienschicht angesammelt, kann es deren oxygene Photosynthese und Wachstum hemmen.

2.2 Biomarkeruntersuchungen an Mikrobenmatten

Die molekulare Zusammensetzung von Umweltproben kann genutzt werden, um eine mikrobielle Gemeinschaft näher zu beschreiben (z.B. Philp et al., 1978; Zeng et al., 1992a, b; Rontani und Volkman, 2005). Allerdings muss in einer Arbeit, die im Bereich Biogeochemie angesiedelt ist, der Begriff Biomarker geklärt werden, da er in der mikrobiellen Ökologie anders definiert ist als in der organischen Geochemie. In beiden Forschungsbereichen beruht die Benutzung von Biomarkern auf der Beobachtung, dass einige Verbindungen jeweils nur von einer bestimmten Gruppe von Organismen gebildet werden.

Die mikrobielle Ökologie untersucht die Beziehung zwischen Mikroorganismen und ihrer natürlichen Umwelt (Brock, 1987). Der Begriff Biomarker wird hier als

chemische Verbindung von Mikroorganismen definiert, welche direkt aus der Umwelt analysiert werden können und welche sowohl quantitative als auch qualitative Rückschlüsse auf die *in situ*-Biomasse zulassen (Parkes, 1987). Dabei sollen Biomarker schnell nach dem Zelltod überarbeitet werden, sodass sie nur für lebende Biomasse und nicht für die Überreste von Lebewesen indikativ sind, die sich über die Zeit akkumuliert haben. Die auf diese Weise meistgenutzten Biomarker sind intakte Phospholipide und Phospholipidfettsäuren, welche sowohl in Bakterien als auch in Eukaryonten gefunden werden (Boschker und Middelburg, 2002).

In der Organischen Geochemie wird der Begriff anders definiert. Hier meint der Begriff organische Verbindungen, die in geologischen Proben weit verbreitet sind und Rückschlüsse auf kohlenstoffhaltige Bestandteile von Organismen zulassen (Eglinton und Calvin, 1967). Biomarker sind einzelne Moleküle, die nach ihrer Ablagerung und Diagenese ihre charakteristische Struktur weitestgehend beibehalten. Hierzu gehören Kohlenwasserstoffe, aber auch funktionalisierte organische Verbindungen (z.B. *n*-Alkane, *n*-Alkohole, Fettsäuren, Steroide oder Triterpenoide).

Folglich sind das ökologische und das geologische Biomarkerkonzept einander ähnlich. In dieser Arbeit werden die Lipide aktuell lebender Organismen in rezenten Ökosystemen untersucht, aber auch bereits diagenetisch überarbeitete Verbindungen erlauben Rückschlüsse auf in früheren Zeiten eingetragene Biomasse. Im Folgenden werden die einzelnen Biomarkergruppen, die zur Charakterisierung des organischen Materials herangezogen wurden, näher erläutert.

2.2.1 Aliphatische Kohlenwasserstoffe

Eglinton und Hamilton (1967) stellten schon früh fest, dass *n*-Alkan-Verteilungsmuster einen Hinweis auf die eintragenden Organismen liefern können. Es gibt zahlreiche Untersuchungen, die versucht haben, dieses chemotaxonomische Potential weiter zu verfolgen (z.B. Cranwell, 1973; Cardoso et al., 1983; Collister et al.; 1994; Ficken et al., 1998; Baas et al., 2000).

Kurzkettige *n*-Alkane mit weniger als 20 Kohlenstoffatomen kommen bevorzugt in Algen und Bakterien vor (Blumer et al., 1971; Cranwell, 1974) und sind damit von besonderer Bedeutung bei der geochemischen Analyse von marinen Mikrobenmatten. Insbesondere *n*-Heptadecan ist in diesem Zusammenhang von besonderer Bedeutung, da es als Cyanobakterienbiomarker gilt (z.B. Gelpi et al., 1970; Murata und Nishida, 1987; Grimalt et al., 1992). Somit kann aus einer Dominanz dieses *n*-Alkans auf Cyanobakterien als Hauptprimärproduzenten geschlossen werden.

Typische Indikatoren für den Eintrag von organischem Material aus terrestrischen Quellen in marine Sedimente sind die Verteilungsmuster von langkettigen *n*-Alkanen, wobei das Maximum im Bereich von 27 bis 31

Kohlenstoffatomen mit starker Bevorzugung der ungeradzahligen Homologen liegt (z.B. Eglinton und Hamilton, 1967).

Unter den verzweigten und ungesättigten aliphatischen Kohlenwasserstoffen gibt es weitere, die in der Analytik von Mikrobenmatten von Bedeutung sind: Mittelständig verzweigte kurzkettige Mono-, Di- und Trimethylalkane (z.B. Köster et al., 1999) sowie isomere geradkettige Alkene mit 17 Kohlenstoffatomen (Gelpi et al., 1970; Murata und Nishida, 1987) sind weitere Cyanobakterienbiomarker. *n*-Octadecene sind nützliche Biomarker für autochthone Einträge photosynthetischer Mikroorganismen (Boon und de Leeuw, 1987; Grimalt et al., 1992).

2.2.2 Isoprenoide

Isoprenoide sind Kohlenwasserstoffverbindungen, die aus Isopreneinheiten (2-Methylbuta-1,3-dien) aufgebaut sind. Das bedeutendste Isoprenoid ist Phytol (Abb. 2.2a), welches als Seitenkette von Chlorophyll *a* (bspw. in Cyanobakterien und Phytoplankton) beziehungsweise Bakteriochlorophyll *a* (beispielsweise in Schwefelpurpurbakterien) durch Hydrolyse abgespalten werden kann (Marchand und Rontani, 2003). Durch Dehydrierung bilden sulfatreduzierende Bakterien aus Phytol Phytadiene und Phytene (Grossi et al., 1998), welche somit auf den Eintrag photosynthetischer Organismen gleichzeitig aber auch auf biologische Degradation hinweisen.

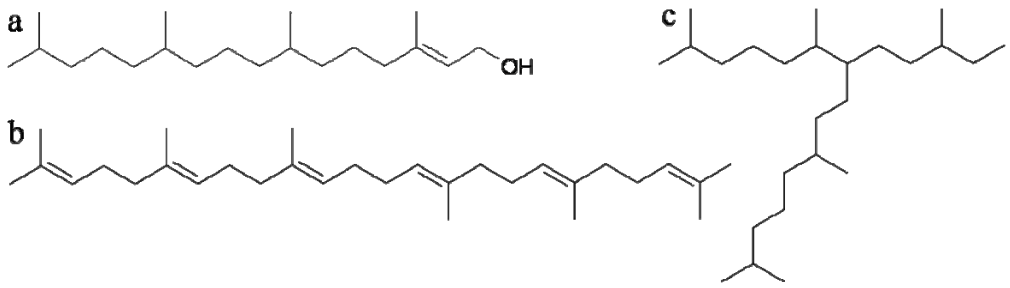

Abb. 2.2: Strukturformeln von a – Phytol, b – Squalen und c- einem C_{25}-HBI ohne Doppelbindungen.

Ein weiterer Isoprenoidbiomarker ist Squalen (Abb. 2.2b). Dieses nicht mit Phytol verwandte Isoprenoid ist die Ausgangsverbindung von Triterpenoiden. Es ist typischer Bestandteil in Mikrobenmatten (Boon et al., 1983; Rontani und Volkman, 2005) und Cyanobakterienreinkulturen (Gelpi et al., 1970).

Da Diatomeen saisonal eine Rolle als Primärproduzenten in marinen Mirkobenmatten spielen können, sind hochverzweigte Isoprenoide (HBI; Abb. 2.2c) von Interesse (Summons et al., 1993; Volkman et al., 1994; Belt et al., 2000). HBIs kommen mit 20 bis 30 Kohlenstoffatomen und häufig 0 bis 6 Doppelbindungen vor und wurden bereits in einer Vielzahl von rezenten Sedimenten (z.B. Rowland und

Robson, 1990 als Übersichtsartikel) und Diatomeenkulturen (z.B. Volkman et al., 1994) nachgewiesen.

2.2.3 Steroide und Hopanoide

Steroide sind Membranbestandteile mariner und terrestrischer Eukaryonten (Hefter et al., 1993) und dienen vor allem als Zellmembranverstärker (Ourisson et al., 1984). Da die Steroidbiosynthese molekularen Sauerstoff benötigt, um aus Squalen das Squalanepoxid zu bilden, werden Steroide ausschließlich von aeroben Organismen synthetisiert (Harwood und Russell, 1984). Sie treten in großer struktureller Vielfalt sowohl in veresterter als auch in freier Form auf (Huang und Meinschein, 1976, 1979; Volkman, 1986). Volkman (1986) verfasste eine umfassende Übersicht über Vorkommen und Bedeutung dieser Biomarker in rezenten Sedimenten. Im Allgemeinen kommen die Steroidalkohole terrestrischer und mariner Herkunft mit einer Kohlenstoffzahl von C_{26} bis C_{30} vor und besitzen an der C-3 Position eine Hydroxylgruppe. Merkmale zur Charakterisierung der Sterolvielfalt sind neben der Größe des Kohlenstoffgerüsts und der Anzahl der Doppelbindungen auch die Position von zusätzlichen Methylgruppen sowie die sterische Konfiguration an chiralen Zentren des Moleküls (Volkman, 1986; Volkman et al., 1993). Die Anwesenheit hoher Gehalte an Stanolen weist auf die mikrobiellen Umwandlung der korrespondierenden Sterole hin (Gaskell und Eglinton, 1975). Bei fortschreitender Diagenese kommt es zur Abspaltung der Hydroxylgruppe und der damit verbundenen Bildung von Sterenen. Beispielsweise ist 5α-Cholest-2-en ein diagenetisches Produkt von Cholest-5-en-3β-ol, das über die Bildung des Cholestan-3β-ol entsteht (Dastillung und Albrecht, 1977; de Leeuw et al., 1989; Abb. 2.3). In Mikrobenmatten werden Steroide hauptsächlich durch aerobe Gemeinschaften in der Oberflächenschicht (Plankton), die mit dem Wasser angespült werden, oder den eventuellen aeolischen Transport terrestrischen Materials eingetragen (Edmunds und Eglinton, 1984).

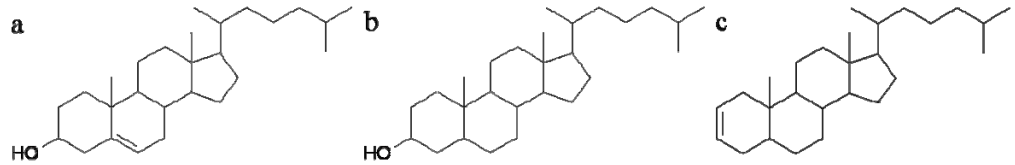

Abb. 2.3: Strukturformeln von a – Cholest-5-en-3β-ol, b – Cholestan-3β-ol und c- Cholest-2-en.

Hopanoide gelten für gewöhnlich als Bakterienbiomarker, da sie bisher überwiegend in Cyanobakterien, photosynthetischen Bakterien und einigen aeroben Bakterien nachgewiesen wurden (z.B. Ourisson et al., 1979; Rohmer et al., 1992; Kannenberg und Poralla, 1999). Sie dienen ebenfalls als membranverstärkende Moleküle (Kannenberg und Poralla, 1999). Die meisten Hopanoide ohne oder mit

einzelnen Hydroxylfunktionen gelten als Abbauprodukte von bakteriellen Polyhydroxyhopanolen (Rohmer et al., 1984; Abb. 2.4a). In Mikrobenmatten sind zumeist Diplopterol (17β,21β-Hopan-22-ol, Abb. 2.4b) und das daraus durch Dehydrierung gebildete Diplopten (17β,21β-Hop-22(29)-en; Abb. 2.4c) die dominanten Hopanoide. Ihr Ursprung kann wahrscheinlich auf Cyanobakterien zurückgeführt werden (Gelpi et al., 1970; Bird et al., 1971). Allerdings sind auch einige andere prokaryontische Organismen dafür bekannt, Triterpenoide zu bilden (z.B. Ourisson et al., 1979).

Summons et al. (1999) beschrieben einen weiteren Cyanobakterienbiomarker unter den Hopanolen: 2-Methylhopanole. Leider lässt sich diese Verbindung vor allem in Süßwassercyanobakterien, aber nur in einer begrenzten Anzahl untersuchter Kulturen mariner Cyanobakterien nachweisen, sodass die Anwesenheit von 2-Methylhopanol auf Cyanobakterien hindeutet, die Abwesenheit allerdings kein Ausschlusskriterium für Cyanobakterieneintrag ist.

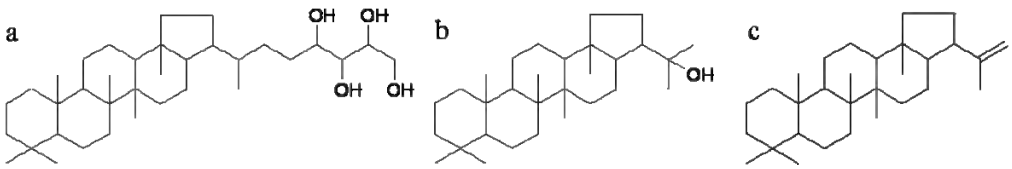

Abb. 2.4: Strukturformeln von a – Bakteriohopantetrol, b – Diplopterol und c- Diplopten.

2.2.4 Fettsäuren

Fettsäuren sind ubiquitär. Neben ihrer Funktion als Energiespeicher (z.B. in Triglyceriden) sind sie Bestandteil der Zellmembran (z.B. in Phospholipiden). Biologische Membranen haben bei allen Lebewesen einen einheitlichen Grundaufbau, der als Phospholipiddoppelschicht beschrieben wird. Phospholipide sind amphipathische Moleküle, d.h. sie bestehen aus einer hydrophilen Komponente (Kopfgruppe) und einer lipophilen Komponente (Acyl- oder Alkoxylketten). Bei Glycerophospholipiden bildet Glycerol das Grundgerüst. An den Positionen 1 und 2 des Glycerols sind Fettsäuren ester- oder ethergebunden. An Position 3 des Glycerols sind über eine Phosphatgruppe die Kopfgruppen gebunden. Diese sind namensgebend für die Phospholipide.

In Umweltproben findet sich eine große Bandbreite an estergebundenen Phospholipidfettsäuren (PLFA). Ein Vorteil der Nutzung von PLFAs als Biomarker ist die Tatsache, dass diese Verbindungen innerhalb von Tagen nach dem Zelltod abgebaut werden (Zelles, 1999 als Übersichtsartikel). In den letzten Jahrzehnten wurde ein immenser Datensatz an kulturspezifischen PLFA-Verteilungsmustern aufgebaut. Seine Verwendung zur taxonomischen Charakterisierung mikrobieller Gemeinschaften und Kulturen beruht auf der Annahme, dass unterschiedliche

Mikroorganismen unterschiedliche Phospholipide enthalten (White et al., 1979; Boschker und Middelburg, 2002). Durch die Phospholipiddoppelschicht ist die Fluidität und die Permeabilität der Zellmembran gewährleistet, wobei diese von den gebundenen Fettsäuren abhängen. Organismen können sich veränderten Umweltbedingungen anpassen, indem die Lipidzusammensetzung variiert wird.

In Sedimenten werden hauptsächlich Fettsäuren mit Kettenlängen zwischen 12 und 36 Kohlenstoffatomen gefunden. *n*-Fettsäuren (Abb. 2.5a) treten aufgrund ihrer Biosynthese aus C2-Einheiten (aus Acetyl-Coenzym A) grundsätzlich mit einer geradzahligen Bevorzugung auf. Ungesättigte Fettsäuren können entweder *de novo* durch das Fettsäure-Synthease-Enzym (anaerober Syntheseweg) oder postsynthetisch durch das Desaturase-Enzym (aerober Syntheseweg) gebildet werden. Dehydrierung führt zu Fettsäuren mit einer oder mehreren konjugierten Doppelbindungen, wobei die sterische Konfiguration der Doppelbindungen vornehmlich *cis* (Abb. 2.5b) ist. Bei prokaryontischen Organismen sind ungesättigte Fettsäuren mit *trans*-Konfiguration (Abb. 2.5c) meist ein Indikator für physiologischen Stress. Die postsynthetischen Modifikationen sind auch diejenigen, die am schnellsten die Membranfluidität regulieren können (Russell, 1984).

Kurzkettige Fettsäuren mit 10 bis 20 Kohlenstoffatomen werden hauptsächlich von Bakterien und planktonischen Organismen gebildet (Volkman et al., 1981; Volkman et al., 1989; Volkman et al., 1991; Findlay und Dobbs, 1993). Die *n*-Hexadecansäure ist ubiquitär in fast allen Organismen (Mancuso et al. 1990; Stoeck et al. 2002). Generell werden gesättigte Fettsäuren mit 14 bis 18 Fettsäuren als typische Bestandteile von Mikroorganismen betrachtet (Findlay und Dobbs 1993).

Langkettige Fettsäuren (>22 C-Atome) mit geradzahliger Kettenlängenbevorzugung sind charakteristisch für die Kutikulawachse höherer Landpflanzen und gelten als Indikatoren für den allochthonen Eintrag detritischen Pflanzenmaterials in marine Ablagerungsräume (z.B. Eglinton und Hamilton, 1967).

Zusätzlich zu den gesättigten Fettsäuren synthetisieren Bakterien hauptsächlich methylverzweigte gesättigte, einfach ungesättigte und *Cyclo*propanfettsäuren (Perry et al., 1979; Parkes und Taylor, 1983; Findlay und Dobbs, 1993). Die methylverzweigten gesättigten Fettsäuren werden in endständig verzweigte und mittelständig verzweigte Fettsäuren unterteilt. Endständig methylverzweigte (*iso*- und *anteiso*-) Fettsäuren (Abb. 2.5d und e) sind Biomarker für anaerobe heterotrophe Bakterien. Diese Fettsäuren treten als Homologe mit Kettenlängen von 12 bis 19 Kohlenstoffatomen auf, wobei *anteiso*-Fettsäuren lediglich als ungeradzahlige Fettsäuren vorkommen.

*Cyclo*propanfettsäuren (Abb. 2.5f) kommen nicht in allen Bakterien vor, jedoch ist ihr Nachweis in Sedimenten ein charakteristischer Indikator für heterotrophe

Bakterien wie zum Beispiel sulfatreduzierende Bakterien und auch andere anaerobe Bakterien (Volkman und Johns 1977; Findlay und Dobbs 1993; Stoeck et al. 2002; Mallet et al. 2004) sowie in Schwefelpurpurbakterien (Grimalt et al, 1992). Allerdings ist es wichtig zu berücksichtigen, dass der Anteil an *Cyclo*propanfettsäuren stark von den Wachstumsbedingungen abhängt, wobei der Anteil grundsätzlich mit zunehmender Wachstumsrate steigt (z.B. Wang et al., 1994; Grogan et al., 1997; Zhang und Rock, 2008).

Mehrfach ungesättigte Fettsäuren kommen in hohen Konzentrationen in Algen vor (z.B. Chuecas und Riley, 1969). Mehrfach ungesättigte und gesättigte Fettsäuren mit mehr als 20 Kohlenstoffatomen sind Biomarker für eukaryontische Organismen wie z.B. Mikroalgen, Protozoen und Diatomeen (Volkman et al. 1980; Findlay und Dobbs 1993).

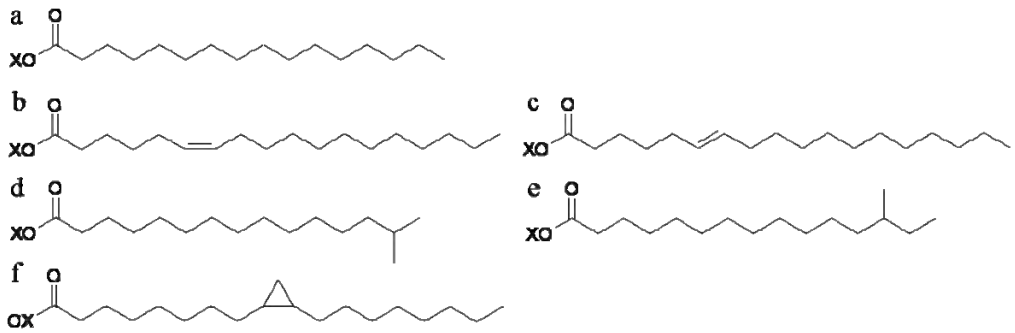

Abb. 2.5: Strukturformeln der verschiedenen Alkylketten in Lipiden. a – geradkettige gesättigt, b - *cis*-ungesättigt, c – *trans*-ungesättigt, d – *iso*-verzweigt, e – *anteiso*-verzweigt, f – *Cyclo*propan, X – Molekülrest.

Grundsätzlich sollte die Interpretation von Phospholipidfettsäuredaten mit Vorsicht erfolgen, da sich Veränderungen in den Wachstumsbedingungen auch auf die Zusammensetzung der Phospholipide und der Fettsäuren auswirken können (Denich et al., 2003; Zhang und Rock, 2008). Außerdem kann eine Überlappung von Lipidmustern in Umweltproben die Korrelation taxonomischer Daten von Einzelgemeinschaften stören (Fang et al., 2000). Es ist bisher nicht möglich von Gesamtzellfettsäureprofilen auf einzelne Organismen zurückzuschließen, aber es herrscht Übereinstimmung, dass eine taxonomische Klassifizierung anhand von Indikatorverbindungen möglich ist.

2.3 Stabile Isotope

Isotope sind Atome des gleichen Elements mit gleicher Protonenzahl und unterschiedlicher Neutronenzahl, welche sich nur geringfügig hinsichtlich ihrer physikalischen und chemischen Eigenschaften unterscheiden. Für das Element Kohlenstoff treten in der Natur drei Isotope auf: ^{12}C, ^{13}C und ^{14}C, wobei ^{12}C und ^{13}C sogenannte stabile Isotope sind. Natürlich vorkommender Kohlenstoff besteht zu über

98,9% aus dem Isotop ^{12}C. Der relative Anteil der stabilen Isotope im organischen Material kann allerdings durch verschiedene physikalische wie auch biochemische Prozesse variieren. Um diesen Unterschied auszudrücken, gibt es den $\delta^{13}C$-Wert, der mathematisch folgendermaßen ausgedrückt wird:

$$\delta^{13}C = \left(\frac{^{13}C_{\mathrm{Pr}} / ^{12}C_{\mathrm{Pr}}}{^{13}C_{Std} / ^{12}C_{Std}} - 1 \right) \cdot 1000$$

mit: Pr = Probe, deren Kohlenstoffisotopenverhältnis ermittelt werden soll und Std = „PDB-Standard“ (aus der Pee Dee Belemnite-Formation)

Für die unterschiedlichen Isotopenverhältnisse in kohlenstoffhaltigen Verbindungen sind Fraktionierungsprozesse verantwortlich. Bei der Primärproduktion spielen das Isotopenverhältnis der verwendeten Kohlenstoffquelle, die Isotopeneffekte im Zusammenhang mit der Assimilation des Kohlenstoffs und die Isotopeneffekte bei der Synthese der Biomasse eine Rolle (z.B. O’Leary, 1988; Hayes, 1993; Schidlowski, 2000).

Autotrophe Primärproduzenten verwenden Bicarbonat beziehungsweise Kohlenstoffdioxid als Kohlenstoffquelle. Daher kann zwischen marinen und terrestrischen Primärproduzenten anhand ihres Isotopenverhältnisses unterschieden werden. Bei der Gleichgewichtsreaktion zwischen atmosphärischem CO_2 und dem Bicarbonatsystem des Meerwassers wird das Bicarbonat des Meeres um 7‰ mit dem schweren ^{13}C angereichert (Schidlowski et al., 1984). Folglich sind von marinen Organismen synthetisierte organische Verbindungen isotopisch schwerer (Durchschnittswert ca. -20‰) als jene, die von terrestrischen Organismen direkt aus atmosphärischem CO_2 gebildet werden (ca. -27‰, Schidlowski et al., 1984). Grundsätzlich wird bei der Photosynthese aufgrund einer enzymatischen Präferenz geringfügig mehr ^{12}C als ^{13}C aufgenommen. Dies führt zu einer Verschiebung der prozentualen Isotopenzusammensetzung zugunsten des leichteren ^{12}C-Isotops. Die damit verbundene Abreicherung an ^{13}C wird als Diskriminierung bezeichnet. Bei heterotrophen Organismen wird die isotopische Zusammensetzung der Biomasse durch die Nahrungsmuster und die isotopischen Fraktionierungen bestimmt, die entlang der Nahrungskette erfolgen.

Das Kohlenstoffisotopenverhältnis von Lipiden wird sowohl durch den $\delta^{13}C$-Wert der Kohlenstoffquelle als auch durch den physikalischen und biochemischen Metabolismus, durch den das jeweilige Molekül gebildet wird, bestimmt. Im Fall des Calvinzyklus, der von grünen Pflanzen, Algen, vielen autotrophen Bakterien sowie

Cyanobakterien zur CO_2-Aufnahme genutzt wird, werden anorganische Kohlenstoffverbindungen bei durch Ribulosebiphosphatcarboxylase (RuBisCO) katalysierten Reaktionen hauptsächlich zu Kohlenhydraten reduziert. Hingegen weisen Bakterien, die entweder den reduktiven Citratzyklus (z.B. *Chlorobium* spp.) oder den 3-Hydroxypropionatmetabolismus (z.B. *Chloroflexus auranticus*) zur Kohlenstoffassimilation nutzen, ein an ^{13}C angereichertes Isotopenverhältnis auf (Quandt et al., 1977; Sirevåg et al., 1977). Folglich ist das Verhältnis von ^{13}C zu ^{12}C im gesamten organischen Material und in einzelnen organischen Verbindungen ein wertvoller Hinweis auf die Herkunft der Verbindungen und des organischen Materials (z.B. O'Leary, 1988), und somit kann die Isotopenbestimmung von Biomarkern Aufschluss über biosynthetische Mechanismen und andere, in die Fraktionierung eingebundene Effekte geben.

Für hypersaline Mikrobenmatten wurden vermehrt isotopisch schwere $\delta^{13}C$-Werte ermittelt (z.B. Schidlowski et al., 1984). Diese können durch die Umweltbedingungen erklärt werden (z.B. verringerte CO_2 Löslichkeit und Verdunstung), welche die Verfügbarkeit von CO_2 für die Photosynthese reduzieren (Schidlowski et al., 1984; Schidlowski, 1985; des Marais et al., 1989; Moers et al., 1993; Schouten et al., 2001). Dies führt zu einer ineffektiven Diskriminierung gegen das ^{13}C, und somit sind die $\delta^{13}C$ Werte photosynthetischer Organismen in diesen Milieus erhöht. Weiterreichende Forschung hat allerdings gezeigt, dass dies nicht der einzige Grund für die Anreicherung an ^{13}C sein kann, da bisher kein konsequenter Trend für Mikrobenmatten, die bei unterschiedlichen Salinitäten vorkommen, gefunden wurde (des Marais et al., 1989; Schidlowski et al., 1994). Daraus folgend wurde vermutet, dass die hohe Produktivität, die häufig in Mikrobenmatten beobachtet wird, und die damit einhergehende CO_2-Limitierung ein weiterer Grund für die herabgesetzte Fraktionierung zwischen den Isotopen sein kann (Schouten et al., 2001).

2.4 Das Probennahmegebiet

Das Probennahmegebiet befindet sich in der Gezeitenzone der Vereinigten Arabischen Emirate südwestlich der Halbinsel Al Dhabaiya (auch Zubaiya: z.B. Whittle et al., 1998, je nach Transkription; Abb. 2.6). Das Untersuchungsgebiet umfasst Bereiche der unteren, mittleren und oberen Gezeitenzone. Alle Bereiche sind teilweise mit morphologisch unterscheidbaren Mikrobenmatten bedeckt.

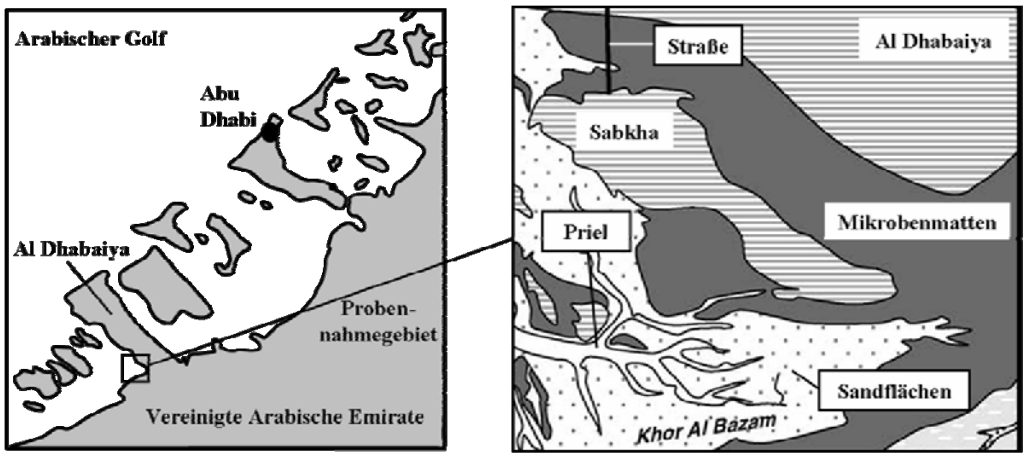

Abb. 2.6: Lokation des Probennahmegebiets an der Küste des Arabischen Golfs, Position ca. 24°11'23''N, 54°10'24''O (Kartenausschnitt rechts aus Alsharhan und Kendall, 2003).

Die Vereinigten Arabischen Emirate befinden sich auf der Nordostseite der Arabischen Halbinsel (Abb. 2.7). Die Küste, die sich über ca. 600 km erstreckt, bildet einen Teil der südlichen Begrenzung des Arabischen Golfs.

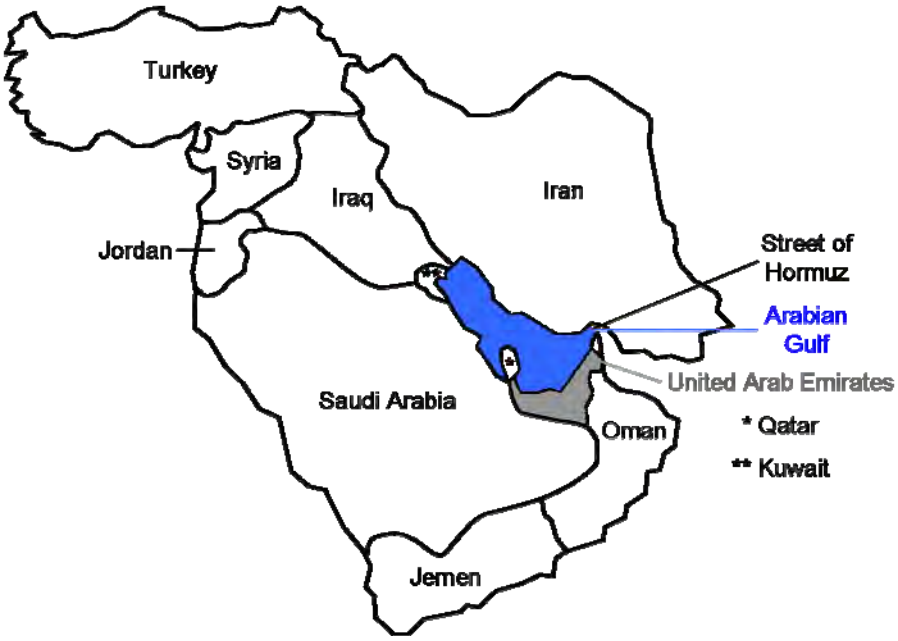

Abb. 2.7: Politische Karte der Arabischen Halbinsel (ohne Israel und Libanon; Quelle: www.brot-fuer-die-welt.de/images/laender/weltkarte_vorderasien_aktuelle-projekte.gif, Stand September 2008).

Das heutige Klima in der Region ist warm und trocken mit jährlichen Niederschlägen von ca. 70 mm entlang der Küste (Evans et al., 1969; Sanford und Wood, 2001) und ca. 40 mm im Flachland (Glennie, 2001). Durch die sehr geringen Niederschlagsmengen besteht der größte Teil der Arabischen Halbinsel aus Wüste. Während des Sommers kann die Lufttemperatur an der Golfküste 50°C und mehr erreichen, wobei die Luftfeuchtigkeit im Schnitt 50 bis 60% beträgt (Glennie, 2001).

Der Arabische Golf erstreckt sich über ca. 900 km Breite und 350 km Länge. Die mittlere Tiefe beträgt 35 m und die maximale Tiefe 100 m. Diese befindet sich in

der Straße von Hormuz (Alsharhan und Kendall, 2002), die zudem auch die Verbindung zum Indischen Ozean ist. Die Frischwasserzufuhr erfolgt über den *Shatt al Arab* sowie einige iranische Flüsse. Die Oberflächenwassertemperaturen an der Südküste des Arabischen Golfs reichen von ca. 23°C im Winter bis ca. 33°C im Sommer. Die durchschnittliche Salinität liegt zwischen 38 und 40. Im Arabischen Golf treten Gezeiten auf, jedoch ist die Fluthöhe trotz starker Gezeitenströme an der Südküste des Golfs nicht höher als 1,5 bis 2,5 m (Chiffings, 1995).

2.4.1 Die Gezeitenzone der Vereinigten Arabischen Emirate

Die Gezeitenzone der Vereinigten Arabischen Emirate erstreckt sich südöstlich des Arabischen Golfs entlang der gesamten Küstenlinie. Es ist ein System, das hauptsächlich aus Lagunen und Sabkhas besteht (z.B. Kendall und Skipwith, 1969; Purser und Evans, 1973). Die Bildung dieses Systems wird durch die Barriereinseln, die *Great Pearl Bank*, begünstigt, die sich – wie auf einer Perlenschnur – in etwa parallel zur Küstenlinie aufreihen (Pilkey, 2003). Landwärts der Barriereinseln befindet sich ein Lagunensystem, welches weit in die hypersaline Küstenebene, die Sabkha, hineinreicht. In diesem Gebiet gibt es eine großflächige Entstehung und Ausbreitung von Mikrobenmatten (z.B. Purser und Evans, 1973; Golubic, 1991).

In der Gezeitenzone findet sich eine Vielzahl von morphologisch unterschiedlichen Mikrobenmatten (z.B. Kendall und Skipwith, 1968; Kinsman und Park, 1976; Kenig et al., 1990; Golubic, 1991; Abed et al., 2007, 2008), die extremen Umweltbedingungen ausgesetzt sind. Die Salinität kann im Sommer je nach Position innerhalb der Gezeitenzone bis zu 200 betragen. Zudem sind die Matten schattenloser Sonneneinstrahlung ausgesetzt, was zu hohen Verdunstungsraten und somit Austrocknung führt. Alle genannten Umweltfaktoren sowie ihre Wechselwirkungen beeinflussen sowohl die Oberflächenstruktur der Mikrobenmatten als auch die Zusammensetzung der Mikrobengemeinschaften in der Gezeitenzone der Vereinigten Arabischen Emirate. Die ausgeprägte zonale Verteilung der verschieden Mattentypen deutet auf individuelle Standortanpassung hin, indem die jeweils bestangepassten und tolerantesten Genotypen unter den Cyanobakterien (Primärproduzenten) dominieren (Golubic, 1991).

2.4.2 Die Entstehung der Gezeitenzone

Die Küste von Abu Dhabi entstand durch Überflutung der äußeren Bereiche der Arabischen Wüste während der flandrischen Transgression vor 8000 Jahren und während einer relativen Regression 4000 Jahre später (Evans et al., 1969; Kinsman und Park, 1976; Sanford und Wood, 2001; Evans und Kirkham, 2002). Die geologische Geschichte in Abu Dhabi während der letzten 8000 Jahre ist reich an

mehrfachen Zyklen abwechselnder Transgression und Regression. Jeder stratigraphisch-sedimentäre Zyklus zeigt einen relativ zügigen Meeresspiegelanstieg an und ist überlagert von Sedimenten, die zunehmend niedrigeres Wasser widerspiegeln.

Heutzutage ist der südliche Teil der Küste des Arabischen Golfs eine progradierende Küste: das Land dehnt sich aus, und das Meer zieht sich zurück, weil die sedimentären Prozesse über die erodierenden überwiegen. Zudem stellt das System eines der wenigen rezenten karbonatischen hypersalinen Sedimentationsgebiete dar.

2.4.3 Die Sabkha

Die Sabkha der Vereinigten Arabischen Emirate ist ein großflächiges supra- und intertidales Habitat. Sabkha ist ein arabisches Wort und bedeutet Salzfläche. Es gibt eine Vielzahl von Regionen, in denen Sabkhas zu finden sind. Im Rahmen dieser Arbeit sind aber nur Küstensabkhas von Bedeutung. Diese haben in der geologischen Literatur viel Aufmerksamkeit erfahren, da es sich hierbei um hypersaline Milieus handelt, in denen auch aktuell die Neubildung von Dolomit beobachtet wird.

Sabkhas sind wegen ihrer Flachheit und der totalen Abwesenheit von terrestrischer Vegetation ausgeprägte geomorphologische Merkmale. Sie finden sich in trockenen Gegenden, in denen die Verdunstung den Niederschlag bei weitem übersteigt, wobei das jährliche Niederschlagsvolumen 250 mm/m^2 nicht übersteigt. Im Fall der Küstensabkhas bietet eine niedrige Küstenlinie den Gezeiten eine große Überflutungsfläche, welche hohe Sedimentationsraten begünstigt. Die ökologische Bedeutung von Sabkhas wurde bisher nicht ergründet (Barth und Böer, 2002).

Die Küstensabkhas im Emirat Abu Dhabi wurden ursprünglich durch Butler (1969), Evans et al. (1969) und Kinsman und Park (1976) untersucht. Die mineralogische Charakterisierung umfasst hauptsächlich Krusten aus Cyanobakterien oder Dolomit, die eine Schicht von Anhydrit überlagern (Evans et al., 1969; Park, 1977; Pilkey, 2003). Die Sabkha der Vereinigten Arabischen Emirate erstreckt sich auf pleistozäne und holozäne Sedimente (Kendall und Skipwith, 1968; Evans et al., 1969; Purser und Evans, 1973; Kenig et al., 1990).

3 Biogeochemistry of high-salinity microbial mats

3.1 Biogeochemistry of high-salinity microbial mats – Part 1: Lipid composition of microbial mats across intertidal flats of Abu Dhabi, United Arab Emirates

Ann-Kathrin Scherf, Jürgen Rullkötter

Institute of Chemistry and Biology of the Marine Environment (ICBM), Carl von Ossietzky University of Oldenburg, P.O. Box 2503, D-26111 Oldenburg, Germany

3.1.1 Abstract

In this paper we present detailed analyses of selected lipid classes of five morphologically different microbial mats from the intertidal area of Abu Dhabi, United Arab Emirates. These mats thrive under extreme environmental conditions as they are exposed to salinities up to 200 and shadowless sunshine exposure for nearly 12 hours per day. The microbial mats are characterized by relatively heavy $\delta^{13}C$ values of the total extractable organic matter (-17 ‰ to -10 ‰) suggesting CO_2 limitation. The lipids reflect the input of the principal mat-building phototrophic and heterotrophic microorganisms. Moderate amounts of hydrocarbons, mainly the cyanobacterial *n*-heptadecane, short-chain monomethylalkanes and diploptene were detected in all mats. Among the free and ester-bound phospholipid fatty acids the ubiquitous *n*-hexadecanoic acid is dominant and changes in the overall composition are observed due to the extreme environmental conditions.

Additionally, from two mats the top layers were analysed to compare the composition with the whole mat results. As would be supposed, the concentrations of cyanobacterial biomarkers exceed those found in the total mats. Most interestingly is the finding of *n*-heneicosadiene as predominating hydrocarbon in the top layer of the so called Gelatinous mat, which thrives under the locally most extreme conditions. As the *n*-alkene was detected to a much lower extent in the intact mat, this hydrocarbon may provide a new biomarker for a so far unknown dominant surface organism of this mat.

3.1.2 Introduction

Microbial mats are stratified organosedimentary structures consisting of millimetre-fine laminae (e.g. Park, 1977; Revsbech et al., 1983; Golubic, 1991; van Gemerden, 1993; Kendall et al., 2002). They are one of the oldest and the smallest ecosystems on Earth and are of considerable geological significance as they are

thought to represent modern analogues of Precambrian stromatolites (e.g. Awramik, 1984; Boudou et al., 1986; van Gemerden, 1993; Schouten et al., 2001). These vertically small-scaled ecosystems, which are often not more than 5 to 10 mm thick, typically consist of a few functional groups of microbes which interact through their metabolic processes (e.g. Boudou et al., 1986; Dobson et al., 1988). The major microbial groups that are typically found in hypersaline mats are cyanobacteria, purple sulphur bacteria, colourless sulphur bacteria and sulphate-reducing bacteria, which are distributed along vertical microgradients of oxygen, sulphide and light (e.g. Revsbech et al., 1983; Boudou et al., 1986; van Gemerden, 1993).

Various types of living and fossil microbial mats from a diversity of environments have previously been investigated in a number of organic geochemical studies (e.g. Philp et al., 1978; Boon et al., 1983; Awramik, 1984; Schidlowski, 1985; Dobson et al., 1988; Robinson and Eglinton, 1990; Shiea et al., 1990; Zeng et al., 1992a; Kenig et al., 1995; Thiel et al., 1997; Wieland et al., 2003). Hypersaline ecosystems, considered recent analogues for ancient evaporitic sediment deposition, were studied, e.g., by Schidlowski et al. (1984) and Friedman and Krumbein (1985).

In the present study we investigated pristine microbial mats from the sabkha region of Abu Dhabi, United Arab Emirates. The coastal plain of Abu Dhabi developed by flooding of the outer parts of the Arabian desert during the Flandrian Transgression 8000 yr BP and a partial regression 4000-5000 yr BP (Evans et al., 1969; Kinsman and Park, 1976; Sanford and Wood, 2001; Evans and Kirkham, 2002). Off the coastline a number of barrier islands formed atop a rocky ridge (Great Pearl Bank) almost parallel to the shore (Pilkey, 2003). Landwards of the barrier islands a lagoonal system fades into a wide hypersaline coastal plain, the sabkha, which comprises Pleistocene to Holocene sediments (Kendall and Skipwith, 1968; Evans et al., 1969; Purser and Evans, 1973; Kenig et al., 1990), consisting mainly of calcium carbonate with gypsum and anhydrite as additional major minerals (Evans et al., 1969; Park, 1977; Pilkey, 2003). The surface is covered with extended microbial mats also referred to as cyanobacterial mats. The coastal intertidal flats of the Arabian Gulf harbour various types of mats (e.g. Kendall and Skipwith, 1968, Kinsman and Park, 1976; Kenig et al., 1990; Golubic, 1991; Abed et al., 2008) that experience extreme environmental conditions. The salinity may reach 200 depending on the mat's tidal position, and the temperature may rise to more than 55°C in hot summers. The mats are exposed to shadowless sunshine, leading to high seawater evaporation rates and desiccation.

We collected five different microbial mats (Table 3.1) from the intertidal area of the United Arab Emirates to analyze them concerning their gross composition as

well as their extractable (non-volatile) free and bound lipids. The lipid composition of the microbial mats allowed to determine the dominant sources of organic matter and the selective diagenetic transformation of specific microbial lipids.

3.1.3 Materials and methods

3.1.3.1 Site and sample description

The microbial mat samples were collected in December 2004 from the sabkha of Abu Dhabi (Arabian Gulf coast, United Arab Emirates) during low tide. The sampling site is located on the west coast of the Al Dhabaiya peninsula (also Zubaiya depending on transcription; e.g. Whittle et al., 1998; see Fig. 3.1). The investigated area includes the upper, lower and middle intertidal zones. Different mat types were identified across the investigated intertidal area when moving landwards from the waterline. The tidal position, salinity at sampling, the distribution of the dominant cyanobacteria, and a description of surface structure and water exposure are summarized in Table 3.1. The salinity of the overlying water ranged from 60 to 200 and was highest in the pond covering the Gelatinous mat. It was measured during low tide using a portable refractometer. The water temperature was 32°C. The oxygen penetration varied significantly in the mats from 3 to 4 mm at daytime and less than 0.5 mm in the dark (Abed et al., 2007), and the photosynthesis rates decreased from lower to higher intertidal mats (Abed et al., 2007). In the field, samples were stored on ice in a cooling box and transferred within a few hours to a deep freezer in the lab, where they were kept frozen till they were shipped to Germany.

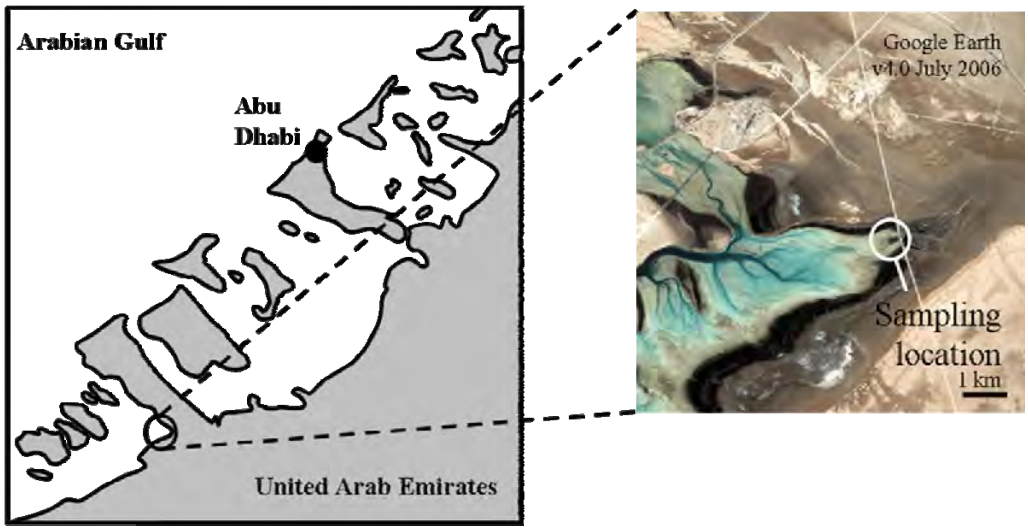

Fig. 3.1. Map showing the location (south-west corner of the Al Dhabaiya peninsula) of the studied microbial mats along the Arabian Gulf coast of Abu Dhabi and a satellite image of the sampling site.

The lower intertidal zone is dominated by mats that are almost always covered by water (Table 3.1, Reddish and Olive mats). They are smooth, leathery and typically

consist of a thin (ca. 3 mm) layer that is firmly attached to the sediment beneath. The middle intertidal area is dominated by two very different mat types, a flat mat that is periodically exposed to air but water logged and a pinnacle mat which covers well-drained elevated hills between pools, channel levees and their slopes. The flat mats have a pink-coloured and smooth surface (Table 3.1). The surfaces of the Pinnacle mat (Table 3.1) grew in the form of upwards-pointing cones (i.e. pinnacles) about 0.5 to 2 cm high. The surface of this mat is inhabited by cyanobacteria. Beneath this layer are a thin, often incomplete layer of purple sulphur bacteria and an equally faint black layer indicating a transient anoxic zone.

The pools and channels in the upper intertidal area are covered by finely laminated gelatinous mats (Table 3.1) which are always inundated. This type of mat has the most clearly visible lamination with each layer representing a distinct functional group of microorganisms. The mat surface is homogeneous, smooth, gelatinous and reddish in colour, although the original dark-red colour of the mat surface changed to green within minutes after sampling (see Abed et al., 2006, 2008). For detailed information concerning community structure and morphotypes of cyanobacteria the authors like to refer to the publications by Abed et al. (2007, 2008).

Table 3.1. Macroscopic characteristics, environmental settings at the time of sampling and dominant microorganisms of the studied mats (abbr. of dominant bacterial groups: *Alphap.* – *Alphaproteobacteria*, CFB – *Cytophaga*/*Flavobacteria*/*Bacteroidetes*, *Chlorofl.* – *Chloroflexus*, Cyanob. – Cyanobacteria; abbr. of dominant cyanobacteria: *A*.s. – *Aphanothece* sp., *E.m.* – *Entophysalis major*, *L.a.* – *Lyngbya aestuarii*, *L*.s. – *Leptolyngbya* sp., *M.c.* – *Microcoleus chthonoplastes*, *S.s.* – *Schizothrix splendida*, data from [a] from Abed et al., 2008, [b] Abed et al., 2007); n.d. – not determined

	Reddish	Olive	Pink	Pinnacle	Gelatinous
Intertidal position [a]	lower	lower	middle	middle	high
Salinity [a]	60	60	90	100	200
Dominant bacterial groups within 16S rRNA clone libraries[b]	62 % Cyanob. 20 % *Alphap.*	n.d.	53 % Cyanob. 35 % *Chlorofl.*	n.d.	53 % CFB 11 % *Alphap.*
Dominant cyanobacteria [a]	*E.m.*, *L.a.*, *L.*s., *M.c.*	*E.m.*, *L.a.*, *M.c.*	*E.m.*, *L.a.*	*L.a.*, *S.s.*	*A*.s., *E.m.*, *L.a.*, *M.c.*
Surface [a]	flat leathery smooth	flat smooth	smooth often covered with gypsum crystals	pinnacles	gelatinous, distinct lamination
Water exposure [a]	submerged	exposed	exposed	elevated	submerged
Desiccation [a]	→ I n c r e a s i n g →				

3.1.3.2 Gross composition

Total carbon (TC) and total sulphur (TS) contents were obtained from the lyophilised and ground samples using a CS-500 Analyser (Eltra GmbH). Nitrogen data

were measured using an EA1108-Elemental Analyser (Carlo Erba Instruments). Total inorganic carbon (TIC) was determined as carbonate using a CO_2-coloumeter 5012 (UIC incorporation). Total organic carbon (TOC) values were calculated as difference between TC and TIC.

Stable carbon isotopic analysis was performed on total organic extracts (see 2.3) by automated on-line combustion with a Carlo Erba CHNS 1108 elemental analyser coupled to a Finnigan MAT 252 isotope ratio mass spectrometer. The data are reported in the delta notation relative to the VPDB standard. All samples were measured in duplicate and values averaged.

3.1.3.3 Extraction

The uppermost centimetre of all mats and in addition the top layers of the Reddish and Gelatinous mats were extracted using a modified Bligh and Dyer method (Bligh and Dyer, 1959; White et al., 1979; Fang and Findlay, 1996). To the homogenised wet mat samples, a single-phase solvent mixture of methanol/dichloromethane/ammonium acetate buffer (pH 7.6, 2:1:0.8 v/v) was added and the suspension ultrasonicated. After centrifugation the supernatant was collected in a separatory funnel. The entire procedure was repeated ten times. Dichloromethane and distilled water were added to the combined extracts until a ratio of methanol/dichloromethane/ammonium acetate buffer of 1:1:0.9 (v/v) was obtained. The organic phase containing the extracted lipids was removed and the methanol-water phase washed three times with dichloromethane. The combined dichloromethane phases were evaporated to dryness and the residue stored at -20°C.

3.1.3.4 Separation of lipid classes

Lipid extracts were dissolved in 1 ml dichloromethane/methanol 9:1 (v/v) and separated by column chromatography according to the method of Zink and Mangelsdorf (2004). The resulting fractions – (1) neutral lipids, (2) free fatty acids, (3) glycolipids and (4) phospholipids – were evaporated to dryness and the residues stored at -20°C.

3.1.3.5 Derivatization

Aliquots of the free fatty acids were treated with N-methyl-N-trimethylsilyltrifluoroacetamid (MSTFA, 70°C, 2 h) to yield the corresponding trimethylsilyl esters. Aliquots of the phospholipid fractions were transesterified with trimethylsulfonium hydroxide as described by Müller et al. (1990) to yield the corresponding methyl esters.

3.1.3.6 Gas chromatography, gas chromatography-mass spectrometry

Samples were analysed on a Hewlett Packard Series 6890 gas chromatograph equipped with a flame ionization detector (FID). Gas chromatography-mass spectrometry (GC-MS) was performed with a Finnigan MAT SSQ 710B mass spectrometer (Finnigan-Thermoquest, San Jose, CA). Both gas chromatographs were equipped with a cold injection system (Gerstel KAS3 (GC-FID) or KAS4 (GC-MS), Gerstel, Mühlheim a. d. Ruhr, Germany) and a DB-5HT fused-silica column (30 m x 0.25 mm, 0.1 µm film thickness, J&W Scientific, USA). Helium was used as carrier gas (constant head pressure 12.5 psi). The temperature program was 60°C (1 min) to 350°C at 3°C/min (held 5 min). The FID was operated at 300°C. The hydrocarbons, trimethylsilyl esters and phospholipid fatty acid methyl esters obtained were identified by interpretation of their mass spectra or comparison with published spectra and/or from their relative retention times.

3.1.4 Results and discussion

3.1.4.1 Gross composition

Total carbon, total inorganic and organic carbon, total nitrogen and total sulphur data as well as the stable carbon isotope ratios of the total extractable organic matter of the five microbial mats and the top layers of the Reddish and the Gelatinous mat are displayed in Table 3.2. Total carbon (TC) contents vary from 6 to 14% showing the highest value for the top layer of the Reddish mat. There is a difference of 2.5% between the TC content of the total Reddish mat and that of the top layer. This difference can essentially be attributed to the difference in TOC content of these samples. The total organic carbon (TOC) values in the total mats range from 0.7% in the Pink mat to 2.4% in the Gelatinous mat, whereas they are considerably higher in both top layer samples (4.6% in the Reddish mat and 6.6% in the Gelatinous mat). The same range of TOC values were measured in a previous study of coastal microbial mats from Abu Dhabi by Kenig (1991).

The amounts of total inorganic carbon range from 8.6% to 9.6% in all samples except the Gelatinous mat, where 3.7% (total mat) and 6.4% (top layer) were determined. Nitrogen values range from 0.3 to 0.7% being highest in the top layer of the Reddish mat. The total sulphur content is particularly high only in the Gelatinous mat (3.4%) and consistent with the high pore water sulphide concentrations measured by Abed et al. (2006) as well as with the intense black colouration of the deeper mat section. All other samples contain less than 1% total sulphur.

Table 3.2. Gross composition of microbial mats: n.d. – not determined

	$\delta^{13}C$ (total extract, ‰)	TC (%)	TOC (%)	TIC (%)	TN (%)	TS (%)
Reddish	-14.3	11.2	1.9	9.2	0.45	0.44
Top Reddish	-11.8	13.7	4.6	9.1	0.69	0.64
Olive	-15.6	10.5	1	9.5	0.27	0.34
Pink	-14.1	9.4	0.7	8.6	0.31	0.29
Pinnacle	-15.9	10.7	1.1	9.6	0.35	0.39
Gelatinous	-16.7	6.2	2.4	3.7	0.33	3.4
Top Gelatinous	-10.5	13	6.6	6.4	n.d.	n.d.

The stable carbon isotope ratios of the total extractable organic matter range from -10.5 to -16.7‰, the heaviest values of -10.5 and -11.8‰ were found in the top layers of the Reddish and the Gelatinous mat, respectively. The Reddish and the Pink mat (-14.3 and -14.1‰) and the Olive and the Pinnacle mat (-15.6 and -15.9‰) resemble each other in their stable carbon isotope values. Remarkably high is the difference of 6.2‰ between the stable carbon isotope ratio of the total Gelatinous mat (–16.7‰, lightest value in the sample series) and its top layer. Heavy $\delta^{13}C_{TOC}$ values of up to -5‰ were reported before for microbial mats from hypersaline environments (e.g. Schidlowski et al., 1984; des Marais et al., 1989; Kenig et al., 1994). Kenig (1991) determined bulk $\delta^{13}C$ values of kerogen isolated from different types of microbial mats from different locations of the Abu Dhabi intertidal area of around -11.8 ± 1.3‰. Such heavy stable carbon isotope ratios for high-salinity microbial mats can be explained by environmental factors (e.g. reduced CO_2 solubility and precipitation) that limit the availability of CO_2 for photosynthesis (Schidlowski et al., 1984; Schidlowski, 1985; des Marais et al., 1989; Moers et al., 1993; Schouten et al., 2001). This results in an ineffective discrimination against ^{13}C commonly associated with photosynthesis due the enzymatic preference for $^{12}CO_2$ (e.g. Freeman and Hayes, 1992). Additional factors, however, appear to control the isotopic composition because microbial mats living at different salinities (as can also be seen in our samples) do not exhibit a consistent trend in their $\delta^{13}C$ values (des Marais et al., 1989; Schidlowski et al., 1994). It was suggested that the high productivity typically encountered in microbial mats is also responsible for the reduced carbon fractionation (Schouten et al., 2001). This hypothesis is consistent with the fact that both top layers of the Abu Dhabi microbial mats, which have the highest photosynthesis rates, are the most enriched ones in ^{13}C.

3.1.4.2 Lipid class composition

Specific community structures in the different microbial mats will lead to differences in the lipid biomarker distribution. The following sections will focus on major or indicative compounds within the fractions obtained by columns chromatography. A total of 83 aliphatic and alicyclic hydrocarbons were identified in the low-polar lipid fraction of the mat extracts comprising *n*-alkanes, *n*-alkenes as well as branched, isoprenoid, steroid and hopanoid hydrocarbons. Additionally, wax esters, sterols and hopanols as well as functionalised isoprenoids such as phytol and α-tocopherol were detected. The phospholipid fractions were analysed as methanolysis products. They yielded different distribution patterns of a total of 63 fatty acids. The free fatty acid fractions showed compositions similar to those of the PLFAs.

Table 3.3. Relative abundances (%) of compound classes among the total hydrocarbons

	Reddish	TOP Redd.	Olive	Pink	Pinnacle	Gelat.	TOP Gelat.
n-Alkanes	46.4	43.4	46.6	37.9	38.1	32.3	32.0
n-Alkenes	27.5	39.0	12.8	28.8	36.6	40.9	53.4
Isoprenoids and HBIs	16.3	12.6	22.4	20.7	8.1	16.6	9.9
Branched alkanes and alkenes	3.5	4.6	6.7	5.6	15.3	7.9	3.9
Sterenes	1.5	n.d	1.8	2.2	0.2	0.8	0.05
Hopanes and hopenes	4.8	0.5	9.7	4.9	1.8	1.4	0.7

3.1.4.3 Alkanes and alkenes

The *n*-alkanes range from *n*-pentadecane to *n*-tritriacontane (Fig. 3.2). They account for 32% (top layer of the Gelatinous mat) to 47% (Olive mat) of total hydrocarbons (Table 3.3). The dominant *n*-alkane in all mats is *n*-heptadecane, which has by far the highest concentration in the top layer of the Reddish mat (22 mg/g organic extract). The *n*-alkane distributions are bimodal in all mat extracts. *n*-Heptacosane and *n*-nonacosane are the dominant compounds among the long-chain *n*-alkanes. All *n*-alkane distributions exhibit an odd-over-even-predominance in the range from *n*-heneicosane (Reddish, Pink and Pinnacle mats), *n*-tricosane (Olive mat) or *n*-pentacosane (Gelatinous mat) to *n*-tritriacontane, respectively (Fig. 3.2). The amounts of the long-chain *n*-alkanes are relatively low with summed concentrations of 0.2 to 3.3 mg/g organic extracts. An exception is the Olive mat, in which nearly 50% of *n*-alkanes are long-chain homologues.

Short-chain monomethyl alkanes with 17 to 19 carbon atoms occur in all samples. Concentrations of summed monomethyl alkanes are presented in Fig. 3.2.

The Pinnacle mat contains the highest relative amount of monomethyl alkanes (12% of total hydrocarbons). In this mat 7- and 8-methylheptadecane represent 5.3% and 5.9% of total hydrocarbon, respectively.

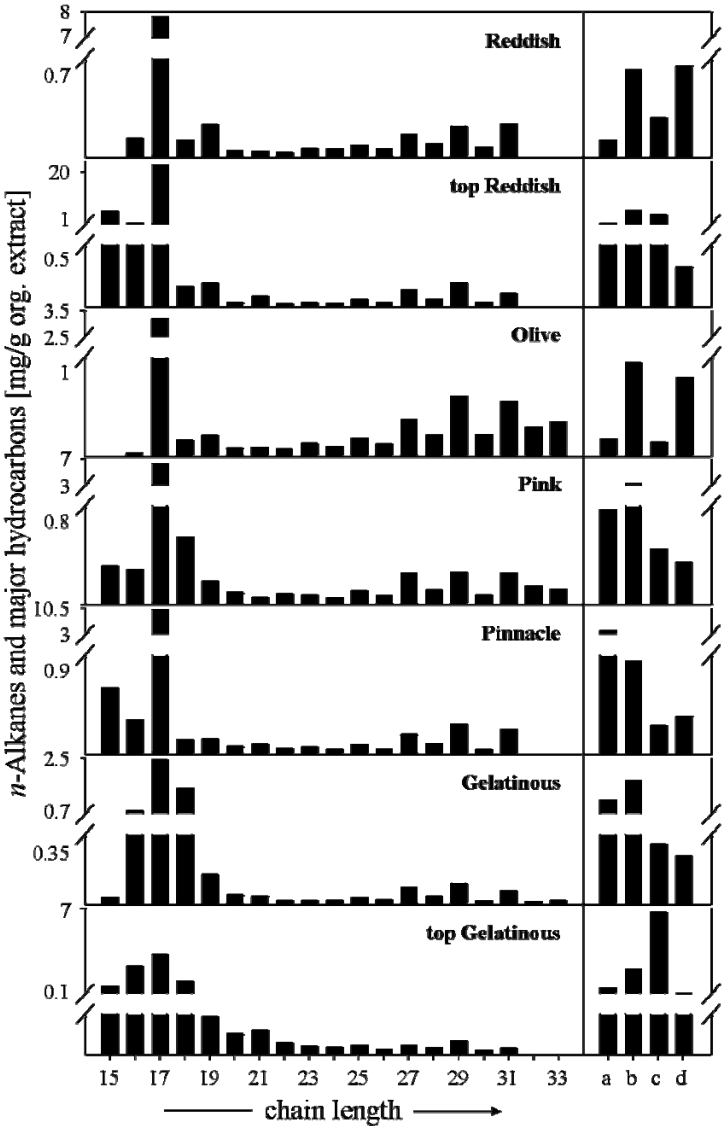

Fig. 3.2. Concentrations of *n*-alkanes and major hydrocarbons in the Abu Dhabi microbial mats: a – methyl alkanes (sum of all C_{17} – C_{19} isomers), b – phytenes (sum of all isomers), c – *n*-heneicosadiene, d – 17β,21β-hop-22(29)-ene.

A large variety of *n*-alkenes in the C_{17} to C_{27} range with one, two and three double bonds were detected in the Abu Dhabi microbial mats. In the range of 21 to 27 carbon atoms only *n*-alkenes with odd carbon numbers were identified. Total contents of *n*-alkenes amount from 12.8% in the Olive mat to 53.4% in the top layer of the Gelatinous mat. In the intact Gelatinous mat as well as in its top layer *n*-alkenes are the most abundant hydrocarbons due to the very high concentration of *n*-heneicosadiene (4.5 and 6.7 mg/g organic extract, respectively). Also in the top layer of the Reddish mat 4.5 mg *n*-heneicosadiene/g organic extract were detected, but

in this and in all other mat samples several isomers of *n*-heptadecene and *n*-octadecene are the major *n*-alkenes.

Overall, the high relative content of *n*-heptadecane (43 to 82% of total *n*-alkanes), the most abundant hydrocarbon detected in all microbial mats except the Gelatinous mat, signifies an abundance of cyanobacteria (cf. Gelpi et al., 1970; Murata und Nishida, 1987; Grimalt et al., 1992). The strong contribution of cyanobacteria to the hydrocarbon fraction is corroborated by large amounts of 7- and 8-methylheptadecane, which are specific cyanobacterial markers (Köster et al., 1999 and references therein). In the intact mats, the summed isomers of *n*-octadecene, also considered a useful biomarker for autochthonous input from photosynthetic microorganisms (Boon and de Leeuw, 1987; Grimalt et al., 1992), are also major hydrocarbons. Volkman et al. (1980) reported diatoms to be a source of *n*-alkenes with less than 20 carbon atoms and even carbon number predominance.

An enigma is the occurrence of *n*-heneicosadiene, which dominates the low-polar lipid fraction of the top layer of the Gelatinous mat. The high abundance in the top layer but its low significance in the intact Gelatinous mat suggests that this compound is biosynthesized by an aerobic organism. Even though the occurrence (in minor amounts) in microbial mats has been reported before (Edmunds and Eglinton, 1984; Boudou et al 1986; Dobson et al., 1988) the origin of *n*-heneicosadiene remains unclear.

3.1.4.4 Isoprenoids

The contents of isoprenoids including highly branched isoprenoids (HBIs) in the aliphatic hydrocarbon fractions range from 8.1% in the Pinnacle mat to 22.4% in the Olive mat. Several isomers of phytene, a phytadiene and phytane are the major isoprenoid hydrocarbons in the microbial mats. They account for 135 to 511 µg/g organic extract and are considered to derive from the microbial diagenetic degradation of phytol (Grossi et al., 1998 and references therein) including the anaerobic formation of phytadienes and phytenes by sulphate-reducing bacteria (Grossi et al., 1998). Phytol itself may derive from the hydrolysis of phytoplanktonic or cyanobacterial chlorophyll *a* as well as from bacteriochlorophyll *a* of certain purple sulphur bacteria (Marchand and Rontani, 2003). Both pigments were detected in all mats (Abed et al., 2008). The concentrations of chlorophyll *a* in the Pink, Pinnacle and Gelatinous mats were notably higher than those of bacteriochlorophyll *a* suggesting a higher relative contribution of phytol and the related hydrocarbons from cyanobacteria in these mats.

We also detected squalene with concentrations of up to 2.3 mg/g organic extract in the top layer of the Reddish mat. This, not phytol-related, isoprenoid is a precursor

of triterpenoids and has been reported before in cyanobacterial mats (Boon et al., 1983, Rontani and Volkman, 2005) and cultures (Gelpi et al., 1970).

Low amounts (< 0.5 mg/g organic extract) of several C_{30} HBIs with three to five degrees of unsaturation were detected in the Reddish, Pinnacle and Gelatinous mats. HBIs were reported to occur in a variety of recent and ancient sediments (reviewed by Rowland and Robson, 1990) and reflect the contribution of diatoms to primary production in microbial mats (Summons et al., 1993; Volkman et al., 1994; Belt et al., 2000). As the Reddish and the Gelatinous mat are submerged even during low tide the presence of benthic diatoms appears reasonable, and an association of cyanobacteria and diatoms is known from the oxygenic layers of microbial mats (Gerdes et al., 1993; Pearl and Pinckney, 1996).

Two vitamins – E (α-tocopherol) and K1 (phylloquinone) – were detected in the Abu Dhabi microbial mats. Both isoprenoids are constituents of the chloroplasts in photosynthetic organisms including higher plants. Cyanobacteria are the only prokaryotic microorganisms known to contain phylloquinone (Collins and Jones, 1981; Hiraishi, 1999). Based on comparison with the mass spectrum published by Rontani and Volkman (2005) the C_{21} isoprenoid γ-lactone 4,8,12,16-tetramethyl-4-olide was found to occur in the Pink mat and in the top layer of the Gelatinous mat. In a couple of recent publications, Rontani et al. (2007, 2008) demonstrated the production of γ-lactone from α-tocopherol via autoxidation mediated by aerobic marine bacteria.

3.1.4.5 Steroids and hopanoids

Sterenes with 27 to 29 carbon atoms occur as minor compounds (maximum concentration 0.5 mg/g organic extract in the Pink mat) in all analyzed mats except the top layer of the Gelatinous mat. The most abundant sterene, 5α-cholest-2-ene, was reported before to be present in microbial mats (Schouten et al., 2001; Hefter et al., 1993).

Fig. 3.3 shows a partial total ion current chromatogram with the sterol and hopanol distribution in the Pink mat, and a compilation of the concentrations of sterols and hopanols of all samples studied is displayed in Fig. 3.4. The top layer of the Reddish mat and the intact Gelatinous mat do not contain any sterols. In the Gelatinous mat they may still have been present at the trace level because they were detected in the top layer of this mat. Among the sterols, cholest-5-en-3β-ol and 5α-cholestanol as well as their 24-methyl and 24-ethyl analogues are the most abundant compounds with concentrations of 0.2 to 2 mg/g organic extract and the 24-methyl compounds always having the lowest concentrations.

Stanols and sterols with the same number of carbon atoms occur in all samples in more or less equal concentrations. The presence of high contents of stanols indicates microbial reduction of the corresponding sterols (Gaskell and Eglinton, 1975). 24-Ethylcholesterol is commonly associated with terrestrial higher plants (e.g. Huang and Meinschein, 1979), but as cyanobacteria were shown to contain C_{27}- and C_{29}-Δ^5 sterols in similarly high amounts (Volkman, 1986 and references therein), these organisms are most likely to be the major contributors also of C_{29} sterols to the mats. 24-Methylcholesterol is present in diatoms, dinoflagellates and green algae in moderate amounts (Volkman, 1986 and references therein), and among them diatoms are the most likely source in the case of the mats studied. Other sterols detected in the microbial mats comprise 24-methyl-cholesta-22-en-3β-ol, 24-ethyl-cholesta-22-en-3β-ol, 24-ethyl-cholesta-5,22-dien-3β-ol (most abundant in this suite and known as a major sterol in green algae; Volkman, 1986 and references therein) and 4-methyl-24-ethyl-cholesta-22-en-3β-ol. The overall sterol distribution does not suggest any significant amounts of terrestrial higher plant material transported to the tidal flats.

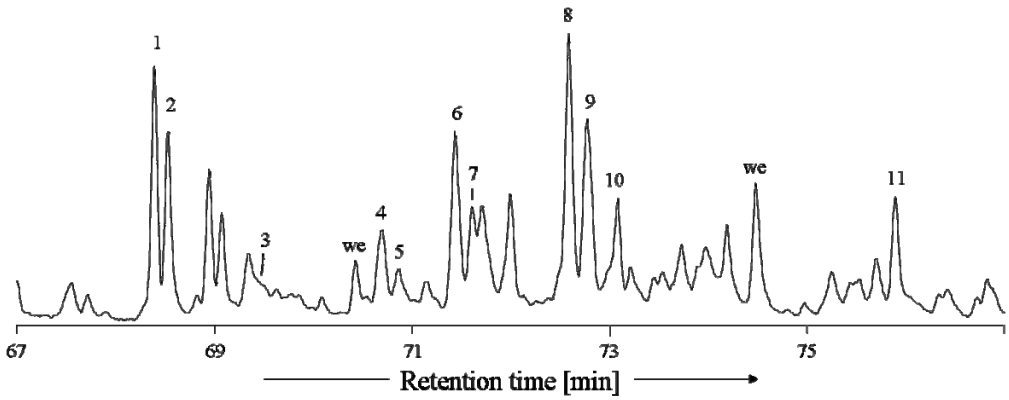

Fig. 3.3. Partial total ion current chromatogram of hydroxyl compounds in the Pink mat (see Table 3.4 for compound identification; we = wax ester).

Hopanes and hopenes have summed concentrations of 0.2 mg/g organic extract (top layer of and intact Gelatinous mat) to 1.5 mg/g organic extract (Olive mat). The top layers of the Gelatinous and the Reddish mat contain by far the lowest amounts of hopanoid hydrocarbons relative to total hydrocarbons (0.5 and 0.7%, respectively), whereas the Olive mat accounts for the highest relative abundance (9.7%). In general, 17β,21β-hop-22(29)-ene (diploptene) is the most abundant representative of this compound group, but in the Olive and Pink mats a unknown compound with a mass spectrum resembling a C_{28} pentacyclic triterpene (M^+ 384 [14%], 369 [7%], BP 191) contributes significantly. The absence of a significantly abundant m/z 163 fragment together with the long relative retention time

(> 17α-hopane) shows that this compound is not 28,30-*dinor*-hopane (Seifert et al., 1978).

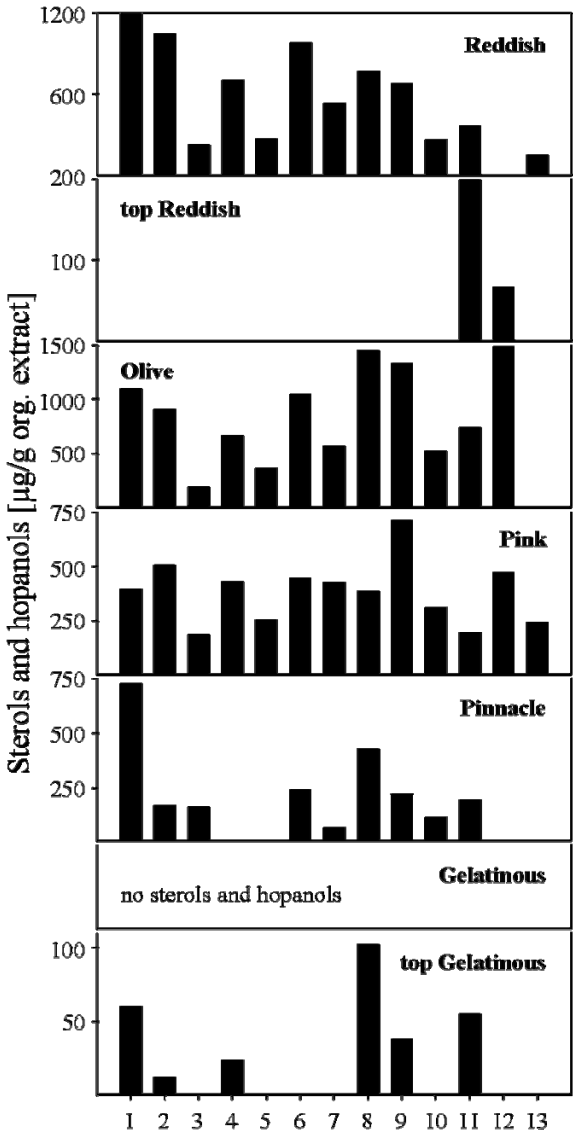

Fig. 3.4. Concentrations of sterols and hopanols in the microbial mats from Abu Dhabi (see Table 3.4 for compound identification).

As can be seen from Table 3.4 and Fig. 3.4, hopanols were also identified in the microbial mats. In the top layer of the Gelatinous mats as well as in the Pinnacle mat only 17β,21β-hopan-22-ol (diplopterol) occurs in low concentrations (<200 µg/g organic extract). The other mats in addition contain various amounts of 17α,21β-*homo*-hopanol and/or 17β,21β-*bishomo*-hopanol both of them having the hydroxy group in the side chain. In the extract of the intact Gelatinous mat none of these compounds are present above the detection limit, but a 17α,21β-*tetrakishomo*-hopanol was detected with a concentration of 113 µg/g organic extract. Hopanoids are of (aerobic) bacterial origin (e.g. Ourisson et al., 1979; Kannenberg and Poralla, 1999) and the compounds detected in our mats are considered degradation products of bacterial polyhydroxy hopanoids (Rohmer et al., 1984). The presence of diplopterol

and its dehydration product diploptene is probably mainly due to direct cyanobacterial input (Gelpi et al., 1970; Bird et al., 1971), because other cyanobacterial biomarkers are also present in significant amounts.

Table 3.4. Hydroxyl compounds annotated in Figs. 3.4 and 3.5

Annotation	Compound
1	Cholest-5-en-3β-ol
2	5α-Cholestan-3β-ol
3	24-Methylcholest-22-en-3β-ol
4	24-Methylcholest-5-en-3β-ol
5	24-Methylcholestan-3β-ol
6	24-Ethylcholesta-5,22-dien-3β-ol
7	24-Ethylcholest-22-en-3β-ol
8	24-Ethylcholest-5-en-3β-ol
9	24-Ethylcholestan-3β-ol
10	4-Methyl-24-dimethylcolest-22-en-3β-ol
11	17β.21β-Hopan-22-ol
12	17α.21β-*homo*-Hopanol
13	17β.21β-*bishomo*-Hopanol

3.1.4.6 Free fatty acids and phospholipid fatty acids

The results of the fatty acids analyses are presented as summed concentrations of compound groups. As it can be seen from the partial gas chromatograms of the free fatty acids and the methanolysis products of the phospholipids (PLFA; Fig. 3.5), the distribution patterns of both fractions strongly resemble each other. Free fatty acids, which account for only a minor portion of total acids in the microbial mats, can be released, e.g., from wax esters, triacylglycerols, glycolipids and phospholipids.

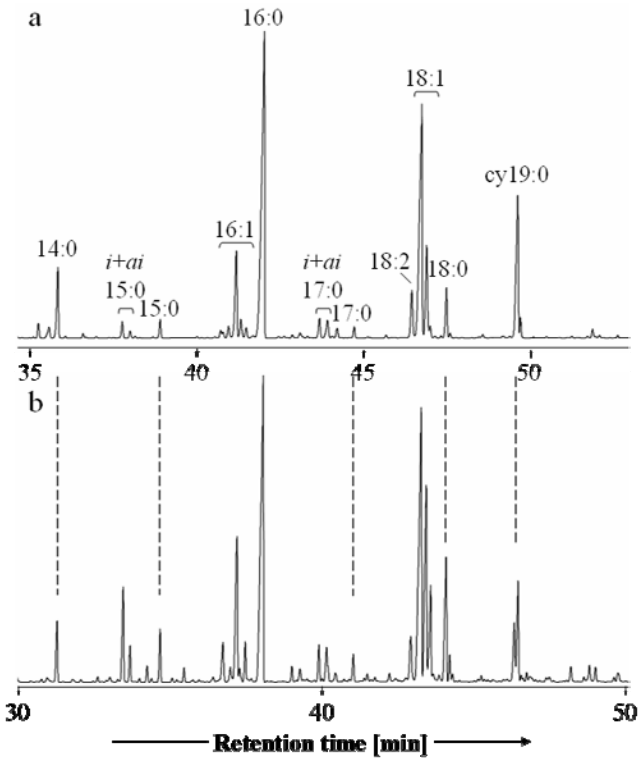

Fig. 3.5. Partial total ion current chromatograms of (a) TMS derivatives of the free fatty acids and (b) phospholipid fatty acid methyl esters from the top layer of the Gelatinous mat.

In the extracts of the top layer of the Reddish mat and the corresponding total mat as well as in the Olive and Pink mats we detected moderate amounts of low-molecular-weight (LMW) free fatty acids (C_9 to C_{14}), which are absent in the other samples. A preliminary version of the overall distribution of PLFAs in these mats in relation to the different adaptation of the mats to environmental stress such as salinity and desiccation was reported elsewhere (Abed et al., 2008). The gross PLFA composition is displayed in Fig. 3.6. This is based on a total of 63 fatty acids – saturated, branched, *cyclo*propyl, mono- and diunsaturated – in the range of C_9 to C_{28}, whereas only very low amounts of straight-chain fatty acids with more than 20 carbon atoms were detected. The amounts of summed PLFAs and major individual PLFAs, expressed as percentage of total PLFAs, are displayed in Table 3.5. The large number of different PLFAs in the different mats is related to the diversity of the microbial population, which comprises cyanobacteria, purple sulphur bacteria, sulphate-reducing bacteria and other aerobic and anaerobic heterotrophic bacteria (Abed et al., 2008). The most striking difference between the mat samples is the high amount of saturated fatty acids in the Gelatinous mat and the corresponding low relative proportion of monounsaturated acids. The Pink mat has a comparably small content of *cyclo*propyl fatty acids. On the compound-specific level *n*-hexadecanoic acid is the dominant fatty acid in all samples, followed by *n*-octadecanoic acid, two isomers of

cyclo-nonadecanoic acid and a number of isomeric mono-unsaturated fatty acids with 16 and 18 carbon atoms.

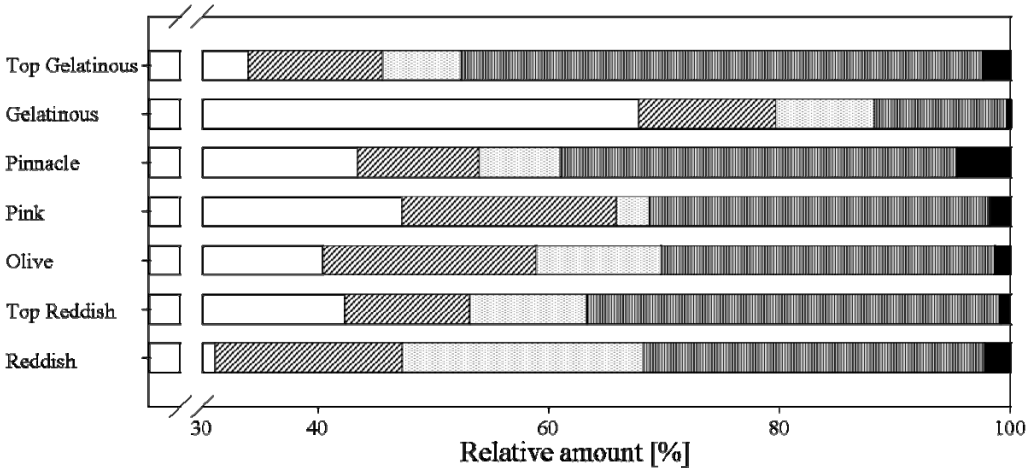

Fig. 3.6. Relative amounts of summed PLFA groups in the Abu Dhabi microbial mats: open bars – saturated fatty acids, hatched bars – branched saturated fatty acids, dotted bars – cyclic fatty acids, vertically lined bars – monounsaturated fatty acids, closed bars – polyunsaturated fatty acids.

Straight-chain fatty acids (SFA) were detected in the carbon number range of 9 to 24 with an expected preference of the even-carbon-numbered homologues and a predominance of the C_{14}, C_{16} and C_{18} compounds, only in the Pinnacle mat the SFAs extend up to 28 carbon atoms. *n*-Hexadecanoic acid is always the most abundant compound ranging from 18.9% relative abundance in the Pinnacle mat to 25.3% in the Reddish mat (Table 3.5; cf. also Abed et al., 2008). As *n*-hexadecanoic acid is ubiquitous in most organisms (Mancuso et al., 1990; Stoeck et al., 2002) it does not contribute significantly to the interpretation of microbial community variations among the mats. The *n*-octadecanoic acid is the second-most abundant PLFA in all mats, remarkably high is the amount of *n*-tetradecanoic acid, which accounts for 10.6% of total PLFA in the Gelatinous mat. Saturated straight-chain fatty acids in the range of C_{14} to C_{18} are considered typical constituents of microorganisms, but with differences in their distribution patterns (Findlay and Dobbs, 1993).

Branched saturated fatty acids (BSFA) contribute between 10.5% (Pinnacle mat) and 18.5% (Pink mat, Table 3.5) to the total PLFAs. They are indicative of bacterial biomass. In the compound group of BSFAs we differentiate between mid-chain and terminally branched fatty acids, in order to derive information on the contributing organisms. Except for the top layer of the Reddish mat, the terminally branched SFAs were more abundant than the mid-chain branched isomers in all samples. Terminally branched fatty acids have 15, 16, 17 and 19 carbon atoms. Among these, *i*-pentadecanoic acid is the predominant BSFA in all mat samples. Mid-chain branched saturated fatty acids with 13 to 18 carbon atoms were found mostly in low abundance. In the Reddish mat and its top layer a mid-chain methyl-branched

fatty acid dominates over the *iso* and *anteiso* fatty acids. The overall distribution of BSFAs indicates the presence of Gram-positive (*i*- and *ai*-pentadecanoic acid, *i*-hexadecanoic acid) and sulphate-reducing bacteria (*i*- and *ai*-pentadecanoic acid, 10-methylhexadecanoic acid) in the mats (cf. Grimalt et al., 1992; Findlay and Dobbs, 1993).

Significant amounts of *cyclo*propyl fatty acids with 17 (one isomer) and 19 (two isomers) carbon atoms found in the mats were reported to be major constituents in sulphate-reducing bacteria as well as other anaerobic bacteria (Volkman and Johns 1977; Findlay and Dobbs 1993; Stoeck et al., 2002; Mallet et al., 2004) as well as purple bacteria (Kaur et al., 2005). It is important to note, however, that in most bacteria the amount of *cyclo*propane fatty acids strongly depends on the growth conditions, and the level generally increases when growth rate decreases (e.g. Wang and Cronan, 1994; Grogan and Cronan, 1997; Zhang and Rock, 2008 for a review).

The amounts of monounsaturated fatty acids (MUFAs) range from 11.5% in the Gelatinous mat to 34.3% in the Pinnacle mat (Table 3.5). The major monounsaturated fatty acids are isomeric *n*-hexadecenoic and *n*-octadecenoic acids. In general, MUFAs with 14 to 22 carbon atoms were detected, some of them also contain methyl branches.

The only polyunsaturated fatty acids (PUFAs) in the mats are *n*-octadecadienoic acid, *n*-eicosadienoic acid (two isomers) and *n*-docosadienoic acid. The Pinnacle mat contains the highest amounts of PUFAs (4.7%). PLFAs with more than one degree of unsaturation are thought to be of eukaryotic origin. In recent years also cyanobacteria (Grimalt et al., 1992) and other groups of bacteria, such as *Alpha*- (Fuerst et al., 1993) and *Gammaproteobacteria* (Freese et al., 2008a), were found to contain PUFAs. Edmunds and Eglinton (1984) reported significant amounts of *n*-octadecadienoic acid throughout the upper 2 cm of a microbial mat.

PLFA interpretation is based on the premise that different microorganisms contain different phospholipids and ester-/ether-linked fatty acids (Lechevalier, 1977; White et al., 1979) and that, thus, the distribution of PLFAs is a parameter that can be applied to characterise and compare microbial communities (e.g. Stoeck et al., 2002; Mallet et al., 2004). The overall fatty acid distribution in the Abu Dhabi microbial mats reflects a predominantly bacterial origin. It does not provide more detailed information about the community structure as we combined different active layers of the mats in a single sample and did not detect any specific fatty acid as major compound. Additionally, one must be aware of the ability of microorganisms to adapt their membrane lipids in composition and content during different stages of their growth as well as to changes in environmental conditions (Potts et al., 1987; Denich et al., 2003; Mangelsdorf et al., 2005; Freese et al., 2008b; Zhang and Rock, 2008).

Thus, it is not possible yet to connect the PLFA profiles of the studied mats to specific organisms.

Table 3.5. Relative abundances (%) of the phospholipid fatty acid groups and major PLFAs (S: sum of all isomers)

	Reddish	Top Redd.	Olive	Pink	Pinnacle	Gelat.	Top Gelat.
Saturated *n*-fatty acids	31.1	42.4	40.5	47.3	43.4	67.8	34
n-Hexadecanoic acid	18.9	24.5	23.8	24.2	25.3	21.4	20.1
n-Octadecanoic acid	6.5	8	7.7	7.8	12	11.9	6.1
Branched saturated fatty acids	16.2	10.8	18.4	18.5	10.5	11.8	11.6
terminal	9.1	4.8	12.6	12.5	6.5	9.5	9.5
others	7.1	6.0	5.8	6.0	4.0	2.3	2.0
Cyclopropyl fatty acids	20.9	10.1	10.9	2.9	7.1	8.5	6.8
Monounsaturated fatty acids	29.5	35.8	28.9	29.4	34.3	11.5	45.2
16:1 (S)	5.7	9.0	8.2	6.5	10.3	2.7	9.5
18:1 (S)	20.8	25.8	19.2	21.0	21.7	8.0	33.5
Diunsaturated fatty acids	2.3	0.8	1.3	1.8	4.7	0.3	2.5

3.1.4.7 Evidence of contribution of selected groups of organisms

The major apolar lipids of the Abu Dhabi microbial mats reflect the major mat-building phototrophic microorganisms. *n*-Heptadecane and mid-chain branched monomethyl alkanes with 17 to 19 carbon atoms, which are major compounds in all mats, are indicative of cyanobacteria (Gelpi et al., 1970; Murata and Nishida, 1987; Shiea et al., 1990, 1991; Grimalt et al., 1992; Köster et al., 1999). Furthermore, the abundance of phytol and phytadiene in the mats appear to derive from chlorophyll *a* containing phototrophs (Cardoso et al., 1976, 1978).

Hop-22(29)-ene is an abundant alkene constituent of *Lyngbya aesturii* and occurs in mats populated by this cyanobacterium (Boudou et al., 1986). It is the dominant triterpene found in all analysed mats, where *Lyngbya aestuarii,* among others, is a dominant cyanobacterium (Table 3.1).

The major fatty acids obtained by methanolysis of the phospholipid fraction of the mat samples are saturated and unsaturated straight-chain compounds with 16 and 18 carbon atoms, which are common to many microorganisms (Mancuso et al., 1990; Stoeck et al., 2002). The overall fatty acid distribution investigated in our microbial mats predominantly reflects the bacterial population in the mats, but does not provide more detailed information about the community structure as we pooled the different active layers of the mats and did not detect any specific fatty acid indicative of a

particular layer as major compound. A few of the lipid biomarkers can be attributed to aerobic and anaerobic bacteria involved in metabolic processes within the mats. Such bacteria were found to produce mainly *i*- and *ai*-pentadecanoic and *i*- and *ai*-heptadecanoic acids (Findlay and Dobbs, 1993 and references therein). These fatty acids were among the phospholipid methanolysis products at concentrations secondary to the *n*-fatty acids which are thought to be mainly contributed by phototrophic organisms.

The terrigenous contribution to the upper part of all microbial mats from the intertidal flat is negligible. Only minor amounts of long-chain odd-carbon-numbered *n*-alkanes were found, and the detected sterols can not be unambiguously related to terrestrial plants (Volkman, 1986). PUFAs with more than two double bonds were not found.

The contents of wax esters, which are biomarker compounds for green non-sulphur-like bacteria (GNSLB) from the *Chloroflexus* group (e.g. Shiea et al., 1991; van der Meer et al., 2001), are very low with summed concentrations of 40 µg (Gelatinous mat) to 1.7 mg/g organic extracts (Olive mat). Another GNSLB biomarker, *n*-hentriacontatriene (van der Meer et al., 1999), was not detected in any of the microbial mats studied. It may, however, be possible that the *Chloroflexus* group organisms in the Abu Dhabi microbial mats produce different biomarker lipids, because they are not close relatives of *Chloroflexus auranticus* (Abed et al., 2007). Since attempts of cultivating these bacteria were not successful, their contribution remains unclear from the biogeochemical point of view. This result is also significant regarding the stable carbon isotope signature of the organic matter, as *Chloroflexus*-like bacteria are photosynthetic organisms which are known to have a carbon fixation pathway different from that of other organisms (e.g. van der Meer, 2003). This pathway leads to an increase in the carbon isotope ratio of the produced lipid compounds. Therefore, heavy stable carbon isotope ratios in microbial mats from an extreme environment are consistent with an organic matter contribution from *Chloroflexus*-like bacteria. As the biomarker evidence of *Chloroflexus*-like bacteria is lacking in our mats, the stable carbon isotope ratios of the total lipid extract may be an indication of a CO_2-limited ecosystem (Schouten et al., 2001).

3.1.4.8 Environmental effects on lipids distribution

Environmental conditions are known to influence the microbial composition of intertidal mats. It is also known that microorganisms are able to adapt their membrane structure in response to changes in environmental conditions such as temperature, pressure, pH, hydrological regime, nutrients and salinity as well as during stationary growth phases (Denich et al., 2003). In a previous publication (Abed et al., 2008)

salinity and desiccation tolerance as well as the corresponding adaptation of the mat-inhabiting microorganisms on the basis of pigment and PLFA composition in the Abu Dhabi microbial mats were demonstrated. In Fig. 3.7 three parameters are shown to visualise temperature adaption in membranes. With increasing temperature there is a simultaneous increase of the chain-length of SFAs (increase of the proportion of *n*-octadecane to *n*-hexadecane) and decrease of the proportion of MUFAs to SFAs (cf. Zeng et al., 1992a; Denich et al., 2003 and references therein). Even if the Pinnacle and Gelatinous mats inhabit the upper intertidal area, they will not be exposed to higher temperatures and therefore this may not be the only parameter affecting the ratios in Fig. 3.7. As the related changes in lipid composition tighten the membrane, they may also be stimulated by increasing salinity. This is corroborated by results obtained from a growth experiments with the cyanobacterium *Synechococcus* 6311 in the presence of NaCl by Huflejt et al. (1990). Part of the changes in the unsaturation level and length of the fatty acids may further be related to differences in community composition. For example, a high ratio of saturated to unsaturated fatty acids may be derived from a higher abundance of cyanobacteria.

The occurrence of γ-lactone in the mat samples can also be connected to high irradiance in the intertidal area of Abu Dhabi. γ-Lactone is an autooxidation product of α-tocopherol (Rontani et al., 2005, 2007, 2008), which is produced by all photosynthetic organisms.

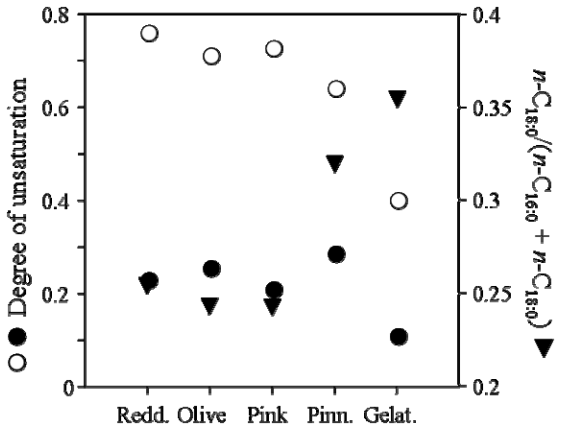

Fig. 3.7. Degree of unsaturation (unsaturated/(saturated + unsaturated) of fatty acid methyl esters; closed circles – *n*-C_{16} FAMEs, open circles – *n*-C_{18} FAMEs from methanolysis of intact phospholipids) and increasing chain-length of fatty acid methyl esters (*n*-octadecanoic acid/(*n*-hexadecanoic acid + *n*-octadecanoic acid)).

3.1.5 Conclusions

The lipid composition of the five microbial mats from Abu Dhabi is similar to that previously found in cyanobacterial mats (e.g. Boon et al., 1983; Cardoso et al., 1976, 1978; Philp et al., 1978; Kenig, 1991; Rontani and Volkman, 2005). The

extractable lipids reflect the complex biogeochemistry in the microbial mat communities as follows:

- The top layers of all mats are built by cyanobacteria as evident from the high amounts of *n*-heptadecane and several methyl-branched alkanes.
- The simultaneous occurrence of sterols with their corresponding stanols and steroid hydrocarbons as well as phytol and phytenes proves the partial biological degradation of selected compounds.
- Differences in the PLFA distributions can be linked to the environmental extremes and resulting changes in the lipid composition.
- The stable carbon isotope ratios of the total lipid extract appear to hint to a CO_2-limited ecosystem. This suggestion requires corroboration by compound-specific stable carbon isotope analysis, which would reveal possible producing organisms because the differences in CO_2 fixation which occur in autotrophic microorganisms lead to differences in the stable carbon isotope ratios in the produced compounds.

The additional comparison with the top layers of the Reddish and the Gelatinous mat revealed

- the "cyanobacterial signal" in the top layer of the Reddish mat exceeding that in the intact mat.
- a predominance of *n*-heneicosadiene in the top layer of the Gelatinous mat, which has not been reported before to this extent. The biological origin of this *n*-alkadiene remains unclear, except of the suggestion that it is derived from an aerobic organism.

From the differences that can be seen in the Reddish and the Gelatinous mats between the total mat and the top layer extracts the interest arises in follow-up analyses concentrating on the different layers of the microbial mats that can be distinguished. Especially the Gelatinous mat exhibits differently coloured thin layers of circa 1 mm thickness each.

3.2 Biogeochemistry of high-salinity microbial mats – Part 2: Vertical distribution of lipids in a microbial mat from Abu Dhabi, United Arab Emirates

Ann-Kathrin Scherf, Jürgen Rullkötter

Institute of Chemistry and Biology of the Marine Environment (ICBM), Carl von Ossietzky University of Oldenburg, P.O. Box 2503, D-26111 Oldenburg, Germany

3.2.1 Abstract

This study is a continuation of our work on microbial mats from the intertidal flats of Abu Dhabi, United Arab Emirates, with a focus on the top layers of the previously described Gelatinous mat. Laminated microbial ecosystems are often characterized by distinct horizontal, differently coloured cohesive layers, which can vary in thickness and in which the primary biological production is restricted to the upper few millimetres or centimetres. We analysed the lipid composition of the different layers of the finely laminated Gelatinous mat by gas chromatography and gas-chromatography-mass spectrometry. The depth profiles of the major lipids illustrate both the imprint of microbial populations and selective diagenetic transformation of specific lipids. The major lipid components of the Abu Dhabi microbial mat are typical of many bacteria. The individual layers of the Gelatinous mat appear to reflect the predicted distribution of microorganisms within the mat's vertical profile. *n*-Heptadecane, short-chain monomethylalkanes and major phospholipid fatty acids (PLFAs) are typical of mat-forming cyanobacteria. These show a maximum in the top 0 to 2 mm and decrease in concentration with depth. Beneath, sulphate-reducing bacteria contribute terminally branched PLFAs. In the deepest section sterols, hopanols and long-chain *n*-alkanes are accumulated.

3.2.2 Introduction

In a previous paper we compared the lipid compositions of a set of morphologically diverse microbial mats from different positions of the tidal flat in the sabkha region of Abu Dhabi, United Arab Emirates. Whereas the preceding investigations were performed on bulk mat samples, we concentrate here on the Gelatinous mat, which shows a distinct vertical lamination. The different colours in the thin layers of the upper part of the mat indicate the presence of several physiological groups of microorganisms (Stal, 1995).

The Gelatinous mat is inundated by highly saline water (Abed et al., 2006, 2007, 2008). In hypersaline ponds the elevated salinity excludes or limits the survival

of higher organisms (Revsbech et al., 1983; Cohen, 1989). Van Gemerden (1993) and several other authors described the predominating microbial communities throughout the vertical profile of microbial mats. Usually, the upper photic and aerobic zone is inhabited by cyanobacteria, aerobic heterotrophic bacteria and photosynthetic bacteria followed downwards by anaerobic heterotrophic bacteria. The mats are often established under extreme environmental conditions (Cohen, 1989), such as high temperature and high salinity like in the case of the mat examined in the present study.

The lipid composition of environmental samples can be used to define the microbial community structure (e.g. Philp et al., 1978; Zeng et al., 1992b; Rontani and Volkman, 2005). In the present study, the distribution of extractable non-volatile lipids (e.g. hydrocarbons, sterols, hopanols and methanolysis products of intact polar lipids) was examined to compare both the vertical distributions of specific lipids with respect to their biological origin and the degradation of selected compound classes.

3.2.3 Materials and Methods

3.2.3.1 Site, sample and layer description

The Gelatinous mat was collected in December 2004 from the intertidal flat of Abu Dhabi (Arabian Gulf coast, United Arab Emirates) during low tide. The sampling site is located on the west coast of the Al Dhabaiya peninsula (also Zubaiya (e.g. Whittle et al., 1998), depending on transcription) (see Fig. 3.7). The intertidal area harbours a variety of microbial mats (Abed et al., 2008). The Gelatinous mat occurs in a little pond in the upper intertidal zone. It is always inundated by highly saline water. The salinity was 200 at the time of sampling. In the field, the collected mat samples were stored on ice in a cool box and transferred within a few hours to a deep-freezer in the laboratory, where they were kept frozen until they were shipped to the Institute of Chemistry and Biology of the Marine Environment, Oldenburg, Germany. In the home laboratory the mat was sliced according to visible distinction.

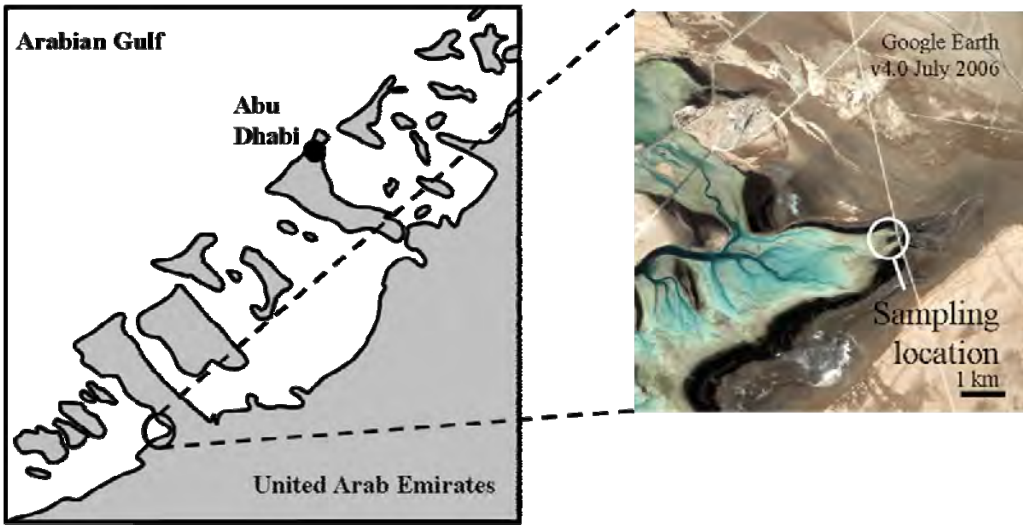

Fig. 3.7. Map showing the location (south-west corner of the Al Dhabaiya peninsula) of the studied microbial mats along the Arabian Gulf coast of Abu Dhabi and a satellite image of the sampling site.

The Gelatinous mat shows a distinct lamination, which is macroscopically visible (Fig. 3.8). Each layer probably represents a specific functional group of microorganisms. The surface layers as well as layers 2 to 4 each comprise more or less 1 mm in thickness. The fifth layer (ca. 3 mm) is slightly thicker than the others. Underneath, lamination continues, but because this zone is deeper than the observed bacterial activity, we collected this horizon as a single sample of ca. 3 mm thickness. Oxygen penetration extends down to 3.4 mm during light penetration and to less than 0.4 mm in the dark (Abed et al., 2007). The volumetric light oxygen consumption exceeds the gross photosynthesis below 3 mm. Below 3.375 mm Abed et al. (2007) did not measure any photosynthesis.

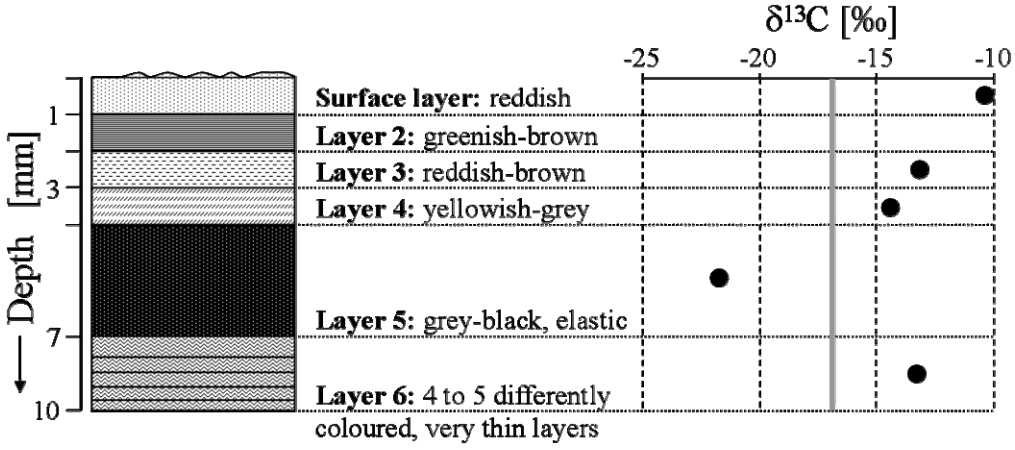

Fig. 3.8. Simplified vertical profile of the Gelatinous mat with stable carbon isotope ratios of the total extractable organic carbon (grey line indicates the $\delta^{13}C$ value of the intact mat; $\delta^{13}C$ values of the surface layer and the intact mat from Scherf and Rullkötter, in prep.).

The mat surface was homogenous, smooth, gelatinous and reddish in colour. The original dark-red colour of the mat surface changed to green within minutes after

sampling (Abed et al., 2006, 2008). The predominant bacterial group revealed by 16S rRNA cloning of the active zone of the Gelatinous mat is the CFB group (*Cytophaga*/*Flavobacteria*/*Bacteroidetes*) with more than 50% of total clones. 45% of those form two clusters related to the species of *Salinibacter ruber* (Abed et al., 2007). A total of ten different morphotypes of cyanobacteria were determined. The dominant taxons are *Microcoleus chtonoplastes*, *Lyngbya aestuarii*, *Entophysalis major* and *Aphanothece sp.* (Abed et al., 2008). For more detailed information concerning the community composition the authors refer to Abed et al. (2007, 2008).

3.2.3.2 Extraction

For extraction of the six layers of the Gelatinous mat a modified Bligh and Dyer method was used (Bligh and Dyer, 1959; White et al. 1979; Fang and Findlay 1996). To the homogenised mat samples, a single-phase solvent mixture of methanol/dichloromethane/ammonium acetate buffer (pH 7.6), 2:1:0.8 (v/v) was added and the mixture ultrasonicated. After centrifugation the supernatants were collected in a separatory funnel. This procedure was repeated ten times. Dichloromethane and distilled water were added to the combined extracts until a ratio of methanol/dichloromethane/ammonium acetate buffer of 1:1:0.9 (by volume) was obtained. The organic phase containing the extracted lipids was separated, removed and the methanol-water phase washed three more times with dichloromethane. The pooled dichloromethane phases were evaporated to dryness and stored at -20°C.

3.2.3.3 Stable carbon isotope analysis of total organic extracts

Stable carbon isotopic ratios of total organic extracts were determined by automated on-line combustion with a Carlo Erba CHNS 1108 elemental analyser coupled to a Finnigan MAT 252 isotope mass spectrometer. The data are reported in the delta notation relative to the VPDB standard. All values were measured as duplicates and averaged.

3.2.3.4 Separation of lipid classes

Lipid extracts were dissolved in 1 ml dichloromethane/methanol 9:1 (by volume) and then chromatographically separated according to Zink and Mangelsdorf (2004). The chromatography yielded four fractions: (1) neutral lipids, (2) free fatty acids, (3) glycolipids and (4) phospholipids. All fractions were evaporated to dryness and stored at -20°C.

3.2.3.5 Derivatization

Aliquots of the phospholipid fractions were transesterified with trimethylsulfonium hydroxide as described by Müller et al. (1990) to yield methyl esters.

3.2.3.6 Gas chromatography, gas chromatography-mass spectrometry

Samples were analysed on a Hewlett Packard 6890 Series gas chromatograph equipped with a flame ionization detector (FID). Gas chromatography-mass spectrometry (GC-MS) was performed with a Finnigan MAT SSQ 710B mass spectrometer (Finnigan-Thermoquest, San Jose, CA). Both gas chromatographs were equipped with a cold injection system (Gerstel KAS3 (GC-FID) or KAS4 (GC-MS), Gerstel, Mühlheim a. d. Ruhr, Germany) and a DB-5HT column (30 m x 0.25 mm, 0.1 µm film thickness, J&W Scientific, USA). Helium was used as carrier gas (constant head pressure 12.5 psi). The temperature program was: 60°C (1 min) to 350°C at 3°C/min (held 5 min). The FID was operated at 300°C. Hydrocarbons and phospholipid fatty acid methyl esters were identified by interpretation of their mass spectra or comparison with published spectra and/or from their relative retention times.

3.2.4 Results and discussion

3.2.4.1 Stable carbon isotope ratios of total lipid extracts

The stable carbon isotope ratios differ strongly throughout the depth profile of the Gelatinous mat (Fig. 3.8). The surface layer is most enriched in ^{13}C (-10.5‰). The $\delta^{13}C$ values of layers 3, 4 and 6 are more or less uniform ranging from -14.5 to -13.3‰. Layer 5 has a $\delta^{13}C$ value of -21.9‰ and, thus, is most depleted in ^{13}C. Suggestions for a specific biological source of the lipids will be made in context with their vertical molecular profiles.

3.2.4.2 Alkanes and alkenes

The *n*-alkanes range from *n*-pentadecane to *n*-tritriacontane (Fig. 3.9, Table 3.7). They account for 15.4% (layer 6) to 32% (surface layer) of total hydrocarbons (Table 3.6), and their proportion decreases with depth. The distribution of *n*-alkanes is displayed in Fig. 3.9. In the surface layer as well as in layers 5 and 6 *n*-heptadecane is the dominant *n*-alkane, whereas in the other three layers *n*-octadecane is slightly more abundant. The maximum concentration of *n*-heptadecane is 3.3 mg/g organic extract in the surface layer. The *n*-alkanes show a bimodal distribution with the *n*-alkanes with less than 21 carbon atoms clearly

dominating. The higher homologues exhibit an odd-over-even carbon number predominance with *n*-nonacosane as the dominant compound. The summed concentrations of the long-chain *n*-alkanes increase with increasing depth through the mat from 0.2 to 0.8 mg/g organic extract.

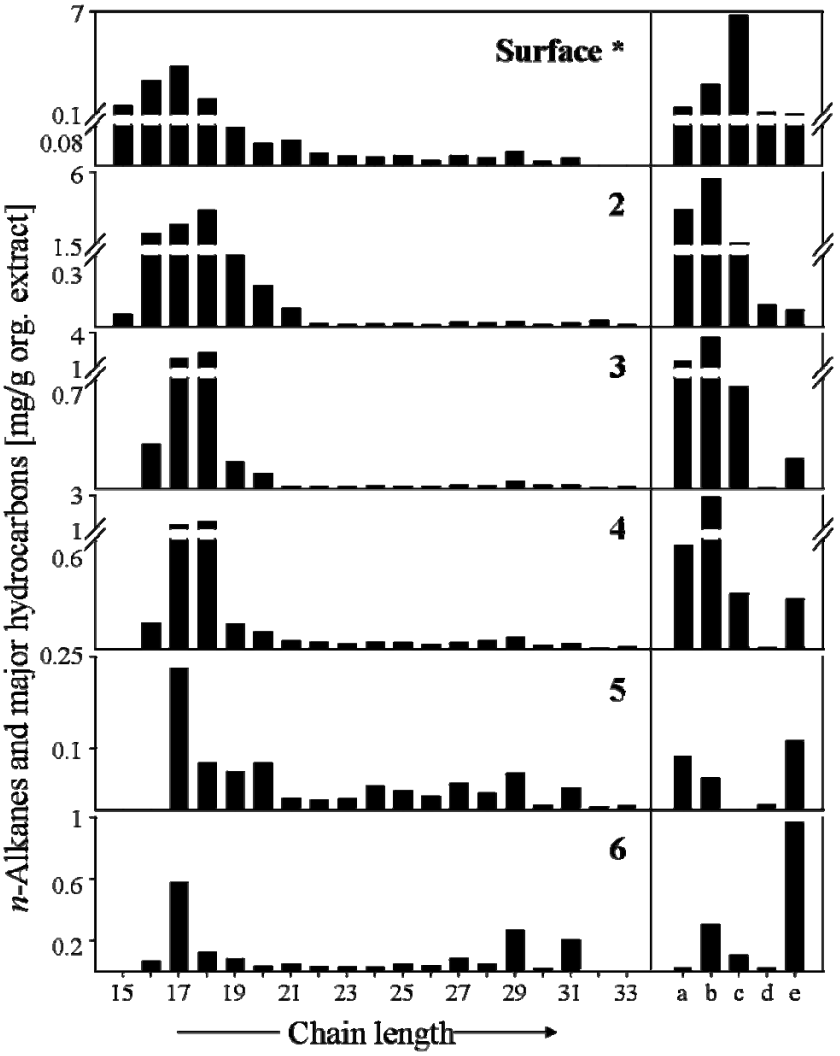

Fig. 3.9. Concentrations of *n*-alkanes and major hydrocarbons: a - *n*-$C_{17:1}$-alkene (sum of all isomers), b – *n*-$C_{18:1}$-alkene (sum of all isomers), c – phytenes (sum of all isomers), d - 5α-cholest-5-ene, e - 17β,21β-hop-22(29)-ene, * from Scherf and Rullkötter, in prep.

Table 3.6. Relative abundances of compound classes in total hydrocarbon fractions

	Surface layer	Layer 2	Layer 3	Layer 4	Layer 5	Layer 6
n-Alkanes	32	29.6	28.5	26.2	23.8	15.4
n-Alkenes	53.4	34.9	25.5	21.8	57.2	5.9
Isoprenoids and HBIs	9.9	18.8	27.9	37.9	11.9	16.9
Branched and alicyclic alkanes and alkenes	3.9	16.5	15.4	9.5	2.7	3.2
Sterenes	0.05	0.03	0.9	1.8	0.3	10.3
Hopanes and hopenes	0.7	0.2	1.7	2.8	4.0	48.4

Table 3.7. Concentrations of *n*-alkanes in µg/g organic extract: n.d. - not determined

	Surface layer	Layer 2	Layer 3	Layer 4	Layer 5	Layer 6
n-pentadecane	650	52	n.d.	n.d.	n.d.	n.d.
n-hexadecane	2308	2166	280	143	n.d.	62
n-heptadecane	3260	2737	1741	1250	230	576
n-octadecane	1104	3607	2291	1437	77	123
n-nonadecane	74	298	168	138	62	82
n-eicosane	42	170	95	91	77	31
n-heneicosane	48	75	14	42	19	45
n-docosane	24	12	14	36	16	29
n-tricosane	18	9	12	26	18	27
n-tetracosane	15	11	22	36	39	24
n-pentacosane	18	12	17	33	31	46
n-hexacosane	10	8	15	23	22	34
n-heptacosane	18	17	25	33	43	85
n-octacosane	14	14	23	43	28	46
n-nonacosane	27	21	48	64	60	267
n-triacontane	8.1	8.5	25	21	8	19
n-heneitriacontane	14	15	28	29	36	202
n-dotriacontane	n.d.	24	8.6	4.8	4.6	n.d.
n-tritriacontane	n.d.	8.7	13	12	7.1	n.d.

Short-chain monomethylalkanes with 17 to 19 carbon atoms occur in all samples. Concentrations of summed monomethylalkanes versus depth are presented in Fig. 3.11a. Between layer 2 and the bottom of the mat they decrease from 3.7 mg/g to 20 µg/g organic extract. The concentration in the surface layer (0.5 mg/g organic extract) is similar to that in layer 4. In the upper four layers 10-methylhexadecane is the dominant monomethylalkane.

A high variety of *n*-alkenes with 17 to 20 carbon atoms and one, two and three double bonds were identified in the different layers of the Gelatinous mat. In the range of 21 to 27 carbon atoms only *n*-alkenes with odd carbon numbers were detected. The concentrations of summed *n*-alkenes decrease from layer 2 downwards from 16.8 to 1.8 mg/g organic extract. The concentration in the surface layer is 15.5 mg/g organic extract. The relative amounts within the hydrocarbon fraction decrease from the surface layer with increasing depth except for a high value of 57.2% in layer 5. In the surface layer *n*-heneicosadiene is the most abundant hydrocarbon with 6.7 mg/g organic extract. In the deeper layers combined isomeric *n*-heptadecenes and *n*-octadecenes are the major *n*-alkenes.

In summary, short-chain compounds with less than 21 carbon atoms dominate the distributions of alkanes and alkenes. *n*-Heptadecane, which is indicative for a

cyanobacterial contribution (e.g. Gelpi et al., 1970; Murata und Nishida, 1987; Grimalt et al., 1992), has the highest concentration in the surface layer and decreases in abundance with depth. Interestingly, *n*-octadecane is more abundant in layers 2 to 4. High concentrations of *n*-octadecane may be attributed to marine bacteria (Nishimura and Baker, 1986) but were also found in cyanobacteria which were exposed to high irradiance for several hours (Walsh et al., 1998). The longer-chain homologues show an odd-over-even carbon number predominance, which suggests a terrestrial plant origin (Eglinton and Hamilton, 1967). They are present in the upper layers, but due to their slightly higher resistance towards degradation their content increases with depth.

3.2.4.3 Isoprenoids

The amounts of isoprenoids including highly branched isoprenoids (HBIs) among the hydrocarbons range from 9.9% in the surface layer to 37.9% in layer 4 (Table 3.6). Several isomers of phytene, a phytadiene and phytane are the major isoprenoids in the microbial mat. A depth profile of summed concentrations of isomeric phytenes in Fig. 3.11a reveals that the highest concentration of 5.6 mg/g organic extract occurs in layer 2. The presence of isomeric phytenes is usually due to degradation of phytol by sulphate-reducing bacteria (Grossi et al., 1998 and references therein). Phytol was detected in all layers, decreasing in abundance very fast with increasing depth (Fig. 3.11b). Phytol can arise from the hydrolysis of chlorophyll *a* of phytoplankton and cyanobacteria as well as from that of bacteriochlorophyll *a* which is a cell component of certain purple sulphur and other phototrophic bacteria (Marchand and Rontani, 2003). As the phytene concentrations also decrease from layer 2 downwards, their turnover appears to be very rapid in the Abu Dhabi mat.

The ubiquitously occurring C_{30} isoprenoid squalene was detected in all layers throughout the mat profile in various amounts ranging from 0.1 mg/g to a maximum of 1.2 mg/g organic extract in layer 4. The occurrence of this isoprenoid, a precursor of pentacyclic triterpenoids, was reported before for cyanobacterial mats (Boon et al., 1983, Rontani and Volkman, 2005) and cultures (Gelpi et al., 1970).

A set of C_{30} HBIs with three to five double bonds were detected in all layers of the Gelatinous mat. The summed concentration increases from the surface layer (64 µg/g) to layer 4 (0.9 mg/g organic extract), then decreases in layer 5 to more or less the concentration at the top and increases again further down. As HBIs were reported to occur in a variety of recent and ancient sediments (reviewed by Rowland and Robson, 1990) and attributed to an origin from diatoms (Summons et al., 1993; Volkman et al., 1994; Belt et al., 2000), it is surprising at first that their concentration increases with depth, but they may have been bound or functionalized and released only by diagenetic transformation. On the other hand, concentrations of diatom

markers in previous studies were found to depend on seasonality (Edmunds and Eglinton, 1984).

In the first part of this publication we reported the occurrence of two vitamins in the microbial mats – E (α-tocopherol) and K1 (phylloquinone). In the context of the vertical distribution of lipids only phylloquinone is of interest, because α-tocopherol was only detected in the surface layer. The depth profile of phylloquinone is similar to the profiles of *n*-octadecane and short-chain monomethylalkanes. The concentrations range from 2 µg/g organic extract (layer 5) to 211 µg/g organic extract (layer 2). In layer 6 it was not detected. Phylloquinone is a constituent of the chloroplasts in photosynthetic organisms and higher plants, whereas cyanobacteria are the only microorganisms found to contain phylloquinone (Collins and Jones, 1981, Hiraishi, 1999).

A single isoprenoid thiophene with 20 carbon atoms was detected in layers 2, 3, 4 and 6. In layers 2 to 4 it shows a slight increase with increasing depth from 11 to 17 µg/g organic extract. Several authors (e.g. Sinninghe Damsté, 1987; Kenig et al., 1995; Barakat and Rullkötter, 1997) reported its occurrence in the past as a reaction product of inorganic sulphur species with phytol, phytenes or phytadiene. As the total sulphide concentration increases with depth (Abed et al., 2006) the absence of the isoprenoid thiophene in layer 5 is surprising. A possible explanation may be a concentration below the detection limit as all extractable organic compounds occurred at very low concentrations in this layer.

3.2.4.4 Steroids and hopanoids

Sterenes with 27 to 29 carbon atoms occur in layers 3, 4 and 6 of the Gelatinous mat. They amount to 146, 232 and 1143 µg/g organic extract, respectively. In layers 3 and 4 24-ethyl-5α-cholest-2-ene and in layer 6 5α-cholest-2-ene are the dominant sterenes, respectively. It is not surprising that the sterenes are absent from the two top layers, as they are diagenetic products derived from the corresponding stanols (Rubinstein et al., 1975). In layer 6 4-methyl-24-ethylcholestane was detected as the second-most abundant compound with 252 µg/g organic extract (Table 3.8). It should be a transformation product of 4-methyl-24-ethylcholesta-22-en-3β-ol, but we failed to detect this sterol both in the intact mat (Scherf and Rullkötter, in prep.) and in any of the layers of the sectioned mat. It may have been incorporated into the mat some time ago (see hereafter) and completely reduced to the saturated hydrocarbon.

Table 3.8. Concentrations of hydroxy compounds in µg/g organic extract: n.d. – not determined

	Surface layer	Layer 2	Layer 3	Layer 4	Layer 5	Layer 6
Phytol	234	92	7	8	9	20
Cholest-5-en-3β-ol	59	5	n.d.	n.d.	n.d.	239
5α-Cholestan-3β-ol	11	n.d.	n.d.	n.d.	n.d.	574
24-Me-cholest-5-en-3β-ol	23	8	n.d.	n.d.	n.d.	292
24-Me-cholestan-3β-ol	n.d.	n.d.	n.d.	n.d.	n.d.	493
24-Et-cholest-5-en-3β-ol	101	n.d.	n.d.	n.d.	n.d.	1017
24-Et-cholestan-3β-ol	37	n.d.	n.d.	n.d.	n.d.	1815
17β,21β-Hopan-22-ol	54	55	55	24	4	718
17α,21β-*homo*-Hopanol	n.d.	117	180	103	2	439
17β,21β-*bishomo*-Hopanol	n.d.	n.d.	n.d.	n.d.	n.d.	699
17α,21β-*tetrakishomo*-Hopanol	n.d.	37	367	345	44	776

In the first part of this study, we determined a variety of sterols and hopanols in the surface layer of the Gelatinous mat, but not in the intact mat. We interpreted this to be due to a very low overall concentration of the compound classes in the total lipid extract of the intact mat. Indeed, in the single layer analysis, apart from the surface layer, we found intact sterols only in layer 6 (Table 3.8) with similar distributions in both layers. Layer 6 contains C_{27} to C_{29} ster-5-en-3β-ols and the corresponding hydrogenated stanols. The concentrations range from 240 to 1815 µg/g organic extract, and both the C_{29} compounds (among the homologues) and the stanols (relative to sterols) clearly dominate. The C_{29} sterols may derive from terrestrial plants (Huang and Meinschein, 1979) or from the unicellular Xanthophyceae algae, which also show a predominance of 24-ethylcholest-5-en-3β-ol over cholest-5-en-3β-ol and no other steroidal compounds (Mercer et al., 1974). The predominance of the stanol over the precursor stenol is consistent with microbial reduction (Gaskell and Eglinton, 1975). It is hard to explain, why sterols were only found in the surface and the deepest layers, but not in the layers between. We suggest that growth of this mat was very slow and that layer 6 was deposited a long time ago and overgrown by a new microbial mat. The internal layering of layer 6 (Fig. 3.8) may indicate that it represents a fossil microbial mat unrelated to the present mat formed by the shallower layers. The fact that the amounts of stanols are almost twice those of the parent sterols may support this hypothesis.

In the case of the hopanols all layers except layer 6 contain low amounts (< 55µg/g organic extract) of 17β,21β-hopan-22-ol (diplopterol). In additional, a 17α,21β-C_{31} and a 17α,21β-C_{34} hopanol with the hydroxy group in the side chain were found. Both appear to be absent from the surface layer, but with 100 to 440 µg/g

organic extract are the dominant hopanoids in layers 2, 3 and 4. In layer 5 only traces of these compounds were detected. A 17β,21β-*bishomo*-hopanol (hydroxy group in the side chain) was detected in layer 6. In this layer, diplopterol as well as the other two hydroxy hopanoids appear to have accumulated, each amounting 440 to 720 µg/g organic extract. Although hopanols are known to be of bacterial origin (Ourisson et al., 1979, Kannenberg and Poralla, 1999), their concentration is highest in the deepest, probably inactive layer. This may be due to accumulation of diagenetic transformation products of bacteriohopanepolyols over time and due to the fact that hopanols are more stable towards degradation than most of the other lipids found in the microbial mat (Ourisson et al., 1987).

3.2.4.5 Phospholipid fatty acids

The methanolysis products of intact phospholipids from the layers of the Gelatinous mat yielded a total of 65 individual PLFAs - saturated, branched, *cyclo*propyl, mono- and diunsaturated - in the range of C_9 to C_{27}. The large number of different PLFAs indicates the diversity of bacterial populations within the layers of the Gelatinous mat. The relative amounts of grouped PLFAs are displayed in Fig. 3.10. The relative concentrations of these groups and major individual PLFAs, expressed as percentage of total PLFAs, are compiled in Table 3.9. Changes in the composition are obvious from the surface towards the deeper layers. In the surface layer the mono-unsaturated fatty acids dominate the PLFA profile with 45% of total PLFAs (cf. also Scherf and Rullkötter, in prep.). Second-most abundant are the saturated fatty acids (SFAs). The strong dominance of SFAs, which was observed in the total mat extract, was found in the sectioned mat only in layer 5. Although the relative content of SFAs is less than 44% in layers 2, 3, 4 and 6, it is the most abundant group of PLFAs. In layer 3 the branched saturated fatty acids (BSFAs) occur in amounts nearly equal to those of the SFAs, and in layer 6 the *cyclo*propyl fatty acids (CFAs) are second-most abundant. In total, layer 5 shows the strongest similarity with the total mat extract. The differences in the PLFA group composition will be further discussed below on the compound-specific level. In general, *n*-hexadecanoic acid, *n*-octadecanoic acid, two isomers of *n*-octadecenoic acid and two isomers of *cyclo*propyl nonadecanoic acid are the dominant compounds.

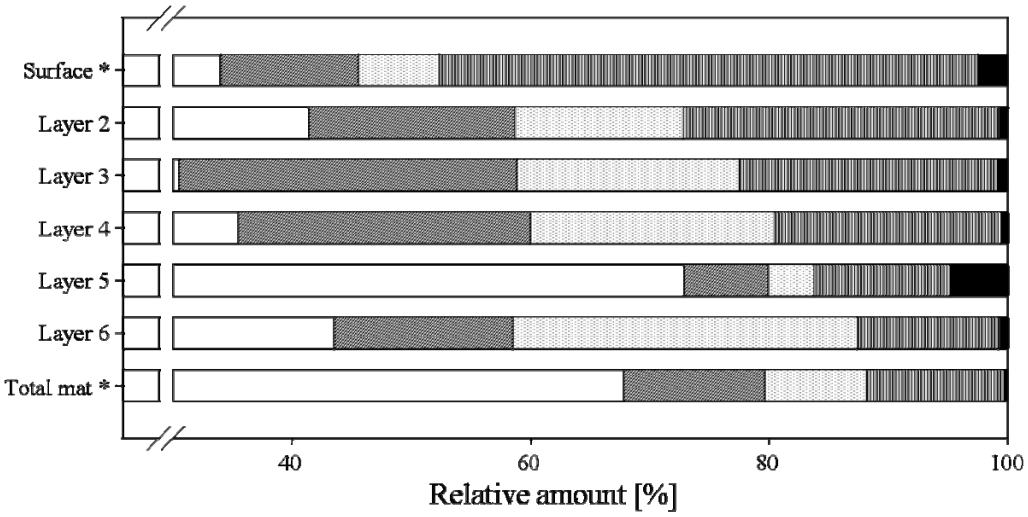

Fig. 3.10. Relative amounts of summed PLFA groups: open bars – saturated fatty acids, diagonally hatched bars – branched saturated fatty acids, dotted bars – cyclic fatty acids, vertically hatched bars – mono-unsaturated fatty acids, solid bars – poly-unsaturated fatty acids, * from Scherf and Rullkötter, in prep.

Straight-chain saturated fatty acids were detected in the range of 9 to 27 carbon atoms. The distribution is dominated by the even-carbon-numbered fatty acids with 14, 16 and 18 carbon atoms, and among these *n*-hexadecanoic acid is the most abundant homologue between the surface layer and layer 4. Layers 5 and 6 contain higher proportions of *n*-octadecanoic acid. *n*-Hexadecanoic acid is known to be ubiquitous in most organisms (Mancuso et al. 1990; Stoeck et al. 2002). So, it does not contribute significantly to the interpretation of the microbial communities over the vertical profile of the mat. In general, saturated straight-chain fatty acids with 14 to 18 carbon atoms are considered typical constituents of microorganisms (Findlay and Dobbs 1993).

A striking feature of the PLFA distributions is the high proportion of branched saturated fatty acids, which are indicative for bacterial contribution. BSFAs were found in amounts from 7% in layer 5 to 28.3% in layer 3. They mainly consist of terminally branched fatty acids (*iso* and *anteiso*) with 15, 16, 17 and 19 carbon atoms. *i*-Pentadecanoic acid dominates over the *anteiso* isomer, whereas *ai*-nonadecanoic acid is more abundant than the *iso* isomer in all layers. Findlay and Dobbs (1993) and Mallet et al. (2004) concluded from their analyses that *i*- and *ai*-pentadecanoic acids and *i*-hexadecanoic acid are characteristic of Gram-positive bacteria, whereas *i*- and *ai*-heptadecanoic acids indicate sulphate-reducing bacteria. Other methyl-branched fatty acids occur in all samples in insignificant relative abundance, except in layer 2, where they are present in amounts similar to those of the terminally branched isomers.

The amount of *cyclo*propyl fatty acids with 17 (one isomer) and 19 (two isomers) carbon atoms ranges between 3.8% (layer 5) and 28.8% (layer 6). CFAs with 17 or 19 carbon atoms have been reported as major constituents in sulphate-reducing

bacteria as well as other anaerobic bacteria (Volkman and Johns, 1977; Findlay and Dobbs 1993; Stoeck et al., 2002; Mallet et al., 2004) and purple bacteria (Grimalt et al, 1992). However, in most bacteria the amount of *cyclo*propane fatty acids strongly depends on the growth conditions, and the level generally increases when growth rate decreases (e.g. Wang et al., 1994; Grogan et al., 1997; Zhang and Rock, 2008 for review). In the surface layer and in layer 3 *cis*-9,10-methylene-octadecanoic acid is dominant with 4.1% and 12.2% of total PLFAs, respectively. In the other layers, *cis*-11,12-methylene octadecanoic acid is the most abundant CFA with 13.8% (layer 2) to 28.8% (layer 6).

The amounts of monounsaturated fatty acids (MUFAs) range from 11.4% in layer 5 to 45.2% in the surface layer. The major monounsaturated fatty acids are isomeric *n*-hexadecenoic and *n*-octadecenoic acids. Summed relative amounts of these MUFAs with 9.5% and 33.5% of total PLFAs, respectively, are highest in the surface layer. Their proportions decrease very fast with increasing depth (Fig. 3.11c).

The only polyunsaturated fatty acids (PUFAs) found in the studied mats were an *n*-octadecadienoic acid, and two *n*-eicosadienoic and *n*-docosadienoic acids each, respectively. The highest amounts of PUFAs were determined in the surface layer and in layer 5 with 2.5% and 4.8% of total PLFA, respectively. In the other layers the contents are less than 1%. *n*-Octadecadienoic acid is always the most abundant PUFA, below layer 3 it is the only one which was detected.

Table 3.9. Relative abundances of the phospholipid fatty groups and major PLFAs (S: sum of all isomers)

	Surface layer	**Layer 2**	**Layer 3**	**Layer 4**	**Layer 5**	**Layer 6**
Saturated fatty acids	34	41.4	30.6	35.5	72.9	43.5
n-hexadecanoic acid	20.1	22.4	14.7	16.3	25.9	14.1
n-octadecanoic acid	6.1	8.7	8.4	11.3	36.9	17.9
Branched saturated fatty acids	11.6	17.2	28.3	24.5	7	15
terminal	9.6	9.4	20.5	21.1	6.1	14
others	2	7.8	7.8	3.4	0.9	1
*Cyclo*propyl fatty acids	6.8	14.1	18.7	20.5	3.8	28.8
Monounsaturated fatty acids	45.2	26.5	21.7	19	11.4	11.9
16:1 (S)	9.5	2.3	2.5	1.9	2.2	1.2
18:1 (S)	33.5	19.8	14.5	13.9	7.5	8.3
Polyunsaturated fatty acids	2.5	0.7	0.8	0.6	4.8	0.7

The distribution of ester-linked phospholipid fatty acids (PLFA) is a parameter that can be applied to characterise and compare microbial communities (e.g. Stoeck et

al. 2002, Mallet et al. 2004). It is based on the premise that different microorganisms contain different phospholipids (White et al., 1979). But in the interpretation of the data caution should be exercised as changes in growth conditions can induce significant changes in composition and content of microbial phospholipids and the bound fatty acids (Denich et al., 2003, Zhang and Rock, 2008 for review). In addition, lipid pattern overlap can disturb the taxonomic correlation of individual community members when environmental samples are analysed (Fang et al., 2000).

3.2.4.6 Vertical distribution of lipids

Fig. 3.11a shows lipid biomarkers thought to be mainly contributed by aerobic phototrophic organisms. *n*-Heptadecane shows the highest value in the surface layer and then decreases with increasing depth. But the concentration is not significantly higher in the aerobic photic layers than in deeper layers, as would have been expected. The summed short-chain monomethylalkanes and summed isomeric *n*-heptadecenes and *n*-octadecenes show a vertical distribution different from that of *n*-heptadecane. The highest values were detected in layer 2. Towards greater depth the concentrations decrease. The summed phytenes show a similar vertical profile like the alkenes. Phytol is found in highest concentration in the surface layer (Fig. 3.11b). Its depth profile resembles that of *n*-heneicosadiene, the predominant hydrocarbon in the surface layer. Fig. 3.11a also shows the vertical profile of summed wax esters, which are only minor mat components. The highest concentration (130 µg/g organic extract) was found in the surface layer. In layer 2 the concentration is significantly lower, but it increases again in layer 3. From there on the concentration decreases downwards.

The relative amounts of long-chain *n*-alkanes among the hydrocarbons increase with increasing depth (Fig. 3.9). *n*-Nocasosane, the major long-chain *n*-alkane, which is indicative of terrestrial plants (Eglinton and Hamilton, 1967), shows a depth profile similar to that of 5α-cholest-2-ene (Fig. 3.11b). Also noteworthy is the correlation of the vertical distributions of diploptene, diplopterol and summed hopanols with those of 5α-cholest-2-ene and *n*-nonacosane.

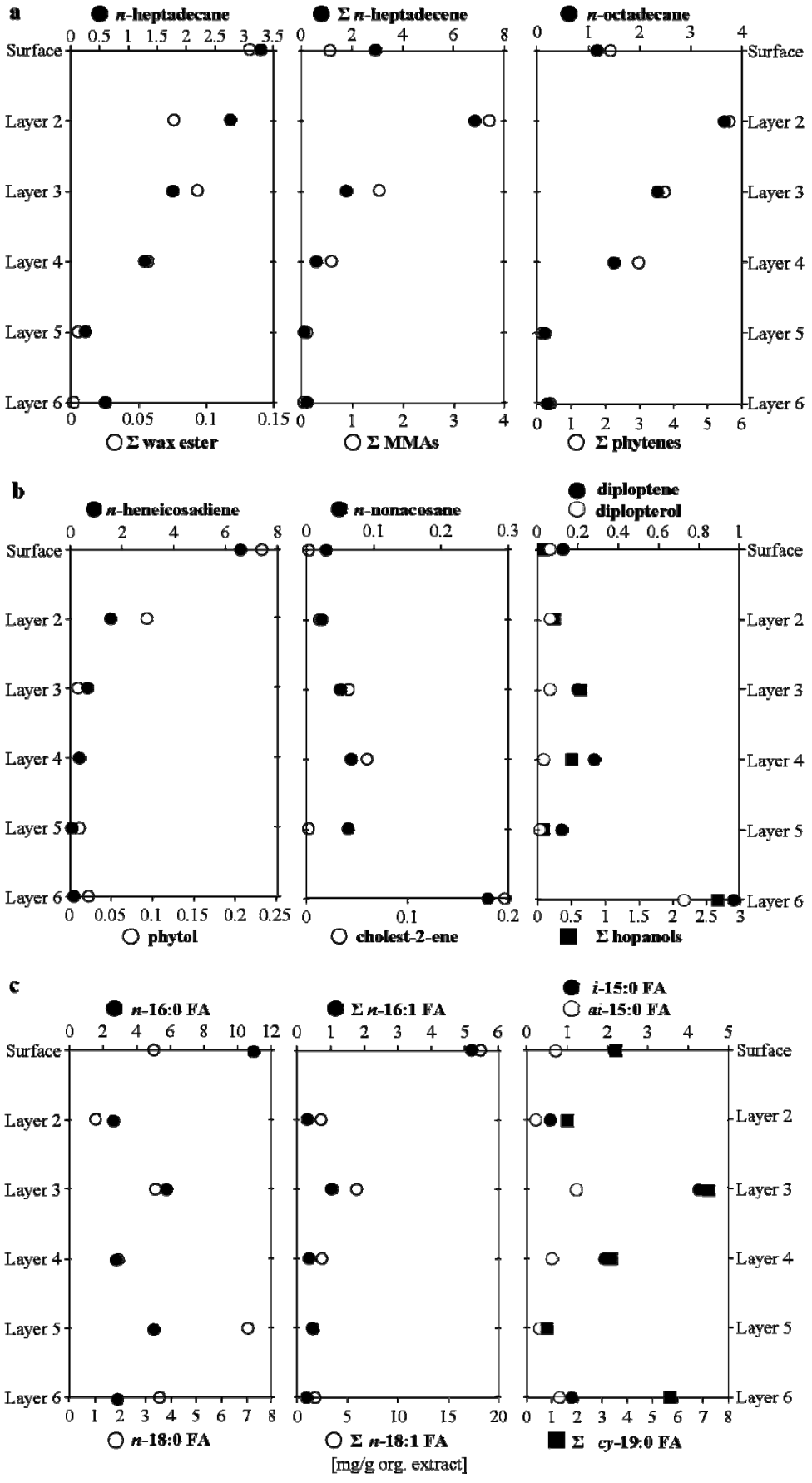

Fig. 3.11a-c. Vertical distribution of selected lipid biomarkers (concentrations in mg/g organic extract).

In Fig. 3.11c the vertical distributions of major PLFAs are displayed. *n*-Hexadecanoic acid and *n*-octadecanoic acid exhibit a scattered vertical distribution. They were found in all layers and exhibit the highest concentration in the surface layer and in layer 5, respectively. Summed concentrations of the isomeric *n*-hexadecenoic acids and *n*-octadecenoic acids have the highest concentrations in the surface layer. They decrease in layer 2 and slightly increase in layer 3 again. Most similarities can be found with the depth profile of the summed wax esters. The terminally branched saturated fatty acids (*i*- and *ai*-pentadecanoic acids) as well as the summed *cyclo*propyl nonadecanoic acids have their highest concentrations in layer 3.

3.2.4.7 Correlations of lipid biomarkers with the community and trophic structure in the mat

In general, the composition of the lipids reflects the microbial communities in the different layers. In the two uppermost layers the cyanobacterial signal is dominant. Analysis of cultured cyanobacteria showed that strains from aquatic environments typically contain high abundances of *n*-heptadecane and/or *n*-heptadecenes and short-chain monomethylalkanes (Han et al., 1968; Gelpi et al., 1970; Shiea et al., 1990; Grimalt et al., 1992). From these results it seems likely that the surface layer is inhabited by cyanobacteria that produce mainly *n*-heptadecane, whereas in layer 2 strains dominate which contribute comparably higher amounts of monomethylalkanes and *n*-heptadecenes. Isomeric *n*-octadecenes show the same vertical distribution. They are also considered to be contributed by photosynthetic microorganisms (Boon and de Leeuw, 1987; Grimalt et al., 1992).

Abed et al. (2007) reported bacteria from the *Chloroflexus* group in the aerobic zone of the Gelatinous mat. The known lipid biomarkers for green non-sulphur-like bacteria (GNSLB) from the *Chloroflexus* group are *n*-hentriacontatriene and wax esters (e.g. Shiea et al., 1991; van der Meer et al., 2001). The alkene was not detected in any of the layers. The concentrations of summed wax esters are generally very low compared to the other biomarker lipids. The unknown *Chloroflexus* group bacteria found in the Gelatinous mat are not close relatives of *Chloroflexus auranticus* from which the lipid biomarkers (*n*-hentriacontatriene and wax esters) were obtained (Abed et al., 2007). Thus, this may be the reason for the absence of specific biomarkers for these bacteria in our analyses.

Sulphate-reducing activity starts directly beneath the surface as isomeric phytenes were found from layer 2 downwards (Grossi et al., 1998). Terminally branched fatty acids (*i*- and *ai*-pentadecanoic acids) which are most abundant in layer 3 can be related to sulphate-reducing bacteria (Findlay and Dobbs, 1993; Mallet et al., 2004). The additional presence of purple sulphur bacteria is possible as the

cyclo-nonadecanoic acids may derive from these anaerobic photosynthetic organisms (Grimalt et al., 1992; Fourçans et al., 2004) and both light penetration and photosynthesis was measured at this depth (Abed et al., 2007). The high concentration of the *cyclo*-nonadecanoic acids in the deepest layer may be due to accumulation or stagnation of growth (e.g. Wang and Cronan, 1994; Grogan and Cronan, 1997; Zhang and Rock, 2008) and preservation. The vertical distribution of major MUFAs shows their dominance in the surface layer. Thus, they derive mainly from aerobic phototrophic or aerobic heterotrophic organisms. In summary, aerobic or anaerobic phototrophic and heterotrophic bacteria can be determined as contributing organisms concerning the PLFA distribution in the Gelatinous mat.

5α-Cholest-2-ene is produced as diagenetic product of cholest-5-en-3β-ol via the formation of the corresponding stanol (Dastillung and Albrecht, 1977; de Leeuw et al., 1989). The source remains unclear, even if the depth distribution of 5α-cholest-2-ene fits with that of *n*-nonacosane. Both individual and summed hopanol concentrations show the same vertical distribution. Thus, both a terrestrial (Huang and Meinschein, 1979) or an algal (Mercer et al., 1974) origin is possible for the 5α-cholest-2-ene. The relative amounts of long-chain *n*-alkanes are highest in layer 5. This appears to be the most probable explanation for the most negative $\delta^{13}C$ value of the total extract from this layer. Stable carbon isotope ratios of total organic carbon in terrestrial plants range from -34‰ to -23‰ and from -14‰ to -12‰ in C_3 and C_4 plants, respectively (Schidlowski, 1987). A decrease from averaged -13‰ to -22‰ suggests a C_3 plant origin of the organic matter in layer 5. The absence of higher plants in viewing distance from the sampling area requires an aeolian transport to the intertidal area, however. From the vertical distribution of phytenes, steroids and hopanoids we conclude that the degradation of the lipids starts very rapidly just below the surface as is obvious from the phytene profiles.

In the first part of this publication (Scherf and Rullkötter, prep.) we suggested an aerobic organism as the source of *n*-heneicosadiene. From the similar depth profiles of *n*-heneicosadiene and phytol (not in concentration but in shape, Fig. 3.11b) we suggest that it is not only derived from an aerobic but more specifically from a phototrophic organism as phytol derives from the phytyl-side chain from either chlorophyll *a* or bacteriochlorophyll *a* in photosynthetic organisms. The most important photosynthetic organisms in the surface layer of the Gelatinous mat are cyanobacteria. Four strains of cyanobacteria were found to be major contributors: *Microcoleus chtonoplastes*, *Lyngbya aestuarii*, *Entophysalis major* and *Aphanothece sp*. (Abed et al., 2008). The first two are typical mat inhabiting strains (Cardoso et al., 1976; Boudou et al., 1986; Grimalt et al., 1992; Thiel et al., 1997). Additionally, the

only major cyanobacterium in the Gelatinous mat, which was not found to be a major contributor to the other microbial mats from the intertidal flat of Abu Dhabi, is *Aphanothece sp.* (Abed et al., 2008; Scherf and Rullkötter, in prep.). Thus, *n*-heneicosadiene may derive from this cyanobacterium or from an unknown organism, whose presence was not revealed by 16S rRNA analysis.

3.2.5 Conclusions

The vertical profiles of lipid biomarkers within the Gelatinous mat reveal a diversity of organic matter sources and provide insight into the community structure in the six horizons. The vertical distribution of lipid biomarkers which can be related to certain organisms occupying different trophic levels within the microbial mat follows the expected distribution relative to light, oxygen and sulphur gradients in the mat. The most abundant lipid biomarkers in the upper layers of the mat are likely to represent phototrophic microorganisms, mainly cyanobacteria. Partially coexisting and directly beneath, sulphate-reducing activity and lipid biomarkers indicative for sulphate-reducing bacteria and anaerobic phototrophic bacteria were observed. In the deepest layer the high concentrations of degraded compounds reflects the activity of heterotrophic mat decomposers throughout the mat profile and organic matter accumulation in this (possibly fossil) layer. The vertical distribution of lipid compounds in the Gelatinous mat shows several similarities with microbial mats which were examined before using biogeochemical analysis (e.g. Philp et al., 1978; Boudou et al., 1985; Boudou et al., 1986; Rontani and Volkman, 2005).

Further efforts must be directed to the isolation and cultivation of the mat-inhabiting microorganisms to clarify the origin of compounds such as *n*-heneicosadiene.

3.2.6 Acknowledgements

The authors would like to thank Dr. Raeid Abed and Dr. Dirk de Beer (Max Planck Institute for Marine Microbiology, Bremen, Germany) and the Dr. Waleed Hamza (University of the United Arab Emirates) for corporation, Kerstin Adolph and Bernd Kopke for analytical support and Deutsche Forschungsgemeinschaft (DFG) for funding (grant no. RU 458/32).

4 Lipid biomarkers, pigments and cyanobacterial diversity of microbial mats across intertidal flats of the arid coast of the Arabian Gulf (Abu Dhabi, UAE)

Raeid M. M. Abed [1], Katharina Kohls [1], Raphaela Schoon [1], Ann-Kathrin Scherf [2], Marion Schacht [3], Katarzyna Palinska [3], Huda Al-Hassani [4], Waleed Hamza [4], Jürgen Rullkötter [2] and Stjepko Golubic [5]

[1] Max Planck Institute for Marine Microbiology, Bremen, Germany

[2] Organic Geochemistry Department, Institute of Chemistry and Biology of the Marine Environment, Carl von Ossietzky University of Oldenburg, D-26111 Oldenburg, Germany

[3] Geomicrobiology Department, Institute of Chemistry and Biology of the Marine Environment, Carl von Ossietzky University of Oldenburg, D-26111 Oldenburg, Germany

[4] Biology Department, Faculty of Science, United Arab Emirates University, Al Ain, UAE

[5] Biological Science Center, Boston University, Boston, MA, USA

4.1 Abstract

Variations in morphology, fatty acids, pigments and cyanobacterial community composition were studied in microbial mats across intertidal flats of the arid Arabian Gulf coast. These mats experience combined extreme conditions of salinity, temperature, UV radiation and desiccation depending on their tidal position. Different mat forms were observed depending on the topology of the coast and location. The mats contained 63 fatty acids in different proportions. The increased amounts of unsaturated fatty acids (12-39%) and the *trans*/*cis* ratio (0.6-1.6%) of the cyanobacterial fatty acid *n*-18:1ω9 in the higher tidal mats suggested an adaptation of the mat microorganisms to environmental stress. Chlorophyll *a* concentrations suggested lower cyanobacterial abundance in the higher than in the lower intertidal mats. Scytonemin concentrations were dependent on the increase in solar irradiation, salinity and desiccation. The mats showed richness in cyanobacterial species, with *Microcoleus chthonoplastes* and *Lyngbya aestuarii* morphotypes as the dominant cyanobacteria. Denaturing gradient gel electrophoresis patterns suggested shifts in the cyanobacterial community dependent on drainage efficiency and salinity from lower to higher tidal zones. We conclude that the topology of the coast and the variable extreme environmental conditions across the tidal flat determine the distribution of microbial mats as well as the presence or absence of different microorganisms.

4.2 Introduction

Microbial mats are among the oldest and most compact ecosystems on earth, sharing very close similarities with the Precambrian fossil stromatolites (Walter et al., 1992; van Gemerden, 1993). They are distributed worldwide in a diverse range of extreme environments, typically where the abundance and activity of grazing organisms is restricted (Javor and Castenholz, 1984; Farmer, 1992). Cyanobacteria, the dominant oxygenic phototrophs in microbial mats, are conjectured to have been the predominant forms of life on early earth for more than 2 billion years, and were likely responsible for the creation of earth's atmospheric oxygen, through their oxygenic photosynthetic metabolism. In modern ecosystems, cyanobacteria prevail whenever conditions become more extreme (Golubic, 1991). Special attention has, therefore, been paid to extreme environments and the organisms therein with the aim being to understand life on early earth and to enable the search of life on other planets. The diversity of cyanobacteria in microbial mats has been studied under extreme conditions of salinity (e.g. hypersaline lakes and marine intertidal flats), temperature (hot springs) and light intensity and UV radiation (hot deserts) (Ferris et al., 1996; Ward et al., 1997; Nübel et al., 1999, 2000; Ward and Castenholz, 2000; Abed and Garcia-Pichel, 2001; Garcia-Pichel and Pringault, 2001).

Coastal intertidal flats of the Arabian Gulf harbour various types of mats that experience the following extreme environmental parameters combined: salinity that may reach over 22% (depending on the mat's tidal position), solar irradiation and temperature increased up to 55°C in hot summers. Rainfall is sporadic, about 40–60 mm $year^{-1}$, as compared with evaporation rates of about 1500 mm $year^{-1}$ (Kinsman and Park, 1976). The mats are exposed to intense sunlight, leading to high evaporation rates of seawater and desiccation. These conditions are expected to attract microbial extremophiles. In spite of the unique environmental settings of the Arabian Gulf mats, little is known about their structure and bacterial diversity. Most previous studies on this mat system focused on the geological record of the area and the description of the landscape (Kendall and Skipwith, 1968, 1969; Purser, 1973; Kinsman and Park, 1976).

The present study applied molecular methods to characterize microbial mats on intertidal flats on the south-eastern coast of the Arabian Gulf at Abu Dhabi, United Arab Emirates (Fig. 4.1). The structure, distribution and composition of cyanobacterial communities were studied using a polyphasic approach that included direct light microscopy, enrichment cultivation, denaturing gradient gel electrophoresis (DGGE), 16S rRNA gene sequencing and distribution of lipid biomarkers and pigments. A combination of these techniques was applied to circumvent the limitations of each

approach. The aim of the study was (1) to investigate the effect of multiple extreme conditions of salinity, temperature, desiccation and irradiation on the development and distribution of mat types as well as on the distribution of their fatty acids and pigments and (2) to explore the diversity of extremophilic cyanobacteria that tolerate the harsh conditions of the arid climate of the Gulf.

Fig. 4.1. Map showing the location of the studied cyanobacterial mats on the Arabian Gulf coast near Abu Dhabi and satellite images of the sampling site modified from Google Earth. Image © 2007 DigitalGlobe.

4.3 Materials and Methods

4.3.1 Mat samples and their environmental settings

Mat samples were collected in December 2004, during low tide (Fig. 4.2). Triplicate mat pieces were collected from different tidal positions along a transect perpendicular to the low waterline, at low, middle and high intertidal ranges. The mat samples were frozen on site and shipped to the Max-Planck Institute in Bremen. The collected mats were different in appearance, texture and ambient salinity (Fig. 4.2). All mats were exposed to 6% salinity during high tide as measured using a portable refractometer. The salinity of the overlying water during the lower tide was found to be 6%, 8–10% and 20% (low, middle and upper intertidal). Air temperature in this region typically reaches above 50°during hot summers and between 15 and 35°C in winter. Thus, the mats experience seasonal temperature difference ranges of 25–35°C. The water temperature in summer was 32°C at high tide, whereas in pools remaining separated during low tide, it reached 50°C.

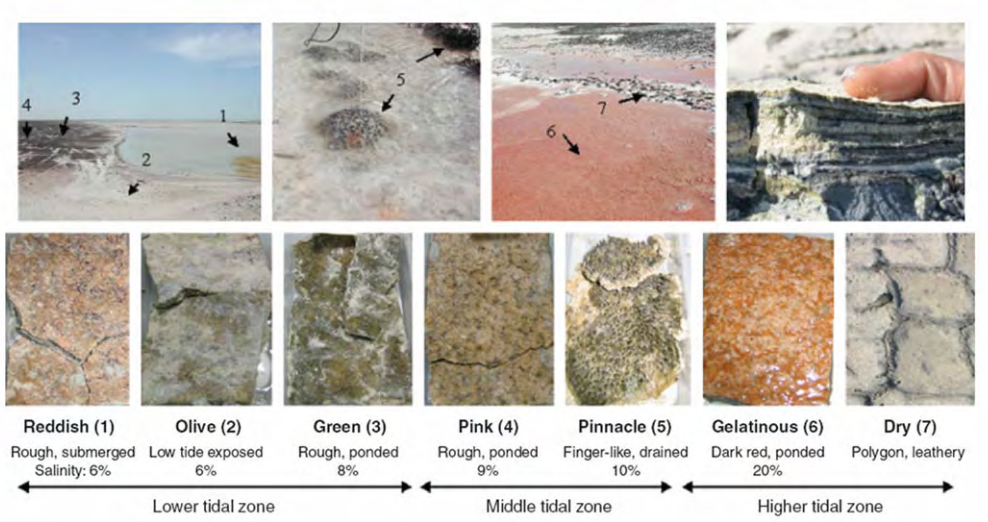

Fig. 4.2. Photographs showing the landscape of the microbial mats in the intertidal flat of Abu Dhabi (top line). The numbers in the top photographs show the tidal positions of the collected mats (bottom line). The mat samples collected from the lower, middle and higher tidal zones show variations in texture, colour and morphology.

4.3.2 Fatty acid analysis

Fatty acids were extracted from the uppermost centimetre of the studied mats using a method modified after Bligh and Dyer (1959), White et al. (1979), and Fang and Findlay (1996). A single-phase solvent mixture of methanol/dichloromethane/ ammonium acetate buffer [pH 7.6, 2:1:0.8 (v/v/v)] was added to the homogenized mat samples. Dichloromethane and distilled water were added to the pooled extracts until a ratio of methanol/dichloromethane/ammonium acetate buffer of 1:1:0.9 (v/v/v) was obtained. The organic phase with the extracted lipids was separated, evaporated to dryness and stored at -20°C. Subsequently, lipid extracts were dissolved in dichloromethane/methanol 9:1 (v/v) and separated using liquid chromatography according to Zink and Mangelsdorf (2004). Four fractions were eluted from the column: (1) neutral lipids, (2) free fatty acids, (3) glycolipids and (4) phospholipids. Aliquots of the phospholipid fractions were transesterified with trimethylsulfonium hydroxide as described by Müller et al. (1990). Identification and quantification of the resulting methyl esters were performed by GC-MS analysis using a Finnigan MAT SSQ 710B mass spectrometer (Finnigan-Thermoquest, San Jose, CA). Individual components were identified by comparing their mass spectra with published spectra or with bacterial fatty acid methyl ester standards (Sigma Aldrich, Taufkirchen, Germany).

4.3.3 Pigment analysis

Triplicate subsamples (top 2–3mm) of the studied mats were used for pigment extraction. The samples were washed in ice-cooled sodium chloride solution (8%

NaCl), vortexed and then centrifuged for 10 min at 2200 g. Extraction of pigments was performed with ice-cooled 100% methanol after sonication and incubation at -20°C for 24 h. The supernatants were filtered through a 0.45 µm Acrodisc® CR 4-mm syringe filter (Pall Gelman Laboratory). The whole procedure was carried out on ice under dim light. The pigments were analyzed using reverse-phase HPLC that consisted of a Waters 996 photo diode array detector (PDA) and a Waters 2690 separation module (Waters, MA). A 125 mm x 4.6 mm vertex column packed with a Eurospher-100 C18 of 5 µm particle size was used (Knauer GmbH, Berlin, Germany). The pigments were identified by comparing the retention time and the spectrum with commercially available pigment standards: chlorophyll *a* (Chl *a*) and β-carotene from DHI Water and Environment, Denmark; bacteriochlorophyll *a* (Bchl *a*) from *Rhodopseudomonas sphaeroides* from Sigma-Aldrich; and scytonemin from Merck, Germany.

4.3.4 Light microscopy and enrichment cultivation

Morphological observations were made using Axiovert and Axioplan Zeiss photomicroscopes equipped with phasecontrast and Nomarski (DIC) optical systems, applying sample preparation as described previously (Palinska et al., 1998). Morphological identification was carried out in accordance with traditional phycological (Geitler, 1932; Komárek and Anagnostidis, 1999, 2005) and bacteriological (Castenholz, 2001) systems, while awaiting further confirmation by molecular sequencing.

Single filaments and cell colonies from the field samples were separated using a binocular microscope and then placed on three different types of media: 'Castenholz'(Castenholz, 1981), 'RC' (van Rijn and Cohen, 1983) and ASNIII (Rippka et al., 1979) solidified with 0.9% agar. Unicyanobacterial cultures were obtained after several transfers of single filaments to fresh media. All cyanobacterial cultures were maintained in ASNIII medium at 35 C. The cultures were illuminated using Osram tungsten light tubes providing a photosynthetic photon flux density (PPFD) of 30.5 mmol photons m^{-2} s^{-1} (measured using a LICOR LI-185B quantum radiometer/photometer equipped with a LI-190SB quantum sensor) and with a light/dark cycle of 12 h/12 h. The 16S rRNA gene sequences of the obtained cultures were phylogenetically analyzed.

4.3.5 Molecular analysis

The photic zones (2–3mm) of mat cores (c. 300–500 mg each) were subjected to nucleic acid extraction, PCR and DGGE as follows: mat cores or pellets, 10 mL of each culture (centrifuged at 4602 g, 5 min, RT), were used for the DNA extraction,

resuspended in 1 mL buffer (100 mM Tris, 100 mM EDTA, 1.5 M NaCl, 1% cetyltrimethylammonium bromide, pH 8.0). After addition of lysozyme (1% final concentration), the samples were incubated at 37°C for 1 h. After five cycles of freeze (in liquid nitrogen) and thaw (at 65°C), 5 mL proteinase K (100 mg mL^{-1}) and 90 mL 10% sodium dodecyl sulfate was added and the samples were incubated at 52°C for 150 min. The samples were centrifuged in a microcentrifuge at 12 000 g for 5 min and the supernatants were extracted twice with phenol, phenol/chloroform and chloroform. The DNA was precipitated from the aqueous phase with 0.6 vol. of 2-propanol, washed with 70% ethanol, vacuum dried and stored in 100 mL TE buffer (10 mM Tris, 1 mM EDTA, pH 8.0).

PCR for the amplification of 16S rRNA genes was carried out using cyanobacteria-specific primers CYA106F (for cultures) or CYA359F (with a 40-nucleotide GC clamp at the 5' end; for DGGE) and CYA781R (Nübel et al., 1997). Thermocycling was performed using a Mastercycler gradient cycler (Eppendorf, Hamburg, Germany). After an initial denaturation step (5 min at 95°C), followed by 80°C for 1 min, Super Taq DNA polymerase (HT Biotechnology, Cambridge, UK) was added. Thirty-five cycles were performed at 94°C for 1 min, 60°C for 1 min (annealing temperature) and 72 C for 1 min. The presence of PCR products was detected by standard agarose gel electrophoresis and ethidium bromide staining.

DGGE was carried out using a Bio-Rad D-Code system and run at 60 C and a constant voltage of 200 V for 3.5 h. The DGGE bands were excised manually under the UV light, the DNA allowed to diffuse out in 50 mL of PCR water at 4°C overnight and PCR reamplified using the same primers (CYA359F and 781R) as described above. The amplification products of the DGGE bands and cultures were purified using the QIAquick PCR Purification Kit (Qiagen, Hilden, Germany) and sequenced in both directions. The primers were the same as for amplification.

4.3.6 Phylogenetic analysis

Sequence alignment and phylogeny of 16S rRNA gene fragments obtained from DGGE bands as well as from the cultures were carried out using the ARB software (Ludwig et al., 1998) version 07.12.17prv and the official database (www.arb-home.de) of February 2005 for small subunit RNA sequences (ssu_jan04_corr_opt.arb). Additionally, cyanobacterial gene sequences available from the GenBank were imported and aligned in the database of the ARB software. These sequences were then aligned with the sequences in the ARB database using the alignment ARB tool. The alignment was corrected manually. The phylogenetic tree was calculated by maximum likelihood, based on long 16S rRNA gene sequences (> 1300 bp). The sequences were inserted into the pre-established tree using the

parsimony ARB tool, while maintaining the overall tree topology without changes. The final tree was minimized for simplicity in presentation.

4.3.7 Nucleotide sequence accession numbers

The sequences determined in this study have been deposited in the GenBank database under accession numbers EU024357–EU024387. Sequences were checked for chimera formation using the CHIMERA CHECK program of the Ribosomal Database Project II database (Cole et al., 2003). The assumption was that true chimeras consist of fragments that each have closer database relatives than the full-length sequence has.

4.4 Results

4.4.1 Intertidal mat landscape

Seven different mat types were identified across the intertidal zone of the coast of Abu Dhabi (Fig. 4.1) by moving from the waterline landward. These mats can be tentatively classified by their position across the range of intertidal flooding and water retention, and recognized by their colour and texture (Fig. 4.2).

Inundated flat mats (Fig. 4.2, Reddish, Olive and Green mats) dominate the lower intertidal zones. These mats are smooth, leathery and typically consist of a thin (ca. 3mm) layer that is firmly adhering to the sediment beneath. The reddish mats are always submerged whereas the olive mats are exposed briefly during the lowest tides. The dark green mats are in ponds in a slightly elevated position.

The middle tidal ranges are dominated by two strikingly different mat types. A flat mat (Fig. 4.2, Pink mat) is periodically air-exposed but water logged, thus leaving a laminated sediment beneath. The mat surface is pink in colour, smooth and often covered by gypsum crystals. In contrast, the Pinnacle mat (Fig. 4.2, Pinnacle) covers well drained elevated hills between pools, channel levees and their slopes. The surfaces of this mat grow in the form of upright pointed cones (i.e. pinnacles) that are 1–2 cm high. Below the surface layer of cyanobacteria, there is a thin, often incomplete layer of purple sulphur bacteria and an equally faint black layer indicating a transient anoxic zone.

Upper tidal ranges are characterized by shallow pools and slightly higher margins covered by a polygonally cracked mostly air-exposed dry mat. The pools are covered by finely laminated, slimy mats (Fig. 4.2, Gelatinous), with each layer representing a distinct functional group of microorganisms, with oxygenic phototrophs on top, underlain by purple and green anoxygenic phototrophs and then by sulphate-reducing bacteria. These mats are, unlike others, exceptionally gelatinous on the

surface. They occupy the ponded channels and depressions exclusively in the upper intertidal zone, and hence are always inundated. Polygonally cracked dry mats (Fig. 4.2, Dry) dominate large areas of the higher intertidal zone, where the water is trapped between tides, but the mat surface is exposed to evaporation. These mats are leathery and often have a convoluted surface. Upon extensive desiccation, these mats crack, forming polygons.

4.4.2 Polyphasic characterization of the cyanobacterial communities

4.4.2.1 Fatty acid fingerprints

The studied mats yielded different lipid patterns based on a total of 63 fatty acids: saturated, branched, cyclopropyl, mono- and diunsaturated, in the range of C_9 to C_{28} (Fig. 4.3). Although the saturated straight-chain fatty acids 16:0 and 18:0 and partially the monounsaturated fatty acids 16:1 and 18:1 dominated all samples (Fig. 4.3a), important quantitative differences were found in the fatty acid distributions in different mat types (Fig. 4.3b). The 16:0 fatty acids accounted for relative amounts between 18.3% (Dry mat) and 25.6% (Pinnacle mat) of the total fatty acids. Branched saturated fatty acids were found in amounts of 8.9% (Pinnacle mat) to 18.5% (Pink mat). They consisted mainly of *iso* (*i*) and *anteiso* (*ai*) fatty acids. Several other methyl-branched saturated fatty acids with 13–18 carbon atoms were found. Most of them were of insignificant relative abundance, except for the *me*-16:0 fatty acids, which accounted for 5.1% of the detected fatty acids in the Reddish mat. The amount of *cyclo*propyl fatty acids ranges between 2.9% (Pink mat) and 21% (Reddish mat). The amounts of monounsaturated fatty acids ranged from 11.5% in the Gelatinous mat to 34.4% in the Pinnacle mat. Nearly equal concentrations of the *cis* and *trans* configurations of the fatty acid *n*-18:1ω9 were detected in all mats. Their sum concentration ranged between 7.7% (Gelatinous mat) and 17.9% (Pinnacle mat) of the total fatty acids. The only polyunsaturated fatty acids found in the studied mats had two double bonds and were represented by an 18:2 fatty acid, two 20:2 and two 22:2 fatty acids. The highest amounts of polyunsaturated fatty acids were estimated in the Pinnacle mat (4.7%). The sum of saturated long-chain fatty acids reached 3.9% in the dry mat, which was more than in any other analyzed mat.

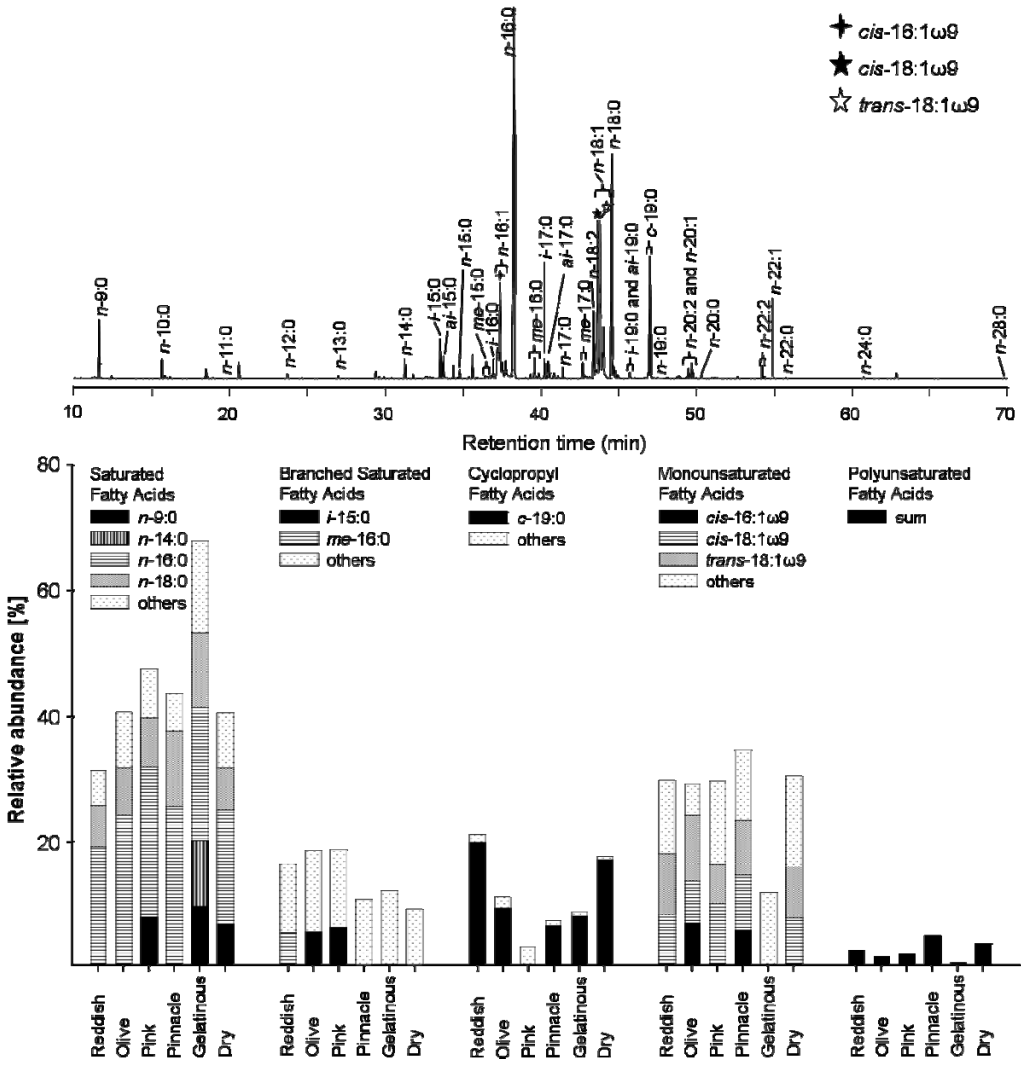

Fig. 4.3. Distribution of fatty acids in the intertidal microbial mats of Abu Dhabi. (a) Total ion current chromatograms of the studied microbial mats. (b) Relative abundances and distribution of different fatty acid groups in the mats.

4.4.2.2 Pigment analysis

The pigments Chl *a*, scytonemin, β-carotene and Bchl *a* were detected in each mat (Fig. 4.4), consistent with the presence of cyanobacteria (Chl *a*, scytonemin and β-carotene) and anoxygenic phototrophic bacteria (Bchl *a*). An additional peak that had a retention time of 17.7 min in the HPLC chromatograms was also detected in all mats; its spectrum resembled that of echinenone. Chl *a* and Bchl *a* concentrations (P values 0.004, df = 10 and 0.002, df = 10, respectively) were significantly higher in the lower tidal mats compared with the higher tidal mats. However, the ratio of Bchl *a* to Chl *a* concentration in the middle tidal mat (Pink mat and Pinnacle mat) was much lower than in other mats (P value 0.001; df = 16). There is a positive correlation between mat exposure to excessive solar irradiation and scytonemin production. Scytonemin exhibited a 10-fold increase in concentration between the submersed

(Reddish and Gelatinous) mats and the frequently drained or air exposed (Pinnacle and Dry) mats.

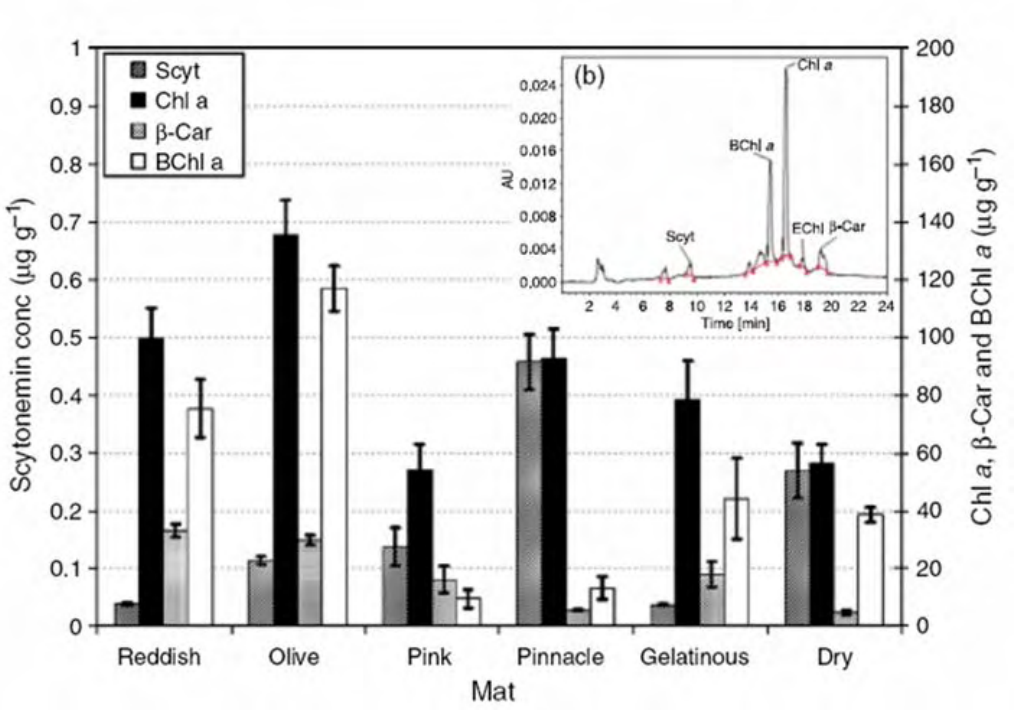

Fig. 4.4. Distribution of intracellular and extracellular pigments among the studied microbial mats. Note that the concentration of Chl *a* is higher in the lower compared with the higher tidal mats while the concentration of scytonemin increases from the lower to the middle tidal mats and then decreases in the higher tidal mats. The insert shows a representative HPLC chromatogram. Note that the scale of scytonemin is different than for other pigments.

4.4.2.3 Light microscopy

Using light microscopy, a total of 15 different cyanobacterial morphotypes were identified (Fig. 4.5, Table 4.1). Each mat harboured a distinct cyanobacterial community with at least five morphotypes. An interesting observation was the detection of a large number of morphotypes in the Gelatinous mat and the Dry mat (11 and 10 morphotypes, respectively), where salinity and desiccation were most extreme. In all mats, the mat-forming *Microcoleus chthonoplastes* Thuret ex Gomont (Fig. 4.5a) and *Lyngbya aestuarii* Liebman ex Gomont (Fig. 4.5b) were often observed as the most dominant cyanobacteria. *Lyngbya aestuarii* was characterized by the presence of a dark scytonemin-coloured sheath and was always present at the surface of the mat above *M. chthonoplastes* filaments. The sunscreen pigment scytonemin was also present in the envelopes of the coccoid cyanobacteria *Entophysalis major* Ercegovic (Fig. 4.5g and h) and *Chroococcus sp.* (Fig. 5i). Morphotype *Schizothrix splendida* Golubic (Fig. 4.5c) largely replaced *Microcoleus* in Pinnacle mats. Other morphotypes such as *Spirulina subtilissima* Kützing ex Gomont (Fig. 4.5d) occurred commonly interspersed in deeper layers of the mat, often colonizing the sheaths of *Microcoleus*. The number of very thin chlorophyll-pigmented filaments corresponding

to *Leptolyngbya* and *Geitlerinema* increased in the lower layers of the mat (Fig. 4.5e and l). *Aphanothece sp.* (Fig. 4.5j) characterized the Gelatinous mats in the upper intertidal ranges. *Rhabdoderma sp*. (Fig. 4.5f), *Chroococcidiopsis sp.* (Fig. 4.5k) *Gomphosphaeria salina* Komárek et Hindak (Fig. 4.5m), *Aphanocapsa sp.* (Fig. 4.5n) and *Oscillatoria spp.* (Fig. 4.5o) were occasionally observed in a single mat but not in others. All mats contained at least two cyanobacteria of those known to produce scytonemin (*L. aestuarii*, *Entophysalis spp.* and *Chroococcus sp.*).

Using enrichment cultivation, a total of 10 strains of cyanobacteria were isolated, most of them showing a simple morphotype of *Leptolyngbya* or *Phormidium* (Fig. 4.5, M1C2, M5C6, M1C10, M4C4, M6C11 andM5C7). Only three cultures showed morphotypic similarity to *M. chthonoplastes* (Fig. 4.5, M7C5, M7C1 and M7C3) and one to *Rhabdoderma sp.* (M7RI).

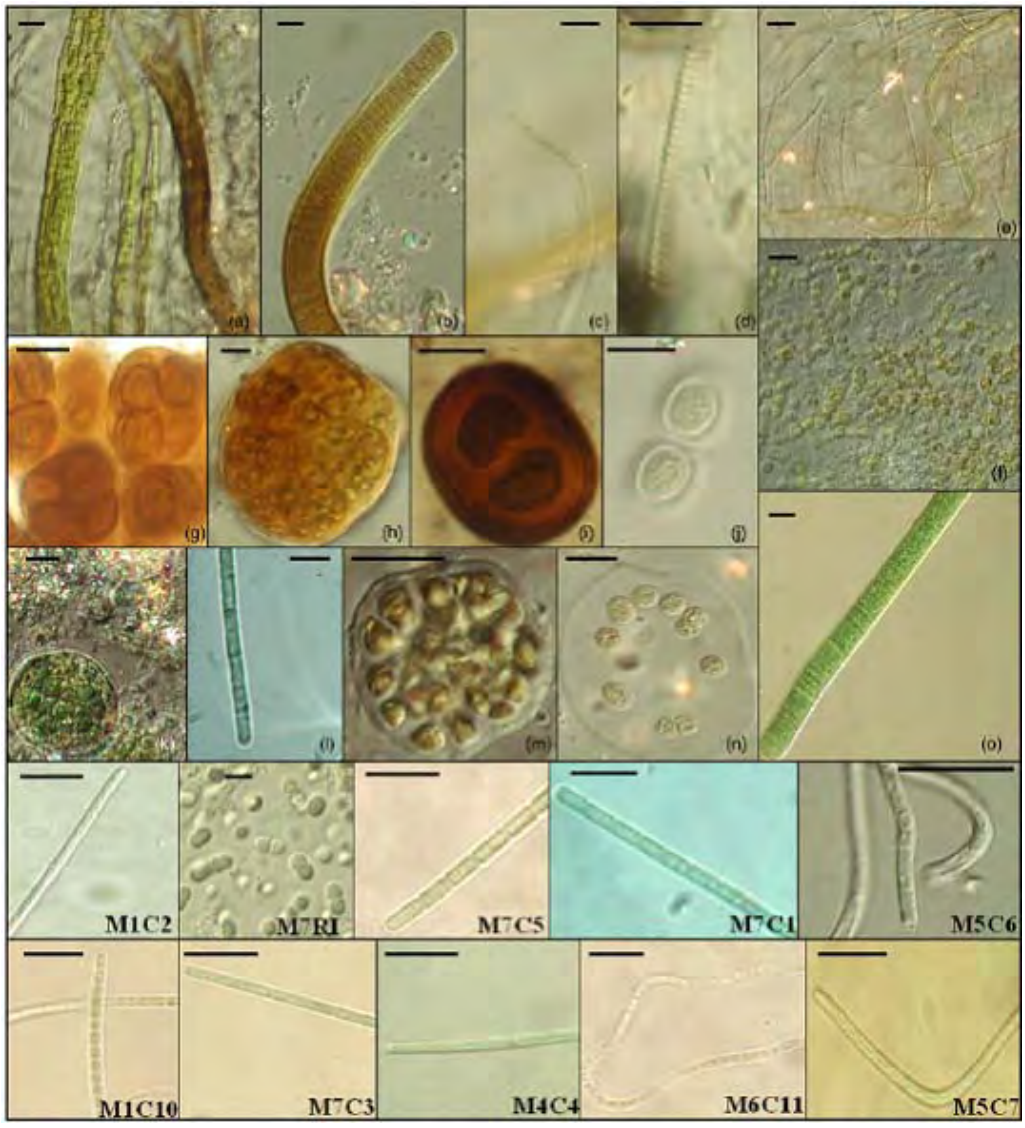

Fig. 4.5. Photomicrographs of identified filamentous and unicellular morphotypes of cyanobacteria in the studied mat samples. Scale bar in 10 µm for all pictures. See text and table 4.1 for the identification of these morphotypes among the mats.

Table 4.1. Comparison of the cyanobacterial community among the studied microbial mats as determined by light epifluorescence microscopy and morphological traits of identified morphotypes (see photographs in fig. 4.5)

Morphotype	Probale taxon*	Cell width (µm)	Cell shape	Colony colour	Mat sample					
					Reddish	Olive	Pink	Pinnacle	Gelatinous	Dry
a	*Microcoleus chtonoplastes*	1.9-5.0	Isodiametric	Dark green	++	++	++	+	++	++
b	*Lyngbya aestuarii*	9.0-16.0	Short discoid	Brown green	++	++	++	++	++	++
c	*Schizothrix splendida*	1.5-3.5	Isodiametric	Pale green	-	+	+	++	+	-
d	*Spirulina subtilissima*	0.8-0.9	Isodiametric	Pale green	-	+	-	-	-	-
e	*Leptolyngbya* sp. 1	1.0-2.1	Isodiametric	Colourless	++	-	+	+	+	+
f	*Rhabdoderma* sp.	3.0-4.0	Cylindrical	Green	-	-	-	-	-	+
g	*Entophysalis major*	6.0-8.0	Spherical	Reddish brown	++	++	+	+	++	-
h	*Entophysalis* sp.	2.5-4.5	Spherical	Reddish brown	+	+	+	-	+	-
i	*Chroococcus* sp.	5.5-8.5	Spherical oval	Dark brown	-	+	+	-	+	-
j	*Aphanothece* sp.	4.0-6.5	Oval isodiametric	Yellowish green	-	-	+	-	++	-
k	*Chroococcidiopsis* sp.	3.0	Spherical	Colourless	-	-	-	-	-	+
l	*Leptolyngbya* sp.2	2.0-3.1	Isodiametric	Colourless	-	-	+	-	-	+
m	*Gomphospheria* sp.	3.0-6.0	Club-shaped	Green	-	+	+	-	-	-
n	*Aphanocapsa* sp.	5.5-7.0	Spherical	Colourless	-	+	+	-	+	-
o	*Oscillatoria* sp.	7.5-8.9	Short discoid	Dark green	-	-	-	-	+	-
M1C2	*Leptolyngbya* sp.	1.0-1.5	Isodiametric	Yellowish green	+	-	-	-	-	-
M7RI	*Rhabdoderma* sp.	4.6-5.1	Oval spherical	Yellowish green						+
M7C5	*Microcoleus* sp.	2.1-2.3	Isodiametric	Dark green						+
M7C1	*Microcoleus* sp.	2.5-5.0	isodiametric	Dark green						+
M5C6	*Halomicronema* sp.	0.8-1.1	Oval	Green				+		
M1C10	*Leptolyngbya* sp.	1.0-1.9	Isodiametric	Dark green	+					
M7C3	*Microcoleus* sp.	2.2-2.5	Oval	Dark green						+
M4C4	*Phormidium* sp.	2.4-5.0	Oval	Green			+			
M6C11	*Leptolyngbya* sp.	1.2-2.0	Isodiametric	Dark green					+	
M5C7	*Halomicronema* sp.	0.8-1.1	Isodiametric	Green				+		

4.4.2.4 DGGE patterns and molecular diversity

The DGGE gel showed a distinct banding pattern for each mat (Fig. 4.6). The phylogenetic tree revealed that the sequences retrieved by DGGE showed variations in the cyanobacterial community composition among different mats (Fig. 4.7). Because DGGE displays dominant members of the bacterial community, the diversity of cyanobacteria detected by DGGE within each mat was, as expected, lower than by direct microscopy. The Pinnacle mat displayed the highest number of DGGE bands, whereas the Dry mat showed a single strong band with few much less prominent ones. The designations based on names submitted with the sequences to GenBank do not have taxonomic validity unless independently confirmed. Sequences related to *M. chthonoplastes* were detected only in the lower tidal mats (Figs. 4.6 and 4.7, Reddish-DGGE band 1, Green-DGGE band 5 and Pink-DGGE band 8) but not in the Pinnacle, Gelatinous and Dry mats, although *M. chthonoplastes* was microscopically observed within these mats. Sequences related to *Leptolyngbya* and *Phormidium* were found in all tidal zones, whereas sequences phylogenetically affiliated with *Plectonema* only in the lower tidal mats (Green-DGGE band 6, Reddish-DGGE band 2 and Olive- DGGE band 3). Sequences related to the extremely halotolerant *Halothece* group were detected only in the Pink and Gelatinous mats (Pink-DGGE band 9 and Gelatinous-DGGE band 15). A single sequence related to *Spirulina subsalsa* was detected in the Pinnacle mat (Pinnacle-DGGE band 10).

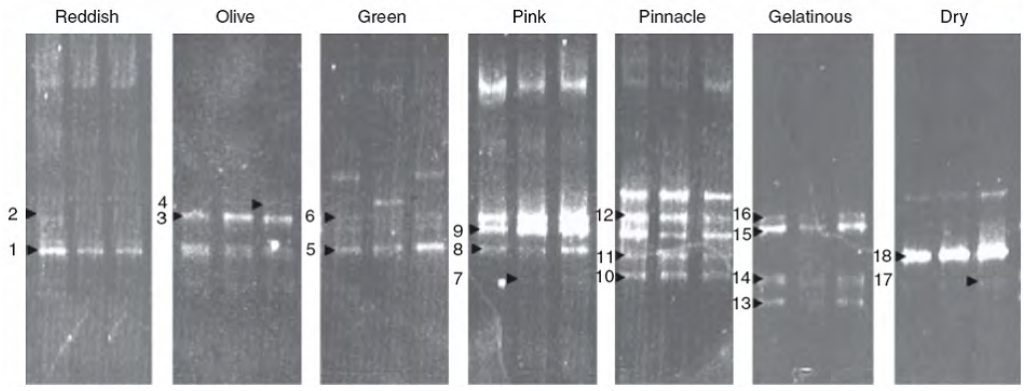

Fig. 4.6. DGGE fingerprints of PCR-amplified 16S rRNA gene fragments obtained from the studied microbial mats using cyanobacteria-specific primers. The shown pictures all belong to the one gel, which was cut and ordered for display. The indicated bands were excides, reamplified and sequenced.

The phylogenetic affiliations of the cultured cyanobacteria showed closeness to sequences of the marine and hypersaline *Phormidium*, *Halomicronema*, *Oscillatoria*, *Microcoleus* and the unicellular *Cyanothece* GenBank designations. Cultures related to *Microcoleus sp.* were obtained from only one particular mat (Dry mat, higher tidal zone). The remaining isolates (M1C2, M5C6, M5C7 and M7RI) were obtained from different mats in higher middle and lower intertidal zones. The sequences of only four

cultures (M1C2, M7C3, M7C5 and M7C1) were related to sequences obtained from DGGE bands.

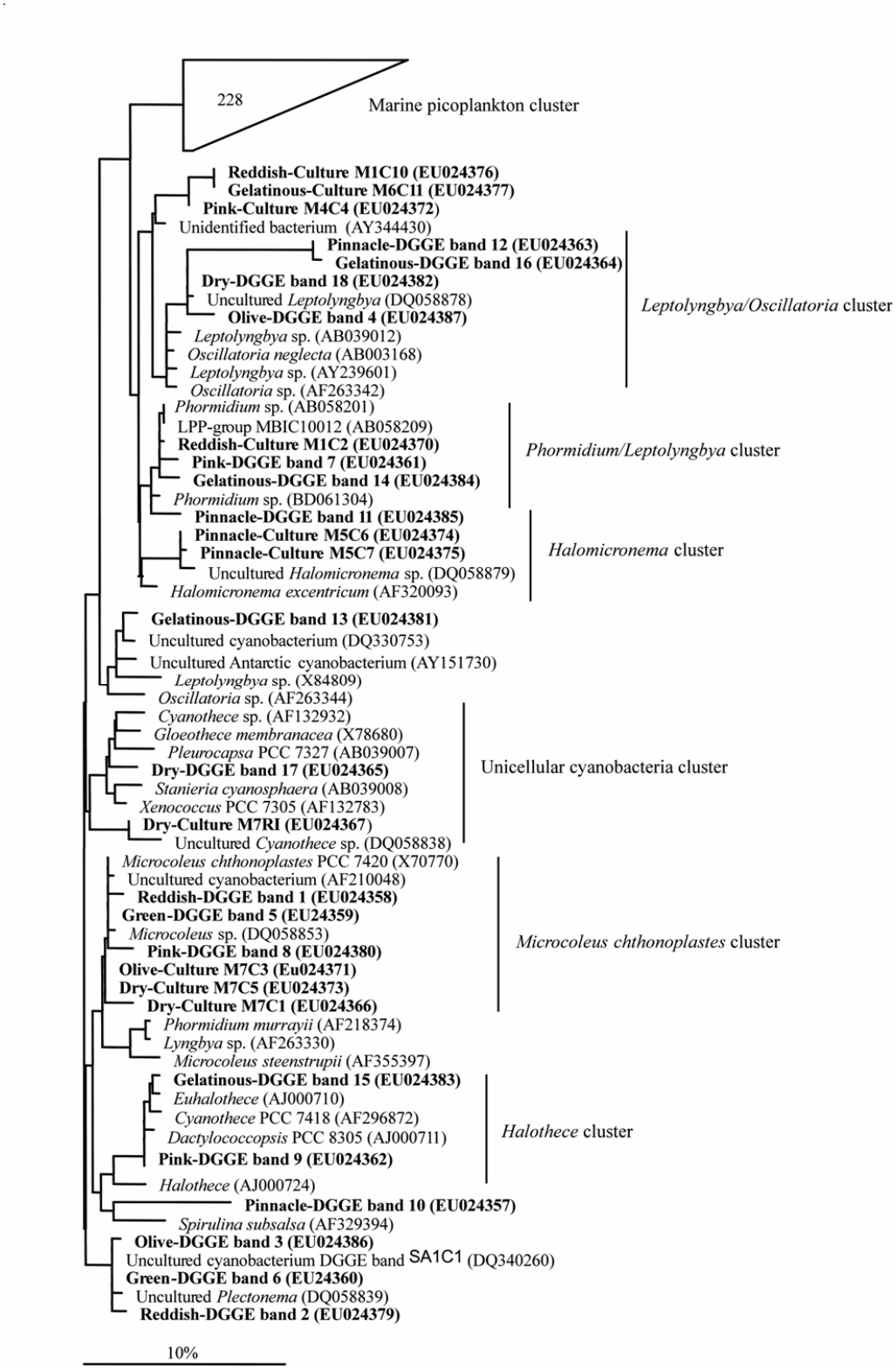

Fig. 4.7. 16S rRNA gene-based phylogenetic reconstruction based on maximum likelihood methods, showing the affiliation of cyanobacterial sequences retrieved from DGGE and cultures obtained from the studied microbial mats. The partial sequences were inserted into the reconstructed tree by applying parsimony criteria without allowing changes in the overall tree topology. Accession numbers are indicated in parentheses. The scale bar indicates 10% sequence divergence. Data received in this study are shown bold.

4.5 Discussion

4.5.1 Effect of the multiply extreme environmental conditions on the effect on the macro- and microstructure of microbial mats

The extent of extreme conditions of salinity, temperature, desiccation and solar irradiation, and their interplay during the tidal cycles across the coastal flats of Abu Dhabi determined the shape of microbial mats as well as the composition of microbial communities, fatty acids and pigments. The distinctive zonal distribution of different mat types reflects the harsh environmental constraints selecting for highly adapted and tolerant genotypes among cyanobacteria, which are the dominant primary producers and architects of these mats (Golubic, 1991). The studied mats are stratified microbial communities, vertically differentiated at mm scale responding to steep physical and chemical gradients, which are especially sharp across oxic–anoxic interfaces. These mats are also horizontally differentiated at different scales. They are significantly drier in the higher compared with the lower tidal zones due to extended exposure to intense solar irradiation and the accompanying high rates of evaporation. The flat mats prevailed in the low tidal zones and in depressions of the middle and high tidal areas where they have adequate water supply. The frequent alteration of air exposure and inundation promoted the growth of contiguous pinnacle mats on well-drained elevations in the middle tidal zones, whereas severe dryness in the higher tidal zones resulted in cracking and polygon formation. Cracking of the mats in channels begins transverse to the flow, and the size of desiccation polygons depends on their tidal position; larger polygons form in the moist centre of channels but become gradually smaller towards the edges, where drying is faster (Golubic, 1991). The number of extracellular polymeric substances (EPS), as assessed by direct visualization, increased from lower to higher tidal mats, which correlated with increased salinities. Previous reports showed that EPS production by phototrophs was stimulated under high salt stress (Liu and Buskey, 2000; Abdullahi et al., 2006).

The extracted Chl *a* quantities from the studied mats suggested that cyanobacteria were most abundant in lower intertidal zones where environmental conditions are optimal. Measured photosynthesis rates using oxygen microsensors decreased from lower to higher tidal mats (Abed et al., 2007). Because the salinity and temperature can reach 20% and 55°C, respectively, in the higher tidal mats, it is likely that the cyanobacteria within these mats are both halotolerant and thermotolerant. The optimum temperature for photosynthesis in these mats was 45°C (Abed et al., 2006). Photosynthesis was still possible up to 60°C and photosynthesis was detectable up to 20% salinity (Abed et al., 2006, 2007). The observed strains of *Aphanothece*, *Halomicronema* and *Microcoleus* are known halotolerant and thermotolerant

cyanobacteria (Karsten, 1996; Nübel et al., 2000; Abed et al., 2002a, b). The detection of *M. chthonoplastes* in mats where salinity reaches 20% is interesting because previous studies on various *Microcoleus* isolates showed a maximum salt tolerance up to 12% salinity (Karsten, 1996). The exclusive occurrence of the desiccation-tolerant *Chroococcidiopsis* in the Dry mat is consistent with the conditions prevalent in this mat. Our DGGE patterns support previous reports that changes in environmental extremes are accompanied by selection and shifts in cyanobacterial community composition (Benlloch et al., 2002; Rothrock and Garcia-Pichel, 2005).

4.5.2 Fatty acids and environmental adaption

The fatty acids obtained could be assigned to known major bacterial groups in microbial mats. Monounsaturated fatty acids are typical for aerobic microorganisms whereas *n*-18:1ω9, and *n*-16:1ω9 together with the polyunsaturated fatty acids 18:2, 20:2 and 22:2, indicate the presence of cyanobacteria (Grimalt et al., 1992). The presence of sulphate-reducing bacteria and other anaerobic bacteria is indicated by the detection of *cyclo*propyl and the terminally branched (*i*- and *ai*-17:0) fatty acids (Findlay and Dobbs, 1993). The *i*-, *ai*-15:0 and *i*-16:0 fatty acids are characteristic of gram-positive bacteria whereas the *cy*-19:0 acid was reported to be abundant in purple phototrophic bacteria (Fourçans et al., 2004). Most of the detected fatty acids in the studied mats were reported previously in other hypersaline mat systems (Grimalt et al., 1992; Wieland et al., 2003; Rontani and Volkman, 2005).

Many reports suggested that lipids may be involved in protection against environmental stress (Huflejt et al., 1990; Khomutov et al., 1990; Ritter and Yopp, 1993). Photosynthetic microorganisms tend to synthesize more unsaturated fatty acids on increasing salinity and temperature, which results in increased fluidity of the membrane. Consequently, the Na^+/H^+ antiport system is activated, resulting in protection of photosystems I and II (Singh et al., 2002). Unsaturated fatty acids were estimated to account for 12–39% of the total fatty acids in our mats. The high *trans*/*cis* ratio (0.6–1.6) of the cyanobacterial fatty acid *n*-18:1ω9 in our mats is also evident with the elevated temperature and salinity in the field. An increase in this ratio with an increase in salinity and temperature was demonstrated in bacterial cultures of *Pseudomonas putida* and in soils (Petersen and Klug, 1994; Heipieper et al., 1996).

4.5.3 Cyanobacteria and solar radiation

The elevated levels of UV and solar radiation in the field favoured the growth of cyanobacteria that contain scytonemin. *Lyngbya aestuarii*, *Entophysalis spp.* and *Chroococcus sp.*, known to possess such sunscreens (Fleming and Castenholz, 2007), were found only in the top layers of all studied mats. Cyanobacteria that lack the

ability to produce scytonemin such as *M. chthonoplastes* protected themselves against UV light by inhabiting deeper horizons in the mat. The quantification of scytonemin by HPLC confirmed our microscopic observations. It correlated with the selection of taxa able to produce this protective extracellular pigment and with their response to maximum irradiation. Accordingly, it was higher in air-exposed Pinnacle and Dry mats, and lower in submerged mats. Dillon et al. (2002) demonstrated that temperature and UV-A irradiation caused a synergistic increase in scytonemin production whereas the synthesis rate of scytonemin declined with increasing salinity. This decrease was correlated with the decreasing growth rate of cyanobacteria with increasing salinity.

In our mat system, the optimum production of scytonemin was detected at 10% salinity in the middle tidal mat, whereas 20% salinity in the high tidal mat apparently limited the growth of cyanobacteria and subsequently the synthesis of scytonemin. The limited growth of cyanobacteria in this mat was clearly reflected by the low concentration of Chl *a*. Periodic desiccation was also shown to induce scytonemin synthesis in cultures of *Chroococcidiopsis* and *Nostoc* (Fleming and Castenholz, 2007). This might explain the higher concentrations of scytonemin in the Dry mat than in the inundated (Gelatinous) mat from the higher tidal zone. Scytonemin is extremely stable and remains largely intact in the sheaths of desiccated cyanobacteria. This would facilitate recovery of desiccated mats upon rehydration by allocating a large fraction of energy to metabolic processes other than UV damage repair. A scytonemin-like pigment was found preserved on the surfaces of silicified Proterozoic stromatolites (Golubic & Hofmann, 1976), suggesting that protection from solar radiation by extracellular pigments is an ancient adaptation.

4.5.4 Cyanobacterial diversity and resistance to desiccation

Desiccation is among the most important factors exerting selective pressure on bacterial communities. Cyanobacterial diversity and species richness have been shown to decrease as the desiccation frequency increases (Rothrock and Garcia-Pichel, 2005). Interestingly, this was not the case in Abu Dhabi mats, where the most desiccated mat in the studied system exhibited a diverse cyanobacterial community as revealed by microscopy (seven morphotypes), DGGE (three phylotypes) and enrichment cultivation (four strains), suggesting the presence of diverse desiccation-tolerant cyanobacteria in these mats. In the submerged, Reddish mat we found five morphotypes, two phylotypes and three strains. Many field cyanobacteria apparently resisted isolation and only a few from each mat outcompeted all others in cultures. Desiccation damages the cells by causing DNA strand breaks, protein denaturation and membrane leakage upon rehydration (Potts, 1994, 1999), however, several cyanobacteria were shown to tolerate an air-dried state and complete dehydration for

prolonged periods. Among such desiccation-tolerant cyanobacteria are *Microcoleus*, *Lyngbya* and *Chroococcidiopsis* (Grilli Caiola et al., 1996; Ohad et al., 2005; Fleming et al., 2007), which were also identified in our Dry mat. Desiccation tolerance of these cyanobacteria can be achieved through the production of polyhydroxyl carbohydrates, which replace the water shell around cellular macromolecules, preventing denaturation (Potts, 1994, 1999). Studies on *Chroococcidiopsis* strains have demonstrated their ability to survive prolonged desiccation through efficient repair of the DNA damage that occurred during dehydration (Billi et al., 2000). Desiccated *Lyngbya*-dominated mats from Baja California, Mexico, were shown to recover within 12 h when rehydrated even after more than one year of dryness (Fleming et al., 2007). This points to the resilience of *Lyngbya* to long-term desiccation and possibly explains the considerable dominance of this cyanobacterium in our mat system. The production of extensive EPS sheaths in *Lyngbya spp.* and other desiccation-tolerant cyanobacteria enables them to survive complete dryness by enhancing water retention and absorption in their sheaths (Tamaru et al., 2005). The increased level of EPS in the higher tidal mats is possibly a response to prolonged exposure to water evaporation and desiccation.

In conclusion, the multiple extreme environmental conditions in the Arabian Gulf and their impact on the diversity and function of microbial mats render this system worthy of further research. More insights into the adaptations of the mats' microorganisms to simultaneous extreme conditions of salinity, UV, desiccation and temperature and their response with changes in these parameters during tidal regime are needed. The properties of these mats identify them as valid modern analogues of ancient stromatolites, and fossil microbial communities of the Proterozoic (Golubic, 1976), and possibly Archaean times (Nisbet and Sleep, 2001).

5 ^{13}C-Labelling of an intact microbial mat from the high-salinity intertidal area of Abu Dhabi, United Arab Emirates - a molecular isotopic study

Ann-Kathrin Scherf, Jürgen Rullkötter

Institute of Chemistry and Biology of the Marine Environment (ICBM), Carl von Ossietzky University of Oldenburg, P.O. Box 2503, D-26111 Oldenburg, Germany

5.1 Abstract

In this paper we present results from an incubation experiment performed on a microbial mat from the Arabian Gulf intertidal area of Abu Dhabi (United Arab Emirates) using ^{13}C-labelled bicarbonate as carbon source for cyanobacteria and other autotrophic organisms. The microbial mat is characterized by a distinct lamination. Natural carbon isotope ratios of the total extractable organic carbon are heavy with δ^{13}C values ranging from -15‰ to -10‰, suggesting that the ecosystem thrives under CO_2 limitation. We applied bicarbonate labelled with ^{13}C to various extents (1%, 10% and 30%). Carbon fixation was measured as the incorporation of ^{13}C into total extractable organic matter as well as in major hydrocarbons and phospholipid ester-linked fatty acids *via* gas chromatography-isotope ratio-mass spectrometry. The strongest enrichment was observed in the cyanobacterial lipid *n*-heptadecane.

5.2 Introduction

In the last decades increasing interest focused on the understanding of the carbon cycle within microbial mats, whose driving force in most cases is photosynthesis by cyanobacteria or aerobic phototrophic bacteria (Boschker and Middelburg, 2002). Microbial mats are one of the oldest and smallest ecosystems on Earth and are of considerable geological significance as they are thought to represent modern analogues of Precambrian fossil stromatolites (e.g. Awramik, 1984; Boudou et al., 1986; van Gemerden, 1993; Schouten et al., 2001). Microbial mats, often not more than 5 to 10 mm in thickness, are vertically laminated organosedimentary structures (e.g. Park, 1977; Revsbech et al., 1983; Golubic, 1991; van Gemerden, 1993; Kendall et al., 2002). The layers typically consist of a few functional groups of microbes, which interact through their metabolic processes (e.g. Revsbech et al., 1983; Boudou et al., 1986; van Gemerden, 1993). The major groups typically found in hypersaline microbial mats are cyanobacteria, purple sulphur bacteria, colourless sulphur bacteria and sulphate-reducing bacteria, which are distributed along vertical microgradients of oxygen, sulphide and light (Boudou et al., 1986; Dobson et al., 1988).

In the recent past, the analysis of the stable carbon isotope composition of organic molecules has led to a deeper understanding of biogeochemical processes (e.g. Hayes, 1993; Boschker et al., 1998; Schouten et al., 1998; Boschker and Middelburg, 2002; van der Meer et al., 2005). The application of ^{13}C-labelled substrates to soils, sediments or laboratory cultures and the subsequent analysis of biomarker lipids provide information about the groups of microorganisms which utilize the given substrate (Hall, 1995; Middelburg et al., 2000; Zhang, 2002; Evershed et al., 2006; Lipp, 2008). The basic idea behind this approach is that a portion of the added labelled substrate is incorporated into the biomass of the metabolically active populations, a process which has been observed from a variety of biomarkers (Boschker and Middelburg, 2002). Concerning the isotopic difference of dissolved CO_2 and biomass, two effects are of relevance: first, the fractionation associated with CO_2 fixation and production of biomass by primary producers; second, fractionation associated with secondary biological processes, e.g. heterotrophy and bacterial reworking (Hayes, 1993).

Labelling experiments with ^{13}C-bicarbonate can be used to determine autotrophic organisms involved in the uptake of inorganic carbon (Boschker and Middelburg, 2002; van der Meer et al., 2005; Evershed et al., 2006). Different autotrophic organisms use different CO_2 fixation pathways (Ratledge and Wilkinson, 1988). A variety of phototrophs, including cyanobacteria and purple bacteria, are known to use the Calvin cycle to fix CO_2 (Ormerod, 1992; Zhang et al., 2004), which under normal conditions leads to a fractionation of up to -25‰ in the organic matter relative to the δ^{13}C value of the CO_2 from which it was formed (e.g. Madigan et al., 1989; Moers et al., 1993; Sakata et al., 1997). Several *Chloroflexus* group bacteria, which are common constituents of many microbial mats (e.g. van der Meer et al., 1998, 2000, 2001), were proven to use the 3-hydroxypropionate pathway for inorganic carbon fixation (Holo and Sirevåg, 1986; Strauss and Fuchs, 1993; van der Meer et al., 2000, 2001, 2003; Klatt et al., 2007), which leads to a depletion of only -14‰ in the δ^{13}C value relative to the inorganic carbon from which it was formed. Thus, biomarker lipids of *Chloroflexus*-like bacteria are enriched in ^{13}C by ca. 8–12‰ relative to cyanobacterial lipids (Sakata et al., 1997; van der Meer et al., 2000; Jahnke et al., 2004) and, therefore, compound-specific stable carbon isotope analysis is a suitable tool to identify specific types of organisms (van der Meer et al., 2005).

In this study we used ^{13}C-labelling of lipids to identify the dominant primary producers in a microbial mat system from the Arabian Gulf intertidal area of Abu Dhabi, United Arab Emirates. The coastal intertidal flats of the Arabian Gulf harbour various types of mats (e.g. Kendall and Skipwith, 1968; Kinsman and Park, 1976;

Kenig et al., 1990; Golubic, 1991; Abed et al., 2007, 2008) that live under extreme environmental conditions. The salinity may reach 200 depending on the mat's tidal position, and the temperature may rise to more than 55°C in hot summers. The mats are exposed to shadowless sunshine, leading to high seawater evaporation rates and desiccation. The comparison of the isotopic composition of the mat lipids in the different stages of the labelling experiment should gain insight into the uptake of substrate by primary producers.

5.3 Methods

5.3.1 Site and sample description

The microbial mat chosen for this experiment is the Gelatinous mat, which has been described before (Abed et al., 2008). The mat was collected in December 2006 from the intertidal flat of Abu Dhabi (Arabian Gulf coast, United Arab Emirates) during low tide. The sampling site is located on the west-coast of the Al Dhabaiya peninsula (also Zubaiya depending on transcription; e.g. Whittle et al., 1998; see Fig. 5.1). The Gelatinous mat occurs in a little pond in the upper intertidal zone. It is always inundated by highly saline water. The salinity was 200 at the time of sampling. The mat surface was homogeneous, smooth, gelatinous and reddish in colour. The TOC content of the Gelatinous mat amounts to 6.6% in the uppermost layer and 2.4% in the entire intact mat (Scherf and Rullkötter, unpubl. results).

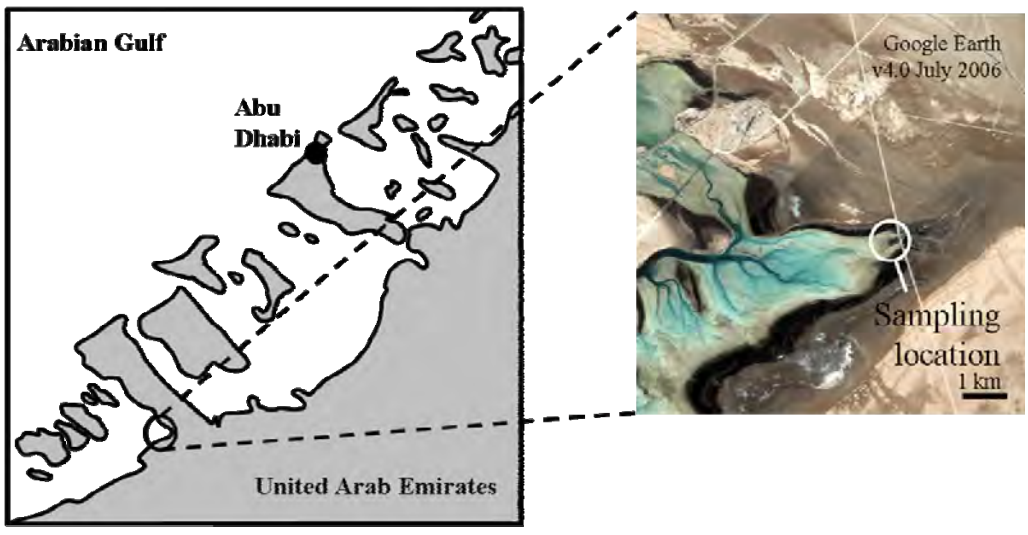

Fig. 5.1. Map showing the location (south-west corner of the Al Dhabaiya peninsula) of the studied microbial mats along the Arabian Gulf coastal area of Abu Dhabi and a satellite image of the sampling site.

The Gelatinous mat shows a well developed lamination, which is macroscopically visible (Fig. 5.2). Each layer probably represents a distinct functional group of microorganisms. Previous analyses to determine the community structure

yielded a huge variety of microorganisms including several being primary producers (Abed et al., 2007, 2008). From chemical analysis of the Gelatinous mat (Scherf and Rullkötter, unpubl. results), the dominating autotrophic microorganisms in the mat are cyanobacteria.

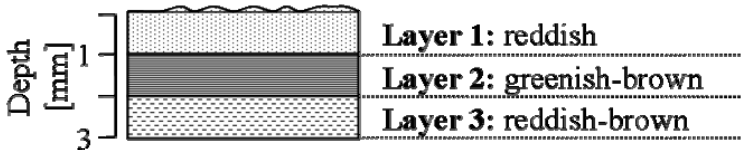

Fig. 5.2. Simplified vertical profile of the photosynthetic zone of the Gelatinous mat.

5.3.2 Labelling experiment

Large pieces of the Gelatinous mat were transported directly to the on-site laboratory. There, small cores of 5 cm in diameter were cut from the mat material. Eight of them were placed in a box filled with artificial seawater (salinity 200) and spiked with 3 mmol bicarbonate, to which 1% ($\delta^{13}C \approx 790‰$), 10% ($\delta^{13}C \approx 8{,}800‰$) and 30% ($\delta^{13}C \approx 26{,}600‰$) ^{13}C-sodium bicarbonate (99%, Cambridge Isotope Laboratories Inc., Andover, USA) were added, respectively. Additionally, a control experiment with unlabelled bicarbonate was performed under the same conditions in a separate box (Fig. 5.3). The first cores were sampled after one hour of dark incubation; this equilibration phase is not further referred to in the text, i.e. 'dark incubation' always means the phase starting at about 7 h. The cores were sliced to recover the superficial 1 mm layer and two deeper layers taken according to visible distinction of layering. The progress of $\delta^{13}C$ incorporation was monitored by collecting samples according to the schedule shown in Fig. 5.3. All samples were frozen immediately and kept frozen until lipid extraction in the home-based laboratory.

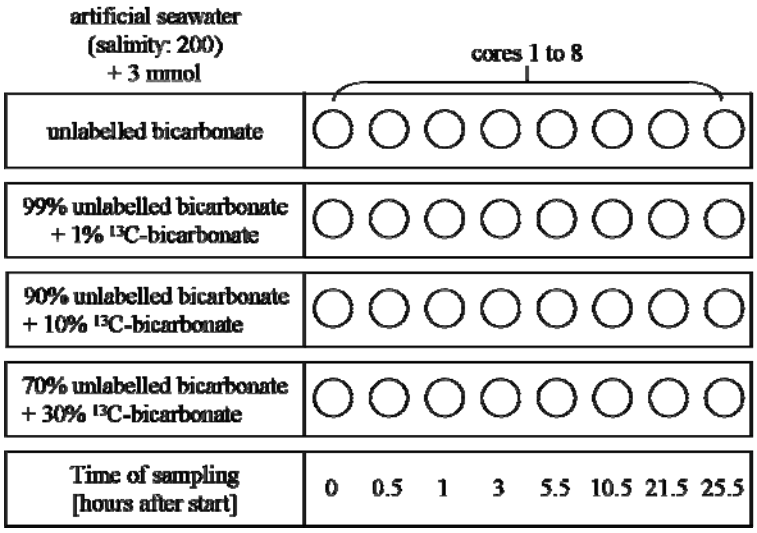

Fig. 5.3. Set–up of the labelling experiment.

5.3.3 Extraction

The layers of the mat were extracted using a modified Bligh and Dyer method (1959; White et al., 1979; Fang and Findlay, 1996). To the homogenised wet mat samples, a single-phase solvent mixture of methanol/dichloromethane/ammonium acetate buffer (pH 7.6, 2:1:0.8 v/v) was added and the suspension ultrasonicated. After centrifugation the supernatant was collected in a separatory funnel. The entire procedure was repeated ten times. Dichloromethane and distilled water were added to the combined extracts until a ratio of methanol/dichloromethane/ammonium acetate buffer of 1:1:0.9 (v/v) was obtained. The organic phase containing the extracted lipids was removed and the methanol-water phase washed three times with dichloromethane. The combined dichloromethane phases were evaporated to dryness and the residue stored at -20°C.

5.3.4 Separation of lipid classes

The lipid extracts were fractionated on a silica gel column (60 mesh, Merck, Darmstadt; Germany) into different polarity classes by sequential elution with dichloromethane, acetone and methanol (modified after Guckert et al., 1985). Column chromatography yielded three fractions: (1) neutral lipids, (2) glycolipids and (3) phospholipids. All fractions were evaporated to dryness and stored at -20°C.

5.3.5 Derivatization

Aliquots of the neutral lipid fractions were treated with N-methyl-N-trimethylsilyltrifluoroacetamid (MSTFA, 70°C, 2 h) to yield the trimethylsilyl esters of the fatty acids. Aliquots of the phospholipid fractions were transesterified via mild alkaline methanolysis modified after White et al. (1979). The phospholipid fraction was suspended in dichloromethane/methanol 9:1 (v/v). An aliquot was transferred into a screw cap vial and filled with methanol to a volume of 1 ml. Then 1 ml of 0.2 N KOH solution (in methanol) was added. The mixture was heated for 15 min at 37°C. After heating the solution was neutralized to pH 6.0 with acetic acid, 2 ml each of chloroform and water were added, and the suspension was vortexed for 2 min. The organic phase containing the phospholipid fatty acid methyl esters was separated and removed and the methanol-water phase washed three more times with dichloromethane. The combined dichloromethane phases were evaporated to dryness and stored at -20°C.

5.3.6 Gas chromatography, gas chromatography-mass spectrometry

Samples were analysed on a Hewlett Packard Series 6890 gas chromatograph equipped with a flame ionization detector (FID). Gas chromatography-mass

spectrometry (GC-MS) was performed with a Finnigan MAT SSQ 710B mass spectrometer (Finnigan-Thermoquest, San Jose, CA). Both gas chromatographs were equipped with a cold injection system (Gerstel KAS3 (GC-FID) or KAS4 (GC-MS), Gerstel, Mühlheim a. d. Ruhr, Germany) and a DB-5HT fused-silica column (30 m x 0.25 mm, 0.1 µm film thickness, J&W Scientific, USA). Helium was used as carrier gas (constant head pressure 12.5 psi). The temperature program was: 60°C (1 min) to 350°C at 3°C/min (held 5 min). The FID was operated at 300°C. The hydrocarbons, fatty acid trimethylsilylesters and phospholipid fatty acid methyl esters were identified by interpretation of their mass spectra or comparison with published spectra and/or from their relative retention times.

5.3.7 Total extractable organic matter stable carbon isotope analysis

The stable carbon isotope ratios of total organic extracts were determined by automated on-line combustion with a Carlo Erba CHNS 1108 elemental analyser (Carlo Erba Instruments, Rodano, Italy) coupled to a Finnigan MAT 252 isotope mass spectrometer (Finnigan-Thermoquest, San Jose, CA). The data are reported in the delta notation relative to the VPDB standard and as $\Delta\delta^{13}C$ values, representing absolute differences between the samples of the different ^{13}C-bicarbonate incubation experiments and the time zero control sample, respectively. All values were measured as duplicates and averaged. Reproducibility of duplicates was better than ±1‰.

5.3.8 Compound-specific stable carbon isotope analysis

Compound-specific stable carbon isotope ratios of neutral lipids and phospholipid fatty acid methyl esters were determined using a Thermo Scientific MAT 253 GC-*irm*MS system (Thermo Fisher Scientific GmbH, Bremen, Germany). The gas chromatograph was equipped with a DB-5 column (30 m x 0.25 µm, 1 µm film thickness, J&W Scientific, USA). The temperature program was: 60°C (2 min) to 320°C at 3°C/min (held 41 min).

Isotopic compositions are reported in standard delta notation relative to the VPDB standard and as $\Delta\delta^{13}C$ values, representing absolute differences between the samples and the time zero control sample of the different ^{13}C-bicarbonate incubation experiments, respectively. All values reported were determined by duplicate analyses and averaged. Reproducibility of duplicates of major hydrocarbons and phospholipid fatty acid methyl esters was better than ±1‰.

5.3.9 Data treatment

To obtain the real stable carbon isotope ratios of the phospholipid fatty acids (PLFAs), the $\delta^{13}C$ values obtained for the derivatized compounds were corrected for the addition of the extra carbon using the mass balance equation

$$n_{dc}\delta^{13}C_{dc}=n_c\delta^{13}C_c+\delta^{13}C_{me}, \quad (1)$$

where n is the number of carbon atoms, "c" the individual compound, "me" the methanol used for derivatisation and "dc" the derivatized compound. The methanol used for mild alkaline hydrolysis had a $\delta^{13}C$ value (average of five measurements) of -45.77‰, as determined by gas chromatography-isotope ratio mass spectroscopy.

All enrichment plots are displayed as difference between the respective sample and the time zero control.

5.4 Results and discussion

5.4.1 Stable carbon isotope ratios of total organic extracts

The stable carbon isotope ratios of the total extractable organic matter in the untreated mat range from -15‰ to -10‰. Kenig (1991) reported bulk $\delta^{13}C$ values of kerogen from microbial mats from a different location within the intertidal area of Abu Dhabi of around -11.8 ± 1.3‰. Overall, $\delta^{13}C$ TOC-values of up to -5‰ (e.g. Schidlowski et al 1984; des Marais et al 1989; Moers et al., 1993) have been reported for microbial mats from various hypersaline environments. The salinity of the water inundating the Gelatinous mat was 200. Due to the high salinity CO_2 may become a limiting nutrient in this water because of reduced solubility and precipitation (Schidlowski et al., 1984, 1985; des Marais et al., 1989; Moers et al., 1993; Schouten et al., 2001). This results in ineffective discrimination against ^{13}C during photosynthesis (Freeman and Hayes, 1992). Consequently, the $\delta^{13}C$ values in the photosynthetic organisms are enriched. Complementary research has shown that this cannot be the only cause for the heavy carbon isotope values as no consistent trends are observed between the isotopic composition of microbial mats living at different salinities (des Marais et al., 1989; Schidlowski et al., 1994).

Fig. 5.4 displays the stable carbon isotope ratios of the total extractable organic matter from the time series with unlabelled bicarbonate. Variations of up to 4‰ were observed during the time of incubation. In layer 1 the variations are most extensive until the dark incubation time starts after about 7 h. Layers 2 and 3 show a slight increase of $\delta^{13}C$ after 30 min of incubation and a stronger decrease after the next

30 min. Then the $\delta^{13}C$ values increase again. During the dark incubation a depletion of ^{13}C was observed, which continues in layer 2 until the next light incubation and the last sampling. In layer 3 the $\delta^{13}C$ value increases towards the 21.5 h sampling and than slightly decreases again.

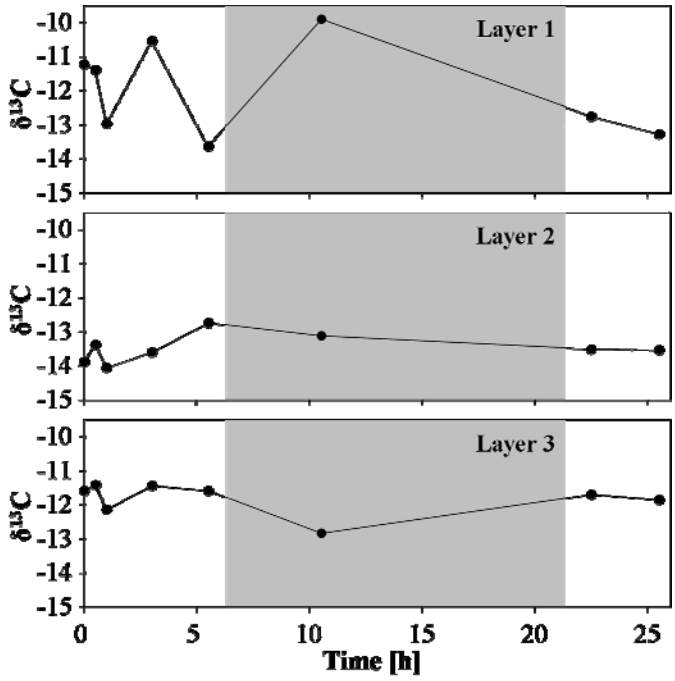

Fig. 5.4. Stable carbon isotope ratios of the total extractable organic carbon of the individual layers over time for incubation with unlabelled bicarbonate (grey area – dark incubation).

Fig. 5.5 shows the incubations with 1% (closed circles), 10% (open circles) and 30% (closed triangles) ^{13}C-bicarbonate. Changes of the $\delta^{13}C$ values are obvious for all three layers. The values were calculated as relative enrichments compared to the time zero. The absolute $\delta^{13}C$ values are listed in Table 5.1. Changes of the carbon isotope ratios during a day-night-day cycle were mainly observed in the uppermost photosynthetic layer. There, enrichment of up to 38‰ was detected at the end of the experiment. In layers 1 and 2 ^{13}C-labelled incubations mainly show the same pattern of enrichment. In layer 2 only the 30% ^{13}C-bicarbonate incubation resulted in a measurable incorporation of ^{13}C in the total extractable organic matter. What is common among all three labelled incubations is that the last sampling shows the highest enrichment. In layer 3, however, even for the incubation with 30% ^{13}C-bicarbonate the variations of the $\delta^{13}C$ values are less than ±1‰ throughout the whole experiment. Therefore, we limited the compound specific stable carbon isotope analysis to layers 1 and 2.

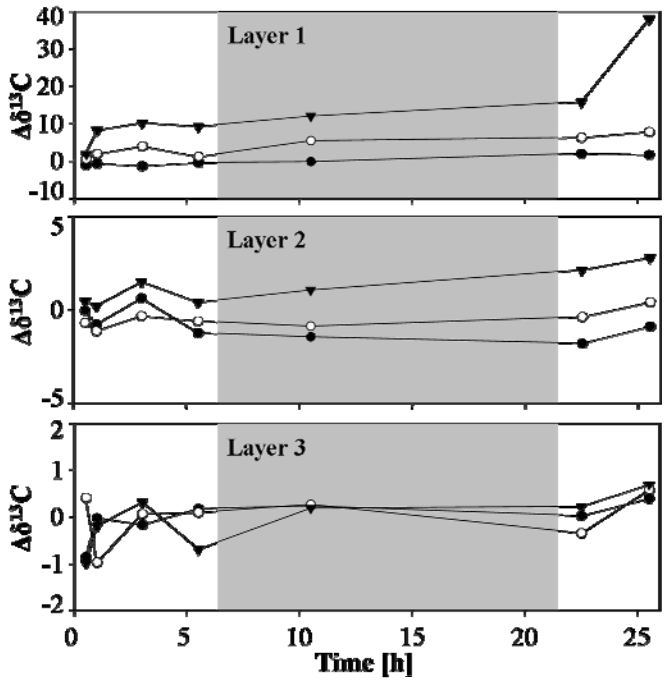

Fig. 5.5. Enrichment plots of ^{13}C in total extractable organic matter from individual layers as a function of time for incubation with 1% (closed circles), 10% (open circles) and 30% (closed triangles) ^{13}C-bicarbonate (grey area – dark incubation).

Table 5.1. $\delta^{13}C$ values of the total extractable organic carbon for layers 1 to 3 with unlabelled and 1%, 10% and 30% ^{13}C-bicarbonate (mean values from duplicate analyses)

Time of sampling [hours after start]	Unlabelled bicarbonate	+ 1% ^{13}C-bicarbonate	+ 10% ^{13}C-bicarbonate	+ 30% ^{13}C-bicarbonate
Layer 1				
0	-11.23	-12.34	-11.52	-11.87
0.5	-11.39	-13.40	-11.05	-10.11
1	-12.97	-13.01	-9.61	-3.62
3	-10.54	-13.64	-7.58	-1.62
5.5	-13.63	-12.80	-10.35	-2.62
10.5	-9.91	-12.56	-6.15	0.09
21.5	-12.76	-10.34	-5.22	3.93
25.5	-13.28	-10.65	-3.69	26.12
Layer 2				
0	-13.88	-12.43	-13.35	-13.92
0.5	-13.38	-12.46	-14.04	-13.43
1	-14.06	-13.20	-14.48	-13.71
3	-13.60	-11.80	-13.68	-12.41
5.5	-12.74	-13.66	-13.95	-13.52
10.5	-13.13	-13.88	-14.23	-12.87
21.5	-13.52	-14.22	-13.73	-11.78
25.5	-13.53	-13.32	-12.94	-11.13
Layer 3				
0	-11.58	-12.09	-12.37	-12.15
0.5	-11.41	-12.94	-11.96	-13.13
1	-12.14	-12.11	-13.34	-12.34
3	-11.44	-12.25	-12.31	-11.83
5.5	-11.58	-11.91	-12.28	-12.84
10.5	-12.84	-11.86	-12.11	-11.97
21.5	-11.70	-12.06	-12.72	-11.93
25.5	-11.85	-11.70	-11.79	-11.46

5.4.2 Stable carbon isotope ratios of major hydrocarbons

The enrichment of ^{13}C in the major hydrocarbons in layer 1 over the time range of the incubation experiment is displayed in Fig. 5.6. Absolute $\delta^{13}C$ values are listed in Table 5.2. The major hydrocarbons selected for compound-specific stable carbon isotope analysis in this study are on the one hand *n*-heptadecane together with an *n*-heptadecene isomer and on the other hand two isomers of *n*-heneicosadiene. The strongest enrichment occurs during the incubation with 30% labelled bicarbonate. Incubation with unlabelled bicarbonate shows a depletion of ^{13}C in *n*-heptadecene and *n*-heptadecane from the beginning of the experiment towards sampling in the dark, for which the most negative $\delta^{13}C$ value was measured. Thus, the $\delta^{13}C$ values of the lipids of the mat organisms become depleted by taking up ^{12}C from the added bicarbonate. Throughout the remainder of the dark incubation ^{13}C becomes enriched in the hydrocarbons but decreases again slightly towards the last sampling time. In the two diunsaturated alkenes the incubation with unlabelled bicarbonate led to an increase in ^{13}C in the first three hours, but towards the next sampling ^{13}C becomes strongly depleted. In the first part of dark incubation the ^{13}C content increases again. Afterwards no significant enrichment or depletion was observed.

The 10% ^{13}C-bicarbonate incubation led to an enrichment of ^{13}C especially in *n*-heptadecene as measured in the 5.5 hour sample. The ^{13}C content stays nearly constant until the dark incubation sampling, but then a decrease was observed in both second day-light incubation samples. Overall, the incubation with 10% ^{13}C-bicarboante leads to an enrichment of less than 10‰ of the $\delta^{13}C$ value in all hydrocarbons. In *n*-heptadecane the enrichment develops over time similar to that in the 30% incubation experiment, but to a lesser extent. In the two *n*-heneicosadienes the shape more closely resembles that measured during the unlabelled incubation. But it is interesting to note, that ^{13}C depletion occurred during the second day-light phase of the 10% ^{13}C-bicarbonate incubation in the two *n*-heneicosadienes. These data are in strong contrast to the other incubations and the behaviour of the other two major hydrocarbons.

Regarding the 30% incubation, *n*-heptadecane and the *n*-heneicosadienes show the same trend as observed for the total organic extract in layer 1 (Fig. 5.5). Actually, the enrichment in *n*-heptadecane and *n*-heneicosadiene (isomer a) exceeds that measured for the total extractable organic matter. Overall, the hydrocarbons *n*-heptadecane and *n*-heneicosadiene mostly show the same trends for all three incubations in layer 1. *n*-Heptadecane and *n*-heptadecene are biomarker compounds assigned to cyanobacteria (e.g. Gelpi et al., 1970; Murata und Nishida, 1987; Shiea et al., 1990, 1991; Grimalt et al., 1992; Köster et al., 1999). *n*-Heneicosadiene emerged

in a previous study of biomarker lipids in the Gelatinous mat as the most abundant hydrocarbons in the uppermost photosynthetic layer (Scherf and Rullkötter, unpubl. results), but remained of unclear origin as these compounds have not been reported before in such high quantities. Even though the occurrence (in minor amounts) in microbial mats was described before (Edmunds and Eglinton, 1984; Boudou et al 1986; Dobson et al., 1988) they cannot be related to a specific organism in the Abu Dhabi mats.

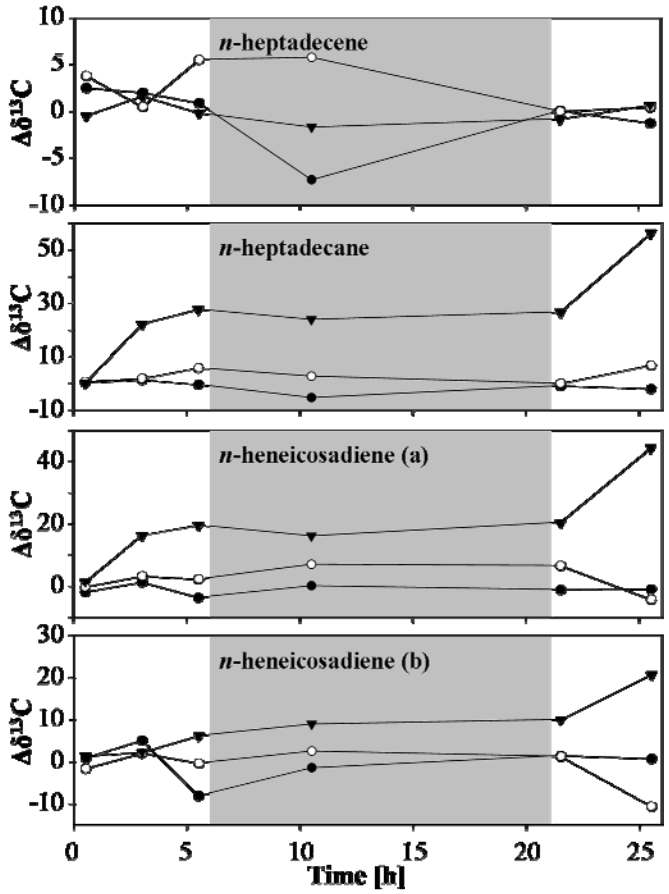

Fig. 5.6. Compound specific enrichment plots of major hydrocarbons from layer 1 as a function of time for incubation with unlabelled bicarbonate (closed circles), 10% (open circles) and 30% (closed triangles) ^{13}C-bicarbonate (grey area – dark incubation).

In Fig. 5.7 the relative enrichment in ^{13}C of the major hydrocarbons in layer 2 are displayed. For incubation with unlabelled bicarbonate a few data points are missing due to very low concentrations. Most remarkable is the overall decrease in ^{13}C content during light incubation in layer 2 in all three hydrocarbons for the incubation with 10% labelled bicarbonate. Towards sampling in the dark a slight enrichment is obvious for *n*-heptadecane, whereas the value stays nearly constant for the *n*-heneicosadienes. Throughout the dark incubation time enrichment of ^{13}C occurs, but the content decreases again during the second day-light incubation. Thus, the ^{13}C from

the substrate may be used in the dark by heterotrophic uptake in the form of metabolites.

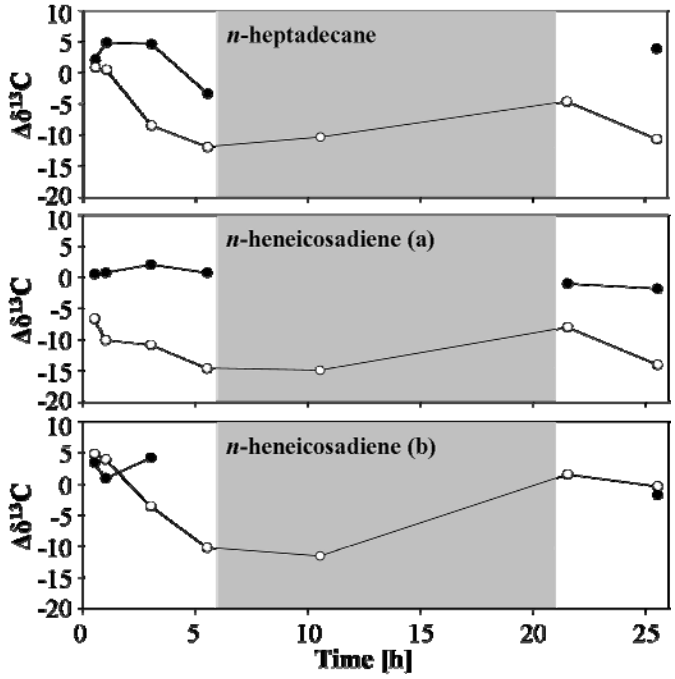

Fig. 5.7. Compound specific enrichment plots of major hydrocarbons from layer 2 as a function of time for incubation with unlabelled bicarbonate (closed circles) and 10% (open circles) ^{13}C-bicarbonate (grey area – dark incubation).

Table 5.2. δ^{13}C values of the major hydrocarbons for layers 1 and 2 with unlabelled, 10% and 30% ^{13}C-bicarbonate (mean values from duplicate analyses, n.d. – not determined, b.d. – below detection)

Time of sampling [hours after start]	Unlabelled bicarbonate	10% ^{13}C-bicarb.	30% ^{13}C-bicarb.	Unlabelled bicarbonate	10% ^{13}C-bicarb.
***n*-heptadecene**		-- Layer 1 --		-- Layer 2 --	
0	-15.9	-23.9	-15.4	n.d.	-18.8
0.5	-13.4	-20.1	-15.9	n.d.	-16.8
1	-15.5	-19.5	-13.8	n.d.	-17.2
3	-13.9	-23.4	-15.6	n.d.	-24.7
5.5	-15	-18.4	-17.2	n.d.	-27.3
10.5	-23.3	-18.2	-16.3	n.d.	-29
21.5	-15.8	b.d.	-14.8	n.d.	-20.7
25.5	-17.2	-23.5	-16.8	n.d.	-29
***n*-heptadecane**					
0	-14.1	-15.6	-14.1	-19	-16.9
0.5	-13.8	-14.9	-14	-16.9	-16.1
1	-15.8	-19.5	8.1	-14.1	-16.5
3	-12.7	-13.8	13.6	-14.4	-25.4
5.5	-14.5	-9.8	9.8	-22.4	-28.9
10.5	-19.4	-12.9	12.6	b.d.	-27.3
21.5	-14.9	b.d.	42.1	b.d.	-21.6
25.5	-16.1	-8.8	18.5	-15.1	-27.6
***n*-heneicosadiene (a)**					
0	-14.9	-16.8	-14.5	-17.2	-13.2
0.5	-17	-17	-13.1	-16.7	-19.9
1	-16.2	-17	1.9	-16.5	-23.3
3	-13.5	-13.6	5.1	-15.2	-24.1
5.5	-18.5	-14.5	1.6	-16.5	-27.9
10.5	-14.7	-9.8	5.9	b.d.	-28.2
21.5	-16	-10.2	29.8	-18.2	-21.3
25.5	-15.8	-21	11.6	-19	-27.3

Table 5.2. continued.

Time of sampling [hours after start]	Unlabelled bicarbonate	10% ^{13}C-bicarb.	30% ^{13}C-bicarb.	Unlabelled bicarbonate	10% ^{13}C-bicarb.
***n*-heneicosadiene (b)**		-- Layer 1 --		-- Layer 2 --	
0	-8.9	-7.7	-7.2	-9	-12
0.5	-8.1	-9.4	-5.8	-5.6	-7.1
1	-7.7	-7.4	-5	-8.1	-8
3	-3.9	-5.7	-1	-4.8	-15.5
5.5	-17.1	-8.1	1.7	b.d.	-22.2
10.5	-10.4	-5.3	2.8	b.d.	-23.6
21.5	-7.5	-6.5	13.5	b.d.	-10.4
25.5	-8.3	-18.4	3	-10.8	-12.3

5.4.3 Stable carbon isotope ratios of major phospholipid fatty acids

The enrichment plots for major phospholipid fatty acids (PLFAs) from layer 1 are displayed in Fig. 5.8. The major PLFAs selected for compound-specific stable carbon isotope analysis in this study are *n*-hexadecanoic acid, *n*-octadecanoic acid, two isomers of *n*-octadecenoic acid and in layer 2 also *cyclo*-nonadecanoic acid. Saturated and unsaturated straight-chain FAMEs with 16 and 18 carbon atoms are common to many microorganisms (Mancuso et al., 1990; Stoeck et al., 2002) and are not specific but widely distributed in cyanobacteria (Thiel et al., 1997; van der Meer et al., 2000). The *cyclo*-propyl fatty acid has been reported as major constituent in sulphate-reducing bacteria as well as other anaerobic bacteria (Volkman and Johns 1977; Findlay and Dobbs 1993, Stoeck et al., 2002; Mallet et al., 2004).

Absolute δ^{13}C values of the PLFAs, listed in Table 5.3, range from -27‰ to -4‰. At the beginning of the incubation experiment compound-specific δ^{13}C values of the major phospholipid fatty acids varied between -20‰ and -12‰. For all fatty acids and both the unlabelled bicarbonate and the 10% ^{13}C-bicarbonate incubation the changes of ^{13}C content can be described as strongly scattering. The incubation with 10% ^{13}C-bicarbonate shows 2‰ enrichment of the ^{13}C content in the *n*-hexadecanoic and *n*-octadecanoic acids after 30 min, followed by depletion within the next 30 min. The highest enrichment overall with 13.2‰ was observed in *n*-octadecanoic acid after three hours of incubation. It is also interesting that the two saturated fatty acids exhibit a strong depletion during the dark incubation period towards the last sampling. *n*-Octadecenoic acid (isomer a) shows the highest enrichment in the dark incubation time, followed by depletion throughout the rest of the dark incubation and another enrichment during the second day-light incubation. For *n*-octadecenoic acid (isomer b) both incubations show parallel enrichment plots with a difference of ca +2‰ between unlabelled and 10% labelled bicarbonate.

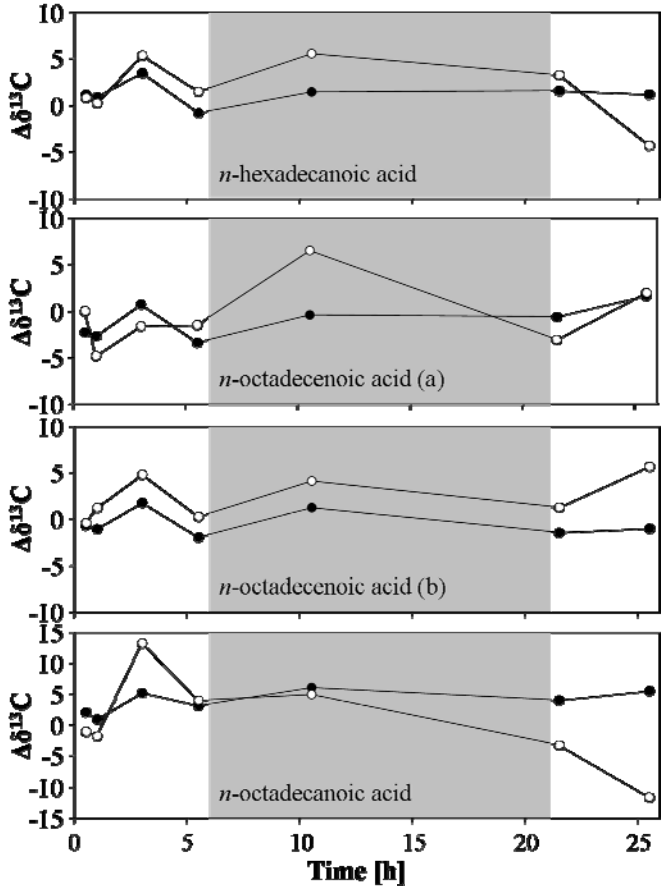

Fig. 5.8. Compound specific enrichment plots of major PLFAs from layer 1 as a function of time for incubation with unlabelled bicarbonate (closed circles) and 10% (open circles) ^{13}C-bicarbonate (grey area – dark incubation).

The enrichment plots of major PLFAs in layer 2 for incubations with unlabelled and 10% ^{13}C-bicarbonate are displayed in Fig. 5.9. The saturated fatty acids (including *cyclo*-nonadecanoic acid) show nearly no change in isotopic composition for the unlabelled incubation, except for a depletion in the three-hour sample. The incubation with 10% ^{13}C-bicarbonate, after an enrichment in the one-hour sample, leads to a continuous depletion until (*n*-hexadecanoic acid) and into (*n*-octadecanoic and *cyclo*-nonadecanoic acid) the dark incubation, respectively. The first second day-light incubation sample shows an enrichment of ^{13}C in all three fatty acids and the enrichment continues towards the last sample except for *n*-octadecanoic acid, in which the ^{13}C content becomes depleted again.

Both *n*-octadecenoic acids show different trends. For these fatty acids enrichment and depletion was observed even upon incubation with unlabelled bicarbonate. In the incubation with 10% ^{13}C-bicarbonate the δ^{13}C values of both fatty acids are less than -21‰ after the initial hour of dark incubation (Table 5.3) and show an increase in ^{13}C within the first 30 min of light incubation. The continuing light incubation leads to different developments of the ^{13}C contents in the two unsaturated fatty acids. *n*-Octadecenoic acid (isomer a) shows a continuous depletion of ^{13}C during

the dark incubation time. In the second day-light incubation sample an increase of ^{13}C was observed. *n*-Octadecenoic acid (isomer b) after one hour of light incubation becomes depleted in ^{13}C followed by another increase. The dark incubation sample is depleted again, but towards the second day-light incubation the enrichment shows the same trend as for the other isomer.

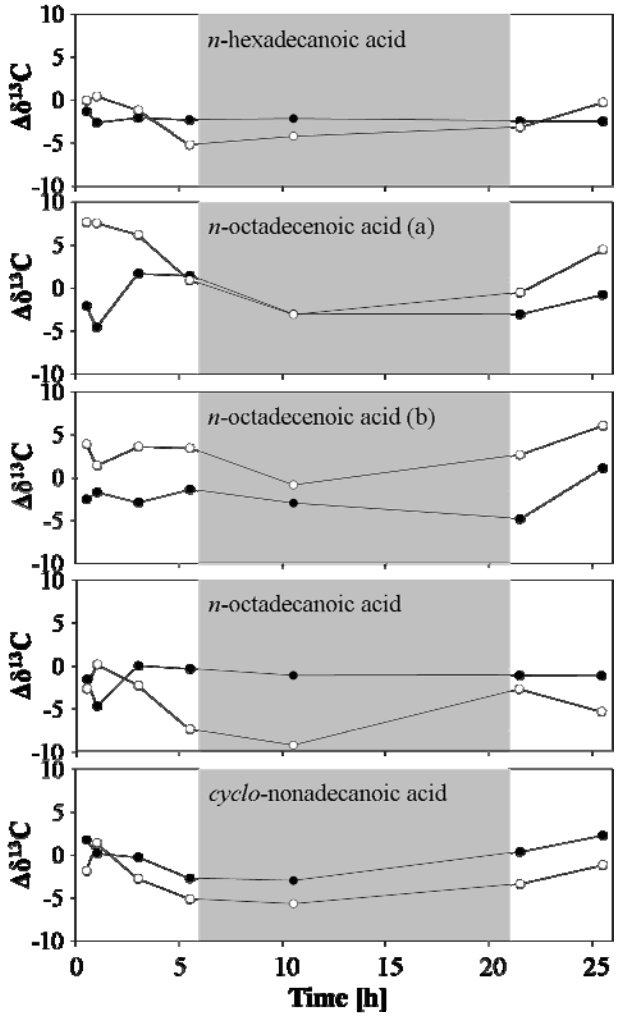

Fig. 5.9. Compound specific enrichment plots of major PLFAs from layer 2 as a function of time for incubation with unlabelled bicarbonate (closed circles) and 10% (open circles) ^{13}C-bicarbonate (grey area – dark incubation).

Altogether, the strongest enrichment of ^{13}C in the fatty acids in layer 1 was observed after the first three hours of light incubation as well as in the dark incubation sample. The last sample, after five hours of light incubation on the second day, shows a strong depletion in the saturated fatty acid compared to the first second day-light incubation sample, whereas the unsaturated fatty acids show an increase in ^{13}C. In layer 2, all fatty acids except *n*-hexadecanoic acid show the dark incubation sample to be most depleted in ^{13}C followed by enrichment towards the end of the experiment. Only *n*-octadecanoic acid shows the same depletion from the first to the second day-

light sample. *n*-Hexadecanoic acid is most depleted in ^{13}C after 5.5 hours of light incubation. Afterwards, the ^{13}C content increases until the end of the experiment.

Table 5.3. $\delta^{13}C$ of the major PLFAs for layers 1 and 2 with unlabelled and 10% ^{13}C-bicarbonate (mean values from duplicate analyses, n.d. – not determined, b.d. – below detection)

Time of sampling [hours after start]	Unlabelled bicarbonate	10% ^{13}C-bicarb.	Unlabelled bicarbonate	10% ^{13}C-bicarb.
***n*-hexadecanoic acid**	-- Layer 1 --		-- Layer 2 --	
0	-17.1	-15.1	-14.4	-17.7
0.5	-15.9	-14.2	-15.7	-17.7
1	-16.2	-14.8	-17.1	-17.2
3	-13.6	-9.67	-16.5	-18.9
5.5	-17.9	-13.6	-16.8	-22.9
10.5	-15.7	-9.5	-16.6	-22
21.5	-15.5	-11.8	-16.9	-20.8
25.5	-15.9	-19.4	-16.9	-18
***n*-octadecenoic acid (a)**				
0	-14.9	-12.8	-14.4	-21.8
0.5	-17.2	-12.8	-16.5	-14.1
1	-17.6	-17.6	-19	-14.2
3	-14.2	-14.4	-12.8	-15.6
5.5	-18.3	-14.3	-13	-20.9
10.5	-15.3	-6.32	-17.5	-24.9
21.5	-15.5	-15.9	-17.5	-22.3
25.5	-13.3	-10.9	-15.2	-17.3
***n*-octadecenoic acid (b)**				
0	-15.9	-14.4	-14.3	-21.3
0.5	-16.6	-14.8	-16.8	-17.4
1	-16.9	-13.1	-16	-19.9
3	-14.1	-9.6	-17.2	-17.7
5.5	-17.9	-14.1	-15.7	-17.9
10.5	-14.7	-10.3	-17.3	-22.2
21.5	-17.3	-13.1	-19.1	-18.7
25.5	-16.9	-8.74	-13.2	-15.3
***n*-octadecanoic acid**				
0	-19.7	-14.4	-17.4	-17.8
0.5	-17.6	-15.4	-19	-20.4
1	-18.7	-16.2	-22.1	-17.6
3	-14.5	-1.17	-17.4	-20
5.5	-16.6	-10.4	-17.8	-25.1
10.5	-13.7	-9.48	-18.6	-27
21.5	-15.7	-17.6	-18.5	-20.4
25.5	-14.2	-26	-18.6	-23.1
***cyclo*-nonadecanoic acid**				
0	n.d.	n.d.	-19.1	-16.7
0.5	n.d.	n.d.	-17.3	-18.5
1	n.d.	n.d.	-18.9	-15.3
3	n.d.	n.d.	-19.4	-19.4
5.5	n.d.	n.d.	-21.8	-21.8
10.5	n.d.	n.d.	-22.1	-22.4
21.5	n.d.	n.d.	-18.7	-20.
25.5	n.d.	n.d.	-16.8	-17.8

5.5 Conclusions

We performed $\delta^{13}C$ analysis of total organic extracts as well as of hydrocarbons and phospholipid ester-linked fatty acids after incubation of a microbial mat with ^{13}C-labelled bicarbonate to determine the development of the isotopic composition as a result of incorporation over a day-night-day cycle. Layer 1 exhibits the most intense

enrichment of ^{13}C in the hydrocarbons as well as in PLFAs. The incubation with the 30% ^{13}C-bicarbonate yielded enrichment plots of *n*-heptadecane and *n*-heneicosadiene which show a shape similar to that for the total extractable organic matter. From these results we conclude that these two hydrocarbons are the major lipids of the constitutive phototrophic microorganisms. From many publications it is clear, that *n*-heptadecane is a cyanobacterial biomarker. *n*-Heneicosadiene is suggested to be contributed by a phototrophic organism, this species being supposed to be on of the major primary producers in the Abu Dhabi mat due to the abundance of its biomarker, but further effort is required to unequivocally identify the source organism.

The incubation with 30% ^{13}C-bicarbonate led during the second day-light incubation in all analysed hydrocarbons in layer 1 to a further enrichment in ^{13}C. For the incubation with 10% ^{13}C-bicarbonate *n*-heptadecane as well as the two mono-unsaturated fatty acids show the same trend, whereas the $\delta^{13}C$ values of the *n*-heneicosadienes and the two saturated fatty acids become depleted in ^{13}C. As this depletion can only be observed for a certain number of the analysed biomarkers we suggest that the source organisms of these biomarkers are most successful in using the natural carbon isotope fractionation and thus, use the ^{12}C from the added substrate. Especially in the *n*-heneicosadienes only minor incorporation of ^{13}C was observed over the whole time of incubation.

In layer 2 mostly a depletion of ^{13}C was observed, which is most pronounced towards the end of the day-light phase or during the night. From this we conclude that assimilation of the label in layer 2 mostly occurs by non-phototrophic, i.e. heterotrophic bacteria, which assimilate and respire ^{13}C during dark incubation. An alternative explanation, suggested by the fact that even *n*-heptadecane shows this enrichment-depletion-trend, is incorporation of label by cyanobacteria through respiration as several cyanobacteria are known to grow heterotrophically in the dark (reviewed by Binder, 1982).

Further analysis should focus on the compound-specific stable carbon isotope analysis of the low molecular weight compounds, which provide information on "cross feeding", e.g. photoassimilation of cyanobacterial products within the mat system.

5.6 Acknowledgements

The authors would like to thank Dr. Dirk de Beer, Dr. Raeid Abed and Katharina Kohls (all Max Planck Institute for Marine Microbiology, Bremen, Germany) and Dr. Waleed Hamza and Huda Al-Hassani (both University of the United Arab Emirates) for their cooperation in the project, Swantje Enge and Steffen Schüler for technical and Bernd Kopke and Dr. Barbara Scholz-Böttcher (all ICBM)

for analytical support as well as Deutsche Forschungsgemeinschaft (DFG) for funding, grant no. RU 458/32.

6 Gesamtbetrachtung

Die Mikrobenmatten, die in der Gezeitenzone der Vereinigten Arabischen Emirate unter extremen Umweltbedingungen wachsen, variieren in ihrer Struktur und Zusammensetzung abhängig von der jeweiligen Position und den damit verbundenen Umweltbedingungen. Es wurde eine Vielzahl morphologisch unterscheidbarer Mikrobenmatten innerhalb des Probennahmeareals identifiziert. Diese Matten beherbergen eine hohe Diversität unterschiedlicher Cyanobakterienarten, welche den durch hohe Salinität, Temperatur, Sonneneinstrahlung und Austrocknung verursachten Umweltstress tolerieren.

6.1 Biomarkerzusammensetzung der Mikrobenmatten

Die biogeochemische Charakterisierung von fünf Mikrobenmatten ergab Lipidzusammensetzungen, die denen anderer Mikrobenmatten aus unterschiedlichen Habitaten weltweit ähneln (z.B. Boon et al., 1983; Cardoso et al., 1976, 1978; Philp et al., 1978; Kenig, 1991; Rontani und Volkman, 2005). Die extrahierbaren Lipide reflektieren die komplexe biogeochemische Zusammensetzung der jeweiligen Matte. Alle Matten sind vorwiegend durch Cyanobakterien aufgebaut, was durch die hohen Gehalte von *n*-Heptadecan und kurzkettigen Monomethylalkanen erkennbar ist. Auch andere Verbindungen konnten ihren Herkunftsorganismen wie autotrophen und heterotrophen Bakterien zugeordnet werden. Die Anwesenheit spezifischer Biomarker gemeinsam mit den physiologischen Bedingungen in der Matte weist auf Biodegradationsprozesse hin. Weiterhin ergaben sich Unterschiede in den Phospholipidfettsäureprofilen, die auf eine Anpassung der Bakterien an die jeweiligen Umweltbedingungen hindeuten.

Die Kohlenstoffisotopenverhältnisse des gesamten extrahierbaren organischen Materials zeigen, dass es an ^{13}C angereichert ist, und weisen somit auf ein CO_2-limitiertes Ökosystem hin. Die alternative Interpretation – die Beteiligung von Bakterien der *Chloroflexus*-Gruppe, welche durch ihren Stoffwechsel bedingt ^{13}C anreichern (van der Meer et al., 2000) – wurde aufgrund des Fehlens spezifischer Biomarker ausgeschlossen.

Die vergleichende Analyse der intakten Matten wurde durch eine Analyse der Biomarkerverteilung über das Vertikalprofil der sogenannten Gelatinösen Matte ergänzt. Diese Matte entstammt der oberen Gezeitenzone und fällt durch ihre besonders ausgeprägte Schichtung auf. Sie wurde unter der Annahme, dass unterschiedlich gefärbte Schichten von unterschiedlichen Artengemeinschaften besiedelt sind, untersucht. Die Tiefenprofile der Biomarker in der Gelatinösen Matte brachten eine Vielzahl an Quellen für das organische Material zum Vorschein und

gaben Einblick in die Zusammensetzung der Mikrobengemeinschaft innerhalb der einzelnen Schichten. Die vertikale Verteilung der Biomarker, welche bestimmten Organismen zugeordnet wurden, die unterschiedliche trophische Ebenen in der Matte repräsentieren, folgt der vermuteten Verteilung entlang der Licht-, Sauerstoff- und Schwefelgradienten in der Matte. Die beiden sauerstoffreichen photosynthetischen Oberflächenschichten sind von Biomarkern geprägt, die auf phototrophe Organismen und speziell auf Cyanobakterien als dominierende Organismen hinweisen. Besonders auffällig ist die hohe Konzentration eines zweifach ungesättigten *n*-Alkens mit 21 Kohlenstoffatomen in der Oberflächenschicht, da dieser Kohlenwasserstoff bisher nicht als spezifischer Biomarker bekannt ist. Aufgrund der hohen Konzentration in der Oberflächenschicht und der wesentlich geringeren Konzentrationen in den tieferen Lagen, wurde ein aerober Organismus als Quelle angenommen. In den Schichten darunter überwiegen die Lipide sulfatreduzierender und von Schwefelpurpurbakterien. Insbesondere die Anwesenheit und Aktivität von sulfatreduzierenden Bakterien wird nicht nur durch die Anwesenheit spezifischer Biomarker belegt, sondern auch durch biodegradierte organische Verbindungen, die bereits direkt unterhalb der obersten Schicht der Mikrobenmatte nachgewiesen wurden. In den tiefsten Lagen unterhalb der aktiven Mikrobenmatte kommt es zur Akkumulation teilweise degradierter Verbindungen und solcher, die wie beispielsweise terrestrische *n*-Alkane vergleichsweise resistent gegenüber dem mikrobiellen Abbau sind.

6.2 Anpassung an die extremen Umweltbedingungen

Durch das Zusammenfügen von Daten aller Kooperationspartner wurde die Anpassung der Mikrobengemeinschaften an die extremen, innerhalb des Untersuchungsgebietes wechselnden Umweltbedingungen nachgewiesen. Diese Anpassung geschieht auf verschiedenen Wegen. In fast allen Matten wurden *Microcoleus chthonoplastes* und *Lyngbya aestuarii* unter anderen als dominante Cyanobakterienarten nachgewiesen. *Microcoleus chthonoplastes* und die nur in der Gelatinösen Matte nachgewiesene *Aphanothece* sp. sind als halo- und thermotolerante Cyanobakterien bekannt (Karsten, 1996; Nübel et al., 2000; Abed et al., 2002a, b). Außerdem wurde das sogenannte „Sonnschutzpigment„ Scytonemin, welches die Zelle vor UV-Strahlung schützt, in allen Matten in unterschiedlichen Mengen nachgewiesen, wobei die Gehalte in den wasserbedeckten Matten wesentlich höher sind als in den trocken liegenden Matten. Von den nachgewiesenen Cyanobakterienarten bilden *Lyngbya aestuarii*, *Entophysalis major* und *Chroococcus* sp. Scytonemin (Fleming und Castenholz, 2007). Somit enthalten alle Matten mindestens zwei Produzenten des Pigments. Des Weiteren verfügen alle Bakterien über die Möglichkeit, ihre Membranlipide an wechselnde Umweltbedingungen

anzupassen. Dies geschieht über die post-synthetische Modifikation der Stereochemie und durch Spaltung von Doppelbindungen der Phospholipidfettsäuren. Ein Beispiel hierfür, das im Rahmen dieser Arbeit nachgewiesen wurde, ist die *cis-trans*-Isomerisierung einer Fettsäuredoppelbindung. Diese beeinflusst durch die Veränderung der Konfiguration maßgeblich die physikalischen Eigenschaften der Zellmembran.

6.3 Cyanobakterien als dominante Primärproduzenten

Aufgrund der extremen Umweltbedingungen, denen die Mikrobenmatten ausgesetzt sind, und der hohen Kohlenstoffisotopenverhältnisse, die auf eine starke Anreicherung an ^{13}C hinweisen, ist der Kohlenstoffmetabolismus in diesen Matten von besonderem Interesse. Inkubationsexperimente mit ^{13}C-Bicarbonat dienen dazu, autotrophe Organismen, die in die Aufnahme von CO_2 involviert sind, ausfindig zu machen (Boschker und Middelburg, 2002). Unter der Annahme, dass die photosynthetischen über die heterotrophen Organismen innerhalb der obersten Mattenschichten überwiegen, wurde solch ein Experiment mit Bicarbonat durchgeführt. Die Kohlenstoffisotopenverhältnisse insbesondere der Einzelverbindungen sollten, gekoppelt mit der Biomarkeranalyse, Aufschluss über die dominanten autotrophen Mirkoorganismen geben. Dazu wurden der organische Gesamtextrakt sowie die Kohlenwasserstofffraktion und die PLFAs nach der Inkubation der Gelatinösen Matte in künstlichem Meerwasser, das mit ^{13}C-markiertem Bicarbonat versetzt war, isotopenmassenspektrometrisch untersucht. Die Inkubation mit 30%igem ^{13}C-Bicarbonat lieferte ähnliche Anreicherungen an ^{13}C im gesamten extrahierbaren organischen Material und in den aliphatischen Kohlenwasserstoffen *n*-Heptadecan und *n*-Heneicosadien. Das lässt vermuten, dass diese zwei dominierenden Lipide die repräsentativen Biomarker der dominierenden autotrophen Organismen sind. *n*-Heptadecan ist seit langem als „Cyanobakterienbiomarker“ bekannt. Der Ursprungsorganismus von *n*-Heneicosadien ist, wie bereits diskutiert, bisher bis auf einige Vermutungen unbekannt.

6.4 Abschließende Zusammenfassung und Ausblick

Frühere Untersuchungen hinsichtlich der mattenbildenden Mikrobengemeinschaften ergaben eine große Anzahl unterschiedlicher Mikroorganismengruppen inklusive diverser Primärproduzenten (Abed et al., 2007, 2008). Die Biomarkeranalyse und das Inkubationsexperiment zeigen hingegen eindeutig, dass Cyanobakterien die mattendominierenden autotrophen Organismen sind. Im Rahmen der geochemischen Charakterisierung wurde eine Vielzahl von Quellen für den Eintrag organischen Materials nachgewiesen. Eine hochauflösende

Analyse der vertikalen Verteilung der Biomarker ergab Tiefenprofile, die dem „Modellaufbau“ einer Mikrobenmatte entsprechen. Ferner ergab die Untersuchung, dass der mikrobielle Abbau organischer Verbindungen ein bedeutender Prozess ist. Die aktive Mikrobenmatte erstreckt sich nur über wenige Millimeter Tiefe - darunter akkumuliert das organische Material. Durch die heterotrophen Prozesse insbesondere in den unteren Schichten herrschen bereits in wenigen Millimetern Tiefe anoxische Bedingungen. Diese ermöglichen besonders gute Erhaltungsbedingungen für das organische Material.

Die Mikrobenmatten aus der Gezeitenzone der Vereinigten Arabischen Emirate sind Vergesellschaftungen einer Vielzahl von Mikroorganismen, die durch ihre Stoffwechselprozesse interagieren. Dass in unmittelbarer Nähe zueinander diese Diversität an morphologisch verschiedenen Mikrobenmatten auftritt, kann auf die Schwankungen der unmittelbaren Umweltbedingungen, bedingt durch die Lage innerhalb der Gezeitenzone, zurückgeführt werden.

Zukünftiges und tiefer reichendes Interesse muss der Isolierung und Kultivierung der unbekannten Mikroorganismen innerhalb der Mattengemeinschaft entgegengebracht werden, um beispielsweise die Herkunft bisher nicht zugeordneter Biomarker wie *n*-Heneicosadien zu ermöglichen. Weiterhin würde eine Analyse der Kohlenstoffisotopenzusammensetzung der niedermolekularen Verbindungen aus dem Inkubationsexperiment zusätzliche Einblicke über „cross-feedings“ wie zum Beispiel die Assimilation cyanobakterieller Ausscheidungsprodukte innerhalb des Mattensystems gewinnen lassen.

7 Literatur

Abdullahi, A.S., Underwood, G.J.C., Gretz, M.R., 2006. Extracellular matrix assembly in diatoms (Bacillariophyceae). V. Environmental effects of polysaccharide synthesis in the model diatom *Phaeodactylum tricornutum*. Journal of Phycology 42, 363-378.

Abed, R.M.M., Garcia-Pichel, F., 2001. Long-term compositional changes after transplant in a microbial mat cyanobacterial community revealed using a polyphasic approach. Environmental Microbiology 3, 53-62.

Abed, R.M.M., Garcia-Pichel, F., Hernández-Mariné, M., 2002a. Polyphasic charaterization of benthic, moderatly halophilic, moderately thermophilic cyanobacteria with very thin trichomes and the proposal of Halomicronema excentricum gen.nov., sp.nov..Archives of Microbiology 177, 361-370.

Abed, R.M.M., Safi, N.M.D., Köster, J., de Beer, D., El-Nahhal, Y., Rullkötter, J., Garcia-Pichel, F., 2002b. Microbial diversity of a heavily polluted microbial mat and its community changes following degradation of petroleum compounds. Applied and Environmental Microbiology 68, 1674-1683.

Abed, R.M.M., Köster, J., 2005. The direct role of aerobic heterotrophic bacteria associated with cyanobacteria in the degradation of oil compounds. International Biodeterioration and Biodegradation 55, 29-37.

Abed, R.M.M., Polerecky, L., Al Najjar, M., de Beer, D., 2006. Effect of temperature on photosynthesis, oxygen consumption and sulphide production in an extremely hypersaline cyanobacterial mat. Aquatic Microbial Ecology 44, 21-30.

Abed, R.M.M., Kohls, K., de Beer, D., 2007. Effect of salinity changes on the bacterial diversity, photosynthesis and oxygen consumption of cyanobacterial mats from an intertidal flat of the Arabian Gulf. Environmental Microbiology 9, 1384-1392.

Abed, R.M.M., Kohls, K., Schoon, R., Scherf, A.-K., Schacht, M., Palinska, K., Al-Hassani, H., Hamza, W., Rullkötter, J., Golubic, S., 2008. Lipid biomarkers, pigments and cyanobacterial diversity of microbial mats across intertidal flats of the arid coast of the Arabian Gulf (Abu Dhabi, UAE). FEMS Microbiology Ecology 65, 449-462.

Alsharhan, A.S., Kendall, C.G.S.C., 2002. Holocene carbonate-evaporites of Abu Dhabi, and their Jurassic ancient analogs. In: Barth, H.-J., Böer, B. (Eds.), Sabkha Ecosystems, Volume 1: The Arabian Peninsula and Adjacent Countries, Tasks for Vegetation Science 36. Kluwer Academic Publishers, Dordrecht, pp. 173-186.

Alsharhan, A.S., Kendall, C.G.S.C., 2003. Holocene coastal carbonates and evaporites of the southern Arabian Gulf and their ancient analogues. Earth-Science Reviews 61, 191-243.

Awramik, S.M., 1984. Ancient stromatolites and microbial mats. In: Cohen, Y., Castenholz, R.W., Halvorson, H.O. (Eds.), Microbial Mats: Stromatolites, Volume 3, MBL Lectures in Biology. Alan R. Liss, New York, pp. 1–22.

Baas, M., Pancost, R., van Geel, B., Sinninghe Damsté, J.S., 2000. A comparative study of lipids in *Sphagnum* species. Organic Geochemistry 31, 535-541.

Barakat, A.O., Rullkötter, J., 1997. A comparative study of molecular paleosalinity indicators: Chromans, tocopherols and C_{20} isoprenoid thiophenes in Miocene lake sediments (Nördlinger Ries, Southern Germany). Aquatic Geochemistry 3, 169-190.

Barth, H.-J., Böer, B., 2002. Introduction. In: Barth, H.-J., Böer, B. (Eds.), Sabkha Ecosystems, Volume 1: The Arabian Peninsula and Adjacent Countries, Tasks of Vegetation Sciences 36. Kluwer Academic Publishers, Dordrecht, pp. 1-5.

Bateson, M.M., Ward, D.M., 1988. Photoexcretion and fate of glycolate in a hot spring cyanobacterial mat. Applied and Environmental Microbiology 54, 1738-1743.

Belt, S.T., Allard, W.G., Massé, G., Robert, J.-M., Rowland, S.J., 2000. Highly branched isoprenoids (HBIs): Identification of the most common and abundant sedimentary isomers. Geochimica et Cosmochimica Acta 64, 3839-3851.

Benlloch, S., López-López, A., Casamayor, E.O., Øvreås, L., Díez, B., Goddard, V.J., Daae, F.L., Smerdon, G., Massana, R., Joint, I., Thingstad, F., Pedrós-Alió, C., Rodríguez-Valera, F. 2002. Prokaryotic genetic diversity throughout the salinity gradient of a coastal solar saltern. Environmental Microbiology 4, 349-360.

Billi, D., Friedmann, E.I., Hofer, K.G., Caiola, M.G., Ocampo-Friedmann, R., 2000. Ionizing-radiation resistance in the desiccation-tolerant cyanobacterium Chroococcidiopsis. Applied and Environmental Microbiology 66, 1489-1492.

Binder, A., 1982. Respiration and photosynthesis in energy-transducing membranes of cyanobacteria. Journal of Bioenergetics and Biomembranes 14, 271-285.

Bird, C.W., Lynch, J.M., Pirt, S.J., Reid, W.W., 1971. The identification of hop-22(29)-ene in prokaryotic organisms. Tetrahedron Letters 34, 3189-3190.

Bligh, E.G., Dyer, W.J., 1959. A rapid method of total lipid extraction and purification. Canadian Journal of Biochemistry and Physiology 37, 911-917.

Blumer, M., Guillard, R.R.L., Chase, T., 1971. Hydrocarbons of marine phytoplankton. Marine Biology 8, 183-189.

Boon, J.J., de Leeuw, J.W., 1987. Organic geochemical aspects of cyanobacterial mats. In: Fay, F., van Baalen, C. (Eds.), The Cyanobacteria. Elsevier, Amsterdam, pp. 471-492.

Boon, J.J., Hines, H., Burlingame, A.L., Klok, J., Rijpstra, W.I.C., de Leeuw, J.W., Edmunds, K.E., Eglinton, G., 1983. Organic geochemical studies of Solar Lake laminated cyanobacterial mats. In: Bjorøy, M. et al. (Eds.), Advances in Organic Geochemistry 1981. John Wiley and Sons, Chichester, pp. 207-227.

Boschker, H.T.S., Middelburg, J.J., 2002. Stable isotopes and biomarkers in microbial ecology. FEMS Microbiology Ecology 40, 85-95.

Boschker, H.T.S., Nold, S.C., Wellsbury, P., Bos, D., de Graaf, W., Pel, R., Parkes, R.J., Cappenberg, T.E., 1998. Direct linking of microbial populations to specific biogeochemical processes by ^{13}C-labelling of biomarkers. Nature 392, 801-805.

Boudou, J.P., Trichet, J., Robinson, N., Brassell, S.C., 1985. Lipid composition of a recent Polynesian microbial mat sequence. Organic Geochemistry 10, 705-709.

Boudou, J.P., Trichet, J., Robinson, N., Brassell, S.C., 1986. Profile of aliphatic hydrocarbons in a recent Polynesian microbial mat. International Journal of Environmental Analytical Chemistry 26, 137-155.

Brock, T.D., 1987. The study of microorganisms in situ: Progress and problems. In: Fletcher, M., Gray, T.R.G., Jones, J.G. (Eds.), Ecology of Microbial

Communities, Forty-first Symposium of the Society for General Microbiology. Cambridge University Press, pp. 1-17.

Bush, P., 1973. Some aspects of the diagenetic history of the sabkha in Abu Dhabi, Persian Gulf. In: Purser, B.H. (Ed.), The Persian Gulf. Springer, Berlin, pp. 395-407.

Butler, G.P., 1969. Modern evaporite deposition and geochemistry of coexisting brines, the sabkha, Trucial Coast, Arabian Gulf. Journal of Sedimentary Petrology 39, 70-89.

Canfield, D.E., des Marais, D.J., 1993. Biogeochemical cycles of carbon, sulfur, and free oxygen in a microbial mat. Geochimica et Cosmochimica Acta 57, 3971-3984.

Canfield, D.E., des Marais, D.J., 1994. Cycling of carbon, sulfur, oxygen and nutrients in a microbial mat. In: Stal, L.J., Caumette, P. (Eds.), Microbial Mats, G 35, NATO ASI Series. Springer, Berlin, pp. 255-263.

Cardoso, J.N., Brooks, P.W., Eglinton, G., Goodfellow, R., Maxwell, J.R., 1976. Lipids of recently-deposited algal mats at Laguna Mormona, Baja California. In: Nriagu, J.O. (Ed.), Environmental Biogeochemistry, Volume1: Carbon, Nitrogen, Phosphorus, Sulfur and Selenium Cycles. Ann Arbor Science Publishers, Ann Arbor, Michigan, pp. 149-174.

Cardoso, J.N., Gaskell, S.J., Quirk, M.M., Eglinton, G., 1983. Hydrocarbon and fatty acid distributions in Rostherne lake sediments (England). Chemical Geology 38, 107-128.

Cardoso, J.N., Watts, C.D., Maxwell, J.R., Goodfellow, R., Eglinton, G., Golubic, S., 1978. A biogeochemical study of the Abu Dhabi algal mats: A simplified ecosystem. Chemical Geology 23, 273-291.

Castenholz, R.W., 1981. Isolation and cultivation of thermophilic cyanobacteria. In: Starr, M.P., Stolp, H., Trüper, H.G., Balows, A., Schlegel, H.G. (Eds), Prokaryotes. Volume 1, Springer, Berlin, pp. 236-246.

Castenholz, R.W., 2001. General characterization of the cyanobacteria. In: Boone, D.R., Castenholz, R.W. (Eds.), Bergey's Manual of Systematic Bacteriology, Volume 1, 2nd Edition. Springer, New York, pp. 474-487.

Chiffings, A.W., 1995. Arabian Seas. In: Kelleher, G., Bleakley, C., Wells, S. (Eds.), A Global Representative System of Marine Protected Areas, Volume 3. The Great Barrier Reef Marine Park Authority, World Bank and IUCN, Washington, D.C., pp. 39-71.

Chuecas, L., Riley, J.P., 1969. Component fatty acids of the total lipids of some marine phytoplankton. Journal of the Marine and Biological Association of the United Kingdom 49, 97-116.

Cohen, Y., 1984. The Solar Lake cyanobacterial mats: Strategies of photosynthetic life under sulfide. In: Cohen, Y., Castenholz, R.W., Halvorson, H.O. (Eds.), Microbial Mats: Stromatolites, Volume 3, MBL Lectures in Biology. Alan R. Liss, New York, pp. 133-148.

Cohen, Y., 1989. Photosynthesis in cyanobacterial mats and its relation to the sulphur cycle: A model for microbial sulphur interactions. In: Cohen, Y., Rosenberg, E. (Eds.), Microbial Mats: Physiological Ecology of Benthic Microbial Communities. American Society for Microbiology, Washington, D.C., pp. 22-36.

Cohen, Y., Rosenberg, E., 1989. Microbial Mats: Physiological Ecology of Benthic Microbial Communities. American Society of Microbioloy, Washington, D.C.

Cohen, Y., Jørgensen, B.B., Revsbech, N.P., Poplawski, R., 1986. Adaptation to hydrogen sulfide of oxygenic and anoxygenic photosynthesis among cyanobacteria. Applied and Environmental Microbiology 51, 398-407.

Cole, J.R., Chai, B., Marsh, T.L., 2003. The Ribosomal Database Project (RDP-II) : Previewing a new autoaligner that allows regular updates and the new prokarytic taxonomy. Nucleic Acids Research 31, 442-443.

Collins, M.D., Jones, D., 1981. Distribution of isoprenoid quinone structural types in bacteria and their taxonomic implications. Microbiological Reviews 45, 316-354.

Collister, J.W., Rieley, G., Stern, B., Eglinton, G., Fry, B., 1994. Compound specific $\delta^{13}C$ analyses of leaf lipids from plants with differing carbon dioxide metabolisms. Organic Geochemistry 21, 619-627.

Cranwell, P.A., 1973. Chain-length distribution of *n*-alkanes from lake sediments in relation to postglacial environments. Freshwater Biology 3, 259-265.

Cranwell, P.A., 1974. Monocarboxcylic acids in lake sediments, indicators, derived from terrestrial and aquatic biota, of paleoenvironmental trophic levels. Chemical Geology 14, 1-14.

Dastillung, M., Albrecht, P., 1977. Δ^2-Sterenes as diagenetic intermediates in sediments. Nature 269, 678-679.

de Leeuw, J.W., Cox, J.C., van Graas, G., van der Meer, F.W., Peakman, T.M., Baas, J.M.A., van de Graaf, B., 1989. Limited double bond isomerisation and selective hydrogenation of sterenes during early diagenesis. Geochimica et Cosmochimica Acta 53, 903-909.

de Wit, R., van Gemerden, H., 1988. Growth and metabolism of the purple sulfur bacterium *Thiocapsa roseopersicina* under combined light/dark and oxic/anoxic regimens. Archives of Microbiology 154, 459-464.

Denich, T.J., Beaudette, L.A., Lee, H., Trevors, J.T., 2003. Effect of selected environmental and physico-chemical factors on bacterial cytoplasmic membranes (Review). Journal of Microbiological Methods 52, 149-182.

des Marais, D.J., 1995. The biogeochemistry of hypersaline microbial mats. In: Jones, G.B. (Ed.), Advances in Microbial Ecology, Volume 14. Plenum Press, New York, pp. 251-274.

des Marais, D.J., Cohen, Y., Nguyen, H., Cheatham, M., Cheatham, T., Munoz, E., 1989. Carbon isotopic trends in the hypersaline ponds and microbial mats at Guerrero Negro, Baja California Sur, Mexico: Implications for Precambrian stromatolites. In: Cohen, Y., Rosenberg, E. (Eds.), Microbial Mats: Physiological Ecology of Benthic Microbial Communities. American Society for Microbiology, Washington, D.C., pp. 191-206.

Dillon, J.G., Tatsumi, C.M., Tandingan, P.G., Castenholz, R.W., 2002. Effect of environmental factors on the synthesis of scytonemin, a UV-screening pigment, in a cyanobacterium (*Chroococcidiopsis* sp.). Archives of Microbiology 177, 322-331.

Dobson, G., Ward, D.M., Robinson, N., Eglinton, G., 1988. Biogeochemistry of hot spring environments: Extractable lipids of a cyanobacterial mat. Chemical Geology 68, 155-179.

Edmunds, K.L.H., Eglinton, G., 1984. Microbial lipids and carotenoids and their early diagenesis in the Solar Lake laminated microbial mat sequence. In: Cohen, Y., Castenholz, R.W., Halvorson, H.O. (Eds.), Microbial Mats: Stromatolites, Volume 3, MBL Lectures in Biology. Alan R. Liss, New York, pp. 343-390.

Eglinton, G., Calvin, M., 1967. Chemical fossils. Scientific American 216, 32.

Eglinton, G., Hamilton, R.J., 1967. Leaf epicuticular waxes. Science 156, 1322-1335.

Evans, G., Kirkham, A., 2002. The Abu Dhabi sabkha. In: Barth, H.-J., Böer, B. (Eds.), Sabkha Ecosystems, Volume 1: The Arabian Peninsula and Adjacent Countries, Tasks for Vegetation Science 36. Kluwer Academic Publishers, Dordrecht, pp. 7-20.

Evans, G., Schmidt, V., Bush, P., Nelson, H., 1969. Stratigraphy and geological history of the sabkha, Abu Dhabi, Persian Gulf. Sedimentology 12, 145-159.

Evershed, R.P., Crossman, Z.M., Bull, I.D., Mottram, H., Dungait, J.A.J., Maxfield, P.J., Brennand, E.L., 2006. ^{13}C-labelling of lipids to investigate microbial communities in the environment. Current Opinion in Biotechnology 17, 72-82.

Fang, J., Findlay, R.H., 1996. The use of a classic lipid extraction method for the simultaneous recovery of organic pollutants and microbial lipids from sediments. Journal of Microbiological Methods 27, 63-71.

Fang, J., Barcelona, M.J., Alvares, P.J.J., 2000. A direct comparison between fatty acid analysis and intact phospholipid profiling for microbial identification. Organic Geochemistry 31, 881-887.

Farmer, J.D., 1992. Grazing and bioturbation in modern microbial mats. In: Schopf, J.W., Klein, C. (Eds). The Proterozoic Biosphere: A Multidisciplinary Study. Cambridge University Press, Cambridge, pp. 295-297.

Ferris, M.J., Muyzer, G., Ward, D.M., 1996. Denaturing gradient gel electrophoresis profiles of 16S rRNA-defined populations inhabiting a hot spring microbial mat community. Applied and Environmental Microbiology 62, 340-346.

Ficken, K.J., Barber, K.E., Eglinton, G., 1998. Lipid biomarker, δ^{13}C and plant macrofossil stratigraphy of a Scottish montane peat bog over the last two millennia. Organic Geochemistry 28, 217-237.

Findlay, R.H., Dobbs, F.C., 1993. Quantitative description of microbial communities using lipid analysis. In: Kemp, P.F., Sherr, B.F., Sherr, E.B., Cole, J.J. (Eds.), Handbook of Methods in Aquatic Microbial Ecology. Lewis Publishers, Boca Raton, Florida, pp. 271-284.

Fleming, E.D., Castenholz, R.W., 2007. Effects of periodic desiccation on the synthesis of the UV-screening compound, scytonemin, in cyanobacteria. Environmental Microbiology 9, 1448-1455.

Fleming, E.D., Bebout, B.M., Castenholz, R.W., 2007. Effects of salinity and light intensity on the resumption of photosynthesis in rehydrated cyanobacterial mats from Baja California Sur, Mexico. Journal of Phycology 43, 15-24.

Fourçans, A., García de Oteyza, T., Wieland, A., Solé, A., Diestra, E., van Bleijswijk, J., Grimalt, J.O., Kühl, M., Esteve, I., Muyzer, G., 2004. Characterization of functional bacterial groups in a hypersaline microbial mat community (Salins-de-Giraud, Camargue, France). FEMS Microbiology Ecology 51, 55.

Freeman, K.H., Hayes, J.M., 1992. Fractionation of carbon isotopes by phytoplankton and estimates of ancient CO_2 levels. Global Biogeochemical Cycles 6, 185-198.

Freese E., Rütters H., Köster J., Rullkötter J., Sass H., 2008a. *Gammaproteobacteria* as a potential source of eicosapentaenoic acid in anoxic intertidal sediments. Microbial Ecology, DOI 10.1007/s00248-008-9443-2

Freese, E., Sass, H., Rütters, H., Schledjewski, R., Rullkötter, J., 2008b. Variable temperature-related changes in fatty acid composition of bacterial isolates from German Wadden Sea sediments representing different bacterial phyla. Organic Geochemistry 39, 1427-1438.

Friedman, G.M., Krumbein, W.E. (Eds.), 1985. Hypersaline Ecosystems: The Gavish Sabkha. Springer, Berlin.

Fuerst, J.A., Hawkins, J.A., Holmes, A., Sly, L.I., Moore, C.J., Stackebrandt, E., 1993. *Porphyrobacter neustonensis* gen. nov., sp. nov., an aerobic bacteriochlorophyll-synthesizing budding bacterium from fresh water. International Journal of Systematic Bacteriology 43, 125-134.

Garcia-Pichel, F., Pringault, O., 2001. Cyanobacteria track water in desert soils. Nature 413, 380-381.

Gaskell, S.J., Eglinton, G., 1975. Rapid hydrogenation of sterols in a contemporary lacustrine sediment. Nature 254, 209-211.

Geitler, L. 1932. Cyanophyceae. In: Kolkwitz, R. (Ed.), Rabenhorst's Kryptogamenflora von Deutschland, Österreich und der Schweiz, Band 14. Akademischer Verlag, Leipzig.

Gelpi, E., Schneider, H., Mann, J., Oró, J., 1970. Hydrocarbons of geochemical significance in microscopic algae. Phytochemistry 9, 603-612.

Glennie, K.W., 2001. Evolution of the Emirates' land surface: An introduction. In: Al Abed, I., Hellyer, P. (Eds.), United Arab Emirates: A new Perspective. Trident Press Ltd., London, pp. 9-27.

Golubic, S., 1976. Organisms that build stromatolites. In: Walter, M.R. (Ed.), Stromatolites: Developments in Sedimentology. Elsevier, Amsterdam, pp. 421-433.

Golubic, S., 1991. Microbial mats of Abu Dhabi. In: Margulis, L., Olendzenski, L. (Eds.), Environmental Evolution: Effects of the Origin and Evolution of Life on Planet Earth. MIT Press, Cambridge, pp. 103-129.

Grilli Caiola, M., Billi, D., Freidmann, E.I., 1996. Effect of desiccation on envelopes of the cyanobacterium *Chroococcidiopsis* sp. (*Chroococcales*). European Journal of Phycology 31, 97-105.

Grimalt, J.O., de Wit, R., Teixidor, P., Albaiges, J., 1992. Lipid biogeochemistry of *Phormidium* and *Microcoleus* mats. Organic Geochemistry 19, 509-530.

Grogan, D.W., Cronan Jr., J.E., 1997. *Cyclo*propane ring formation in membrane lipids of bacteria. Microbiology and Molecular Biology Reviews 61, 429-441.

Grossi, V., Hirschler, A., Raphel, D., Rontani, J.-F., de Leeuw, J.W., Bertrand, J.C., 1998. Biotransformation pathways of phytol in recent anoxic sediments. Organic Geochemistry 29, 845-861.

Guckert, J.B., Antworth, C.P., Nichols, P.D., White, D.C., 1985. Phospholipid, ester-linked fatty acid profiles as reproducible assays for changes in prokaryotic community structure of estuarine sediments. FEMS Microbiology Letters 31, 147-158.

Hall, R.O.J., 1995. Use of a stable carbon isotope addition to trace bacterial carbon through a stream food web. Journal of the North American Benthological Society 14, 269-277.

Han, J., McCarthy, E.D., van Hoeven, W., Calvin, M., Bradley, W.H., 1968. Organic geochemical studies, II. A preliminary report on the distribution of aliphatic hydrocarbons in algae, in bacteria and in a recent lake sediment. Proceedings of the National Academy of Sciences 59, 29-33.

Harwood, J.L., Russell, N.J., 1984. Lipids in Plants and Microbes. George Allen & Unwin, London.

Hayes, J.M., 1993. Factors controlling ^{13}C contents of sedimentary organic compounds: Principles and evidence. Marine Geology 113, 111-125.

Hefter, J., Thiel, V., Jenisch, A., Galling, U., Kempe, S., Michaelis, W., 1993. Biomarker indications for microbial contribution to recent and late Jurassic carbonate deposits. Facies 29, 93-106.

Heipieper, H.J., Meulenbeld, G., Oirschot, Q.V., de Bont, J.A.M., 1996. Effect of environmental factors on the *trans*/*cis* ratio of unsaturated fatty acids in *Pseudomonas putida* S12. Applied and Environmental Microbiology 62, 2773-2777.

Hiraishi, A., 1999. Isoprenoid quinones as biomarkers of microbial populations in the environment. Journal of Bioscience and Bioengineering 88, 449-460.

Hoffmann, L., 1996. Recolonisation of the intertidal flats by microbial mats after the Gulf War oil spill. In: Krupp, F., Abuzinada, A.H., Nader, I.A. (Eds.), A Marine Wildlife Sanctuary for the Arabian Gulf. Environmental Research and Conservation Following the 1991 Gulf War Oil Spill. Senckenbergische Naturforschende Gesellschaft, Frankfurt a.M., pp. 96-115.

Holo, H., Sirevåg, R., 1986. Autotrophic growth and CO_2 fixation of *Chloroflexus auranticus*. Archives of Microbiology 145, 173-180.

Höpner, T., Yousef, M., Berthe-Corti, L., Felzmann, H., Struck, H., Al-Thukair, A., 1996. Cyanobacterial mats on oil polluted sediments: Start of a promising self remediation process? In: Krupp, F., Abuzinada, A.H., Nader, I.A. (Eds.), A Marine Wildlife Sanctuary for the Arabian Gulf. Environmental Research and

Conservation Following the 1991 Gulf War Oil Spill. Senckenbergische Naturforschende Gesellschaft, Frankfurt a.M., pp. 85-95.

Huang, W.-Y., Meinschein, W.G., 1976. Sterols as source indicators of organic materials in sediments. Geochimica et Cosmochimica Acta 40, 323-330.

Huang, W.-Y., Meinschein, W.G., 1979. Sterols as ecological indicators. Geochimica et Cosmochimica Acta 43, 739-745.

Huflejt, M.E., Tremolieres, A., Pineau, B., Lang, J.K., Hatheway, J., Packer, L., 1990. Changes in membrane lipid composition during saline growth of the fresh water cyanobacterium *Synechococcus* 6311. Plant Physiology 94, 1512-1521.

Jahnke, L.L., Embaye, T., Hope, J., Turk, K.A., van Zuilen, M., des Marais, D.J., Farmer, J.D., Summons, R.E., 2004. Lipid biomarker and carbon isotopic signature for stromatolite-forming, microbial mat communities and *Phormidium* cultures from Yellowstone National Park. Geobiology 2, 31-47.

Javor, B., Castenholz, R.W., 1981. Laminated microbial mats, Laguna Guerrero Negro, Mexico. Geomicrobiology Journal 2, 237-273.

Javor, B.J., Castenholz, R.W., 1984. Invertebrate grazers of microbial mat, Laguna Guerrero Negro, Mexico. In: Cohen, Y., Castenholz, R.W., Halvorson, H.O. (Eds.), Microbial mats: Stromatolites, Volume 3. Alan R Liss, New York, pp. 85-94.

Jensen, J., Revsbech, N.P., 1989. Photosynthesis and respiration of a diatom biofilm cultured in a new gradient growth chamber. FEMS Microbiology Ecology 62, 29-38.

Jørgensen, B.B., Cohen, Y., 1977. Solar Lake (Sinai). 5. Sulfur cycle of benthic cyanobacterial mats. Limnology and Oceanography 22, 657-666.

Jørgensen, B.B., des Marais, D.J., 1986. Competition for sulfide among colorless and purple sulfur bacteria in cyanobacterial mats. FEMS Microbiology Ecology 38, 179-186.

Kannenberg, E.L., Poralla, K., 1999. Hopanoid biosynthesis and function in bacteria. Naturwissenschaften 86, 168-176.

Karsten, U., 1996. Growth and organic osmolytes of geographically different isolates of *Microcoleus chthonoplastes* (Cyanobacteria) from benthic microbial mats: Response to salinity change. Journal of Phycology 32, 501-506.

Karsten, U., Kühl, M., 1996. Die Mikrobenmatte - das kleinste Ökosystem der Welt. Biologie in unserer Zeit 26, 16-26.

Kaur, A., Chaudhary, A., Kaur, A., Choudhary, R., Kaushik, R., 2005. Phospholipid fatty acid - a bioindicator of environment monitoring and assessment in soil ecosystem. Current Science 89, 1103-1112.

Kendall, C.G.S.C., Skipwith, Sir P.A.d'E., 1968. Recent algal mats of a Persian Gulf lagoon. Journal of Sedimentary Petrology 38, 1040-1058.

Kendall, C.G.S.C., Skipwith, Sir P.A.d'E., 1969. Geomorphology of a recent shallow-water carbonate province: Khor al Bazam, Trucial Coast, Southwest Persian Gulf. Geological Society of America Bulletin 80, 865-891.

Kendall, C.G.S.C., Skipwith, Sir P.A.d'E., 1969. Holocene shallow-water carbonate and evaporite sediments of Khor al Bazam, Abu Dhabi, Southwest Persian Gulf. AAPG Bulletin 53, 841-869.

Kendall, C.G.S.C., Alsharhan, A.S., Cohen, A., 2002. The Holocene tidal flat complex of the Arabian Gulf coast of Abu Dhabi. In: Barth, H.-J., Böer, B. (Eds.), Sabkha Ecosystems, Volume 1: The Arabian Peninsula and Adjacent Countries, Tasks for Vegetation Science 36. Kluwer Academic Publishers, Dordrecht, pp. 21-36.

Kenig, F., 1991. Sédimentation, distribution et diagenèse da la matière organinique dans un environnement carbonaté hypersalin: Le système lagune-sabkha d'Abu Dhabi. Thèse. Université d'Orléans, France.

Kenig, F., 2000. C_{16} - C_{29} homologues series of monomethylalkanes in the pyrolysis products of a Holocene microbial mat. Organic Geochemistry 31, 237-241.

Kenig, F., Huc, A.Y., Purser, B.H., Oudin, J.-L., 1990. Sedimentation, distribution and diagenesis of organic matter in a recent carbonate environment, Abu Dhabi, U.A.E. Organic Geochemistry 16, 735-747.

Kenig, F., Sinninghe Damsté, J.S., de Leeuw, J.W., Hayes, J.M., 1994. Molecular palaeontological evidence for food-web relationships. Naturwissenschaften 81, 128-130.

Kenig, F., Sinninghe Damsté, J.S., Frewin, N.L., Hayes, J.M., de Leeuw, J.W., 1995. Molecular indicators for palaeoenvironmental change in a Messinian evaporitic sequence (Vena del Gesso, Italy). II: High-resolution variations in abundance and ^{13}C contents of free and sulphur-bound carbon skeletons in a single marl bed. Organic Geochemistry 23, 485-526.

Kenig, F., Sinninghe Damsté, J.S., Kock-van Dalen, A.C., Rijpstra, W.I.C., Huc, A.Y., de Leeuw, J.W., 1995. Occurrence and origin of mono-, di-, and trimethylalkanes in modern and Holocene cyanobacterial mats from Abu Dhabi, United Arab Emirates. Geochimica et Cosmochimica Acta 59, 2999-3015.

Khomutov, G., Fry,, I.V., Huflejt, M.E., Packer, L., 1990. Membrane lipid composition, fluidity, and surface charge changes in response to growth of the fresh water cyanobacterium *Synechococcus* 6311 under high salinity. Archives of Biochemistry and Biophysics 277, 263-267.

Kinsman, D.J.J., Park, R.K., 1976. Algal belt and coastal sabkha evolution, trucial coast, Persian Gulf. In: Walter, M.R. (Ed.), Stromatolites, Developments of Sedimentology. Elsevier, Amsterdam, pp. 421-433.

Klatt, C.G., Brayant, D.A., Ward, D.M., 2007. Comparative genomics provides evidence for the 3-hydroxypropionate autotrophic pathway in filamentous anoxygenic phototrophic bacteria and in hot spring microbial mats. Environmental Microbiology 9, 2067-2078.

Komárek, J., Anagnostidis, K., 1999. Cyanoprokaryota, 1.Teil. *Chroococcales*. In: Ettl, H., Gärtner, G., Heynig, H., Mollenhauer, D. (Eds.), Süßwasserflora von Mitteleuropa. Gustav Fischer Verlag, Jena, pp. 1-548.

Komárek, J., Anagnostidis, K., 2005. Cyanoprokaryota, 2.Teil. *Oscillatoria*. In: Büdel, B., Gärtner, G., Krienitz, L., Schlager, M. (Eds.), Süßwasserflora von Mitteleuropa. Elsevier, München, pp. 1-759.

Köster, J., Volkman, J.K., Rullkötter, J., Scholz-Böttcher, B.M., Rethmeier, J., Fischer, U., 1999. Mono-, di- and trimethyl-branched alkanes in cultures of the

filamentous cyanobacterium *Calothrix scopulorum*. Organic Geochemistry 30, 1367-1379.

Krumbein, W.E., 1983. Stromatolites - the challenge of a term in space and time. Precambrian Research 20, 493-531.

Kühl, M., Fenchel, T., Kazmiercza, J., 2003. Structure, function, and calcification potential of an artificial cyanobacterial mat. In: Krumbein, W.E., Paterson, D.W., Zavarzin, G.A. (Eds.), Fossil and Recent Biofilms - A Natural History of Life on Earth. Kluwer Academic Publishers, Dordrecht, pp. 77-102.

Lechevalier, M.P., 1977. Lipids in bacterial taxonomy - a taxonomist's review. CRC Critical Reviews in Microbiology 5, 109-210.

Lipp, J.S., 2008. Intact membrane lipids as tracers for microbial life in the marine deep biosphere. PhD thesis, University of Bremen, Germany.

Liu, H., Buskey, E.J., 2000. Hypersalinity enhances the production of extracellular polymeric substance (EPS) in the Texas brown tide alga *Aureoumbra lagunensis* (Pelagophyceae). Journal of Phycology 36, 71-77.

Ludwig, W., Strunk, O., Klugbauer, S., Klugbauer, N., Weizenegger, M., Neumaier, J., Bachleitner, M., Schleifer, K.H., 1998. Bacterial phylogeny based on comparative sequence analysis. Electrophoresis 19, 554-568.

Madigan, M.T., Takigiku, R., Lee, R.G., Gest, H., Hayes, J.M., 1989. Carbon isotope fractionation by thermophilic phototrophic sulphur bacteria: Evidence for autotrophic growth in natural populations. Applied and Environmental Microbiology 55, 639-644.

Mallet, C., Basset, M., Fonty, G., Desvilettes, C., Bourdier, G., Debroas, D., 2004. Microbial population dynamics in the sediments of a eutrophic lake (Aydat, France) and characterization of some heterotrophic bacterial isolates. Microbial Ecology 48, 66-77.

Mancuso, C.A., Franzmann, P.D., Burton, H.R., Nichols, P.D., 1990. Microbial community structure and biomass estimates of a methanogenic Antarctic Lake ecosystem as determined by phospholipid analyses. Microbial Ecology 19, 73-95.

Mangelsdorf, K., Zink, K.-G., Birrien, J.-L., Toffin, L., 2005. A quantitative assessment of pressure dependent adaptive changes in the membrane lipids of a piezosensitive deep sub-seafloor bacterium. Organic Geochemistry 36, 1459-1479.

Marchand, D., Rontani, J.-F., 2003. Visible light-induced oxidation of lipid components on purple sulfur bacteria: A significant process in microbial mats. Organic Geochemistry 34, 61-79.

Margulis, L., Barghoorn, E.S., Ashendorf, D., Banerjee, S., Chase, D., Francis, S., Giovannoni, S., Stolz, J., 1980. The microbial community in the layered sediments at Laguna Figueroa, Baja California, Mexico: Does it have Precambrian analogues? Precambrian Research 11, 93-123.

Mercer, E.I., London, R.A., Kent, I.S.A., Taylor, A.J., 1974. Sterols, sterol esters and fatty acids of *Botrydium granulatum*, *Tribonema aequale* and *Monodus Subterraneus*. Phytochemistry 13, 845-852.

Middelburg, J.J., Barranguet, C., Boschker, H.T.S., Herman, P.M.J., Moens, T., Heip, C.H.R., 2000. The fate of intertidal microphytobenthos carbon: An in situ ^{13}C-labeling study. Limnology and Oceanography 45, 1224-1234.

Moers, M.E.C., Jones, D.M., Eakin, P.A., Fallick, A.E., Griffiths, H., Larter, S.R., 1993. Carbohydrate diagenesis in hypersaline environments: Application of GC-*ir*MS to the stable isotope analysis of derivatized saccharides from surficial and buried sediments. Organic Geochemistry 20, 927-933.

Müller, K.-D., Husmann, H., Nalik, H.P., Schomburg, G., 1990. Trans-esterification of fatty acids from microorganisms and human blood serum by trimethylsulfonium hydroxide (TMSH) for GC analysis. Chromatographia 30, 245-248.

Murata, N., Nishida, I., 1987. Lipids of blue-green algae. In: Stumpf, K. (Ed.), The Biochemistry of Plants. Academic Press, Orlando, Florida, pp. 315-347.

Nisbet, E.G., Sleep, N.H., 2001. The habitat and nature of early life. Nature 409, 1083-1091.

Nishimura, M., Baker, E.W., 1986. Possible origin of *n*-alkanes with a remarkable even-over-odd predominance in recent marine sediments. Geochimica et Cosmochimica Acta 50, 299-305.

Nübel, U., Garcia-Pichel, F., Muyzer, G., 1997. PCR primers to amplify 16S rRNA genes from cyanobacteria. Applied and Environmental Microbiology 63, 3327-3332.

Nübel, U., Garcia-Pichel, F., Kühl, M., Muyzer, G., 1999. Quantifying microbial diversity: Morphotypes, 16S rRNA genes and carotenoids of oxygenic phototrophs in microbial mats. Applied and Environmental Microbiology 65, 422-430.

Nübel, U., Garcia-Pichel, F., Clavero, E., Muyzer, G., 2000. Matching molecular diversity and ecophysiology of benthic cyanobacteria and diatoms in communitites along a salinity gradient. Environmental Microbiology 2, 217-226.

Ohad, I., Nevo, R., Brumfeld, V., Reich, Z., Tsur, T., Yair, M., Kaplan, A., 2005. Inactivation of photosynthetic electron flow during desiccation of desert biological sand crusts and *Microcoleus* sp.-enriched isolates. Photochemical and Photobiological Sciences 4, 977-982.

O'Leary, M.H., 1988. Carbon isotopes in photosynthesis. BioScience 38, 328-336.

Ormerod, J.G., 1992. Physiology of the photosynthetic prokaryotes. In: Mann, N.H., Carr, N.G. (Eds.), Photosynthetic Prokaryotes. Plenum Press, New York, pp. 93-120.

Ourisson, G., Albrecht, P., Rohmer, M., 1979. The hopanoids. Pure and Applied Chemistry 51, 709-729.

Ourisson, G., Albrecht, P., Rohmer, M., 1984. The microbial origin of fossil fuels. Scientific American 251, 34-41.

Ourisson, G., Rohmer, M., Poralla, K., 1987. Prokaryotic hopanoids and other polyterpenoid sterol surrogates. Annual Review of Microbiology 42, 301-333.

Paliñska, K.A., Krumbein, W.E., Schlemminger, U., 1998. Ultramorphological studies on *Spirulina* sp.. Botanica Marina 41, 349-355.

Park, R.K., 1976. A note on the significance of lamination in stromatolites. Sedimentology 23, 379-393.

Park, R.K., 1977. The preservation potential of some recent stromatolites. Sedimentology 24, 485-506.

Parkes, R.J., Taylor, J., 1983. The relationship between fatty acid distributions and bacterial respiratory types in contemporary marine sediments. Estuarine, Coastal and Shelf Science 16, 173-174.

Parkes, R.J., 1987. Analysis of microbial communities within sediments using biomarkers. In: Fletcher, M., Gray, T.R.G., Jones, J.G. (Eds.), Ecology of Microbial Communities, Forty-first Symposium of the Society for General Microbiology. Cambridge University Press, pp. 147-177.

Pearl, H.W., Pinckney, J.L., 1996. A mini-review of microbial consortia: Their roles in aquatic production and biogeochemical cycling. Microbial Ecology 31, 225-247.

Perry, G.J., Volkman, J.K., Johns, R.B., Bavor, H.J.J., 1979. Fatty acids of bacterial origin in contemporary marine sediments. Geochimica et Cosmochimica Acta 43, 1715-1725.

Petersen, S.O., Klug, M.J., 1994. Effects of sieving, storage, and incubation temperature on the phospholipid fatty acid profile of a soil microbial community. Applied and Environmental Microbiology 60, 2421-2430.

Philp, R.P., Brown, S., Calvin, M., Brassell, S.C., Eglinton, G., 1978. Hydrocarbon and fatty acid distribution in recently deposited algal mats at Laguna Guerrero, Baja California. In: Krumbein, W.E. (Ed.), Environmental Biogeochemistry and Geomicrobiology, 1. The Aquatic Environment. Ann Arbor Science Publishers, Ann Arbor, Michigan, pp. 255-270.

Pilkey, O.H., 2003. The carbonate islands: Tropical permafrost. In: Pilkey, O.H., Fraser, M.E. (Eds.), A Celebration on World's Barrier Islands. Columbia University Press, New York, pp. 159-181.

Potts, M., 1994. Desiccation tolerance of prokaryotes. Microbiology and Molecular Biology Reviews 58, 755-805.

Potts, M., 1999. Mechanisms of desiccation tolerance in cyanobacteria. European Journal of Phycology 34, 319-328.

Potts, M., Olie, J.J., Nickels, J.S., Parsons, J., White, D.C., 1987. Variation in phospholipid ester-linked fatty acids and carotenoids of desiccated *Nostoc commune* (cyanobacteria) from different geographic locations. Applied and Environmental Microbiology 53, 4-9.

Purser, B.H. (Ed.), 1973. The Persian Gulf: Holocene Carbonate Sedimentation and Diagenesis in a Shallow Epicontinental Sea. Springer, Berlin.

Purser, B.H., Evans, G., 1973. Regional sedimentation along the Trucial coast, SE Persian Gulf. In: Purser, B.H. (Ed.), The Persian Gulf: Holocene Carbonate Sedimentation and Diagenesis in a Shallow Epicontinental Sea. Springer, Berlin, pp. 211-232.

Quandt, L., Gottschalk, G., Ziegler, H., Stichler, W., 1977. Isotope discrimination by photosynthetic bacteria. FEMS Microbiology Letters 1, 125-128.

Revsbech, N.P., Jørgensen, B.B., 1983. Photosynthesis of benthic microflora measured with high spatial resolution by the oxygen microprofile method: Capabilities and limitations of the method. Limnology and Oceanography 28, 749-756.

Revsbech, N.P., Jørgensen, B.B., Blackburn, T.H., Cohen, Y., 1983. Microelectrode studies of the photosynthesis and O_2, H_2S and pH profiles of a microbial mat. Limnology and Oceanography 28, 1062-1074.

Rippka, R., Deruelles, J., Waterbury, J.B., Herdman, M., Stanier, R.Y., 1979. Generic assignments strain histories and properties of pure cultures of cyanobacteria. Journal of General Microbiology 111, 1-61.

Ritter, D., Yopp, J.H., 1993. Plasma membrane lipid composition of the halophilic cyanobacterium *Aphanothece halophytica*. Archives of Microbiology 159, 435-439.

Robinson, N., Eglinton, G., 1990. Lipid chemistry of Icelandic hot spring microbial mats. Organic Geochemistry 15, 291-298.

Rohmer, M., Bouvier-Navé, P., Ourisson, G., 1984. Distribution of hopanoid triterpenes in prokaryotes. Journal of General Microbiology 130, 1137-1150.

Rohmer, M., Bisseret, P., Neunlist, S., 1992. The hopanoids, prokaryotic triterpenoids and precursors of ubiquitous molecular fossils. In: Moldowan, J.M., Albrecht, P., Philp, R.P. (Eds.), Biological Markers in Sediments and Petroleum. Prentice Hall, Englewood Cliffs, New Jersey, pp. 1-17.

Rontani, J.-F., Volkman, J.K., 2005. Lipid characterization of coastal hypersaline cyanobacterial mats from the Camargue (France). Organic Geochemistry 36, 251-272.

Rontani, J.-F., Nassiry, M., Mouzdahir, A., 2007. Free radical oxidation (autooxidation) of a-tocopherol (vitamin E): A potential source of 4,8,12,16-tetramethylheptadecan-4-olide in the environment. Organic Geochemistry 38, 37-47.

Rontani, J.-F., Nassiry, M., Guasco, S., Mouzdahir, A., Bonin, P., 2008. Aerobic metabolism of vitamin E by marine bacteria: Interaction with free radical oxidation (autooxidation) processes. Organic Geochemistry 39, 676-688.

Rothrock, M.J., Garcia-Pichel, F., 2005. Microbial diversity of benthic mats along a tidal desiccation gradient. Environmental Microbiology 7, 593-601.

Rowland, S.J., Robson, J.N., 1990. The widespread occurence of highly branched alicyclic C_{20}, C_{25} and C_{30} hydrocarbons in recent sediments and biota - a review. Marine Environmental Research 30, 191-216.

Rubinstein, I., Sieskind, O., Albrecht, P., 1975. Rearranged sterenes in a shale: Occurrence and simulated formation. Journal of the Chemical Society, Perkin I, 1833-1836.

Russell, N.J., 1984. Mechanisms of thermal adaption in bacteria: Blueprints for survival. Trends in Biochemical Sciences 9, 108-112.

Sakata, S., Hayes, J.M., McTaggart, A.R., Evans, R.A., Leckrone, K.J., Togasaki, R.K., 1997. Carbon isotope fractionation associated with lipid biosynthesis by a cyanobacterium: Relevance for interpretation of biomarker records. Geochimica et Cosmochimica Acta 61, 5379-5389.

Sanford, W.E., Wood, W.W., 2001. Hydrology of the coastal sabkhas of Abu Dhabi, United Arab Emirates. Hydrogeology Journal 9, 358-366.

Scherf, A.-K., Rullkötter, J., in prep. Biogeochemistry of high-salinity microbial mats – Part 1: Lipid composition of microbial mats across intertidal flats of Abu Dhabi, United Arab Emirates. Organic Geochemistry.

Schidlowski, M., 1985. Carbon isotope discrepancy between Precambrian stromatolites and their modern analogues: Inferences from hypersaline microbial mats of the Sinai coast. Origins of Life 15, 263-277.

Schidlowski, M., 1987. Application of stable carbon isotopes to early biochemical evolution on earth. Annual Review of Earth and Planetary Sciences 15, 47-72.

Schidlowski, M., 2000. Carbon isotopes and microbial sediments. In: Riding, R.E., Awramik, S.M. (Eds.), Microbial Sediments. Springer, Berlin, pp. 84-95.

Schidlowski, M., Matzigkeit, I., Krumbein, W.E., 1984. Superheavy organic carbon from hypersaline microbial mats. Naturwissenschaften 71, 303-308.

Schidlowski, M., Gorzawski, H., Dor, I., 1994. Carbon isotope variations in a solar pond microbial mat: Role of environmental gradients as steering variables. Geochimica et Cosmochimica Acta 58, 2289-2298.

Schouten, S., Klein Breteler, W.C.M., Blokker, P., Schogt, N., Rijpstra, W.I.C., Grice, K., Baas, M., Sinninghe Damsté, J.S., 1998. Biosynthetic effects on the stable carbon isotopic compositions of algal lipids: Implications for deciphering the carbon isotopic biomarker record. Geochimica et Cosmochimica Acta 62, 1397-1406.

Schouten, S., Hartgers, W.A., Lopez, J.F., Grimalt, J.O., Sinninghe Damsté, J.S., 2001. A molecular isotopic study of ^{13}C-enriched organic matter in evaporitic deposits: Recognition of CO_2-limited ecosystems. Organic Geochemistry 32, 277-286.

Seifert, W.K., Moldowan, J.M., Smith, G.W., Whitehead, E.V., 1978. First proof of a C_{28}-pentacyclic triterpane in petroleum. Nature 271, 436-437.

Shiea, J., Brassell, S.C., Ward, D.M., 1990. Mid-chain branched mono- and dimethyl alkanes in hot spring cyanobacterial mats: A direct biogenic source for branched alkanes in ancient sediments? Organic Geochemistry 15, 223-231.

Shiea, J., Brassell, S.C., Ward, D.M., 1991. Comparative analysis of extractable lipids in hot spring microbial mats and their component photosynthetic bacteria. Organic Geochemistry 17, 309-319.

Singh, S.C., Sinha, R.P., Häder, D.-P., 2002. Role of lipids and fatty acids in stress tolerance in cyanobacteria. Acta Protozoologica 41, 297-308.

Sinninghe Damsté, J.S., Kock-van Dalen, A.C., de Leeuw, J.W., Schenck, P.A., 1987. The identification of 2,3-dimethyl-5-(2,6,10-trimethylundecyl)-thiophene, a novel sulphur containing biological marker. Tetrahedron Letters 28, 957-960.

Sirevåg, R., Buchanan, B.B., Berry, J.A., Troughton, J.H., 1977. Mechanisms of CO_2 fixation in bacterial photosynthesis studied by the carbon isotope fractionation technique. Archives of Microbiology 112, 35-38.

Stal, L.J., 1995. Tansley Review No. 84: Physiological ecology of cyanobacteria in microbial mats and other communities. New Phytologist 131, 1-32.

Stal, L.J., van Gemerden, H., Krumbein, W.E., 1985. Structure and development of a benthic marine microbial mat. FEMS Microbiology Ecology 31, 111-125.

Stoeck, T., Kröncke, I., Duineveld, G.C.A., Palojärvi, A., 2002. Phospholipid fatty acid profiles at depositional and non-depositional sites in the North Sea. Marine Ecology Progress Series 241, 57-70.

Strauss, G., Fuchs, G., 1993. Enzymes of a novel autotrophic CO_2 fixation pathway in the phototrophic bacterium *Chloroflexus auranticus*, the 3-hydroxypropionate cycle. European Journal of Biochemistry 215, 633-643.

Summons, R.E., Jahnke, L.L., Hope, J.M., Logan, G.A., 1999. 2-Methylhopanoids as biomarkers for cyanobacterial oxygenic photosynthesis. Nature 400, 554-557.

Summons, R.E., Barrow, R.A., Capon, R.J., Hope, J.M., Stranger, C., 1993. The structure of a new C_{25} isoprenoid alkene biomarker from diatomaceous microbial communities. Australian Journal of Chemistry 46, 907-915.

Tamaru, Y., Takani, Y., Yoshida, T., Sakamoto, T., 2005. Crucial role of extracellular polysaccharides in desiccation and freezing tolerance in the terrestrial cyanobacterium *Nostoc commune*. Applied and Environmental Microbiology 71, 7327-7333.

Thiel, V., Merz-Preiß, M., Reitner, J., Michaelis, W., 1997. Biomarker studies on microbial carbonates: Extractable lipids of a calcifying cyanobacterial mat (Everglades, USA). Facies 36, 163-172.

van der Meer, M.T.J., Schouten, S., Sinninghe Damsté, J.S., 1998. The effect of the reversed tricarboxylic acid cycle on the ^{13}C contents of bacterial lipids. Organic Geochemistry 28, 527-533.

van der Meer, M.T.J., Schouten, S., Ward, D.M., Greenevasen, J.A.J., Sinninghe Damsté, J.S., 1999. All-*cis* hentriaconta-9,15,22-triene in microbial mats formed by the phototrophic prokaryote *Chloroflexus*. Organic Geochemistry 30, 1585-1587.

van der Meer, M.T.J., Schouten, S., de Leeuw, J.W., Ward, D.M., 2000. Autotrophy of green non-sulphur bacteria in hot spring microbial mats: Biological explanations for isotopically heavy organic carbon in the geological record. Environmantal Microbiology 2, 428-435.

van der Meer, M.T.J., Schouten, S., van Dongen, B.E., Rijpstra, W.I.C., Fuchs, G., Sinninghe Damsté, J.S., de Leeuw, J.W., Ward, D.M., 2001. Biosynthetic controls on the ^{13}C contents of organic components in the photoautotrophic bacterium *Chloroflexus auranticus*. The Journal of Biological Chemistry 276, 10971-10976.

van der Meer, M.T.J., Schouten, S., Sinninghe Damsté, J.S., de Leeuw, J.W., Ward, D.M., 2003. Compound-specific isotopic fractionation patterns suggest different carbon metabolisms among *Chloroflexus*-like bacteria in hot-spring microbial mats. Applied and Environmental Microbiology 69, 6000-6006.

van der Meer, M.T.J., Schouten, S., Bateson, M.M., Nübel, U., Wieland, A., Kühl, M., de Leeuw, J.W., Sinninghe Damsté, J.S., Ward, D.M., 2005. Diel variations in carbon metabolism by green nonsulphur-like bacteria in alkaline siliceous hot spring microbial mats from Yellowstone National Park. Applied and Environmental Microbiology 71, 3978-3986.

van der Meer, M.T.J., Lammerts, L., Skirnisdottir, S., Sinninghe Damsté, J.S., Schouten, S., 2008. Distribution and isotopic composition of bacterial lipid biomarkers in microbial mats from a sulfidic Icelandic hot spring. Organic Geochemistry 39, 1015-1019.

van Gemerden, H., 1993. Microbial mats: A joint venture. Marine Geology 113, 3-25.

van Rijn, J., Cohen, Y., 1983. Ecophysiology of the cyanobacteria. Journal of General Microbiology 129, 1849-1856.

Volkman, J.K., 1986. A review of sterol markers for marine and terrigenous organic matter. Organic Geochemistry 9, 83-99.

Volkman, J.K., Johns, R.B., 1977. The geochemical significance of positional isomers of unsaturated acids from an intertidal zone sediment. Nature 267, 693-694.

Volkman, J.K., Johns, R.B., Gillan, F.T., Perry, G.J., Bavor, H.J., 1980. Microbial lipids of an intertidal sediment - I. Fatty acids and hydrocarbons. Geochimica et Cosmochimica Acta 44, 1133-1143.

Volkman, J.K., Gillan, F.T., Johns, R.B., 1981. Sources of neutral lipids in a temperate intertidal sediment. Geochimica et Cosmochimica Acta 45, 1817-1828.

Volkman, J.K., Jeffrey, S.W., Nichols, P.D., Rogers, G.I., Garland, C.D., 1989. Fatty acid and lipid composition of 10 species of microalgae used in mariculture. Journal of Experimental Marine Biology and Ecology 128, 219-240.

Volkman, J.K., Dunstan, G.A., Jeffrey, S.W., Kearney, P.S., 1991. Fatty acids from microalgae of the genus *Pavlova*. Phytochemistry 30, 1855-1859.

Volkman, J.K., Barrett, S.M., Dunstan, G.A., 1994. C_{25} and C_{30} highly branched isoprenoid alkenes in laboratory cultures of two marine diatoms. Organic Geochemistry 21, 407-413.

Walsh, K., Jones, G.J., Dunstan, R.H., 1998. Effect of high irradiance and iron on volatile odour compounds in the cyanobacterium *Microcystis aeruginosa*. Phytochemistry 49, 1227-1239.

Walter, M.R., Grotzinger, J.P., Schopf, J.W., 1992. Proterozoic stromatolites. In: Schopf, J.W., Klein, C. (Eds.), The Proterozoic Biosphere. Cambridge University Press, New York, pp. 247-251.

Walter, M.R., Bauld, J., des Marais, D.J., Schopf, J.W., 1992. A general comparison on microbial mats and microbial stromatolites: Bridging the gap between the modern and the fossil. In: Schopf, J.W., Klein, C. (Eds.), The Proterozoic Biosphere. Cambridge University Press, New York, pp. 335-342.

Wang, A.-Y., Cronan Jr., J.E., 1994. The growth phase-dependent synthesis of cyclopropane fatty acids in *Escherichia coli* is the result of an RpoS(KatF)-dependent promoter plus enzyme instability. Molecular Microbiology 11, 1009-1017.

Ward, D.M., Brock, T.D., 1980. Hydrocarbon biodegradation in hypersaline environments. Applied and Environmental Microbiology 35, 353-359.

Ward, D.M., Santegoeds, C.M., Nold, S.C., Ramsing, N.B., Ferris, M.J., Bateson, M.M., 1997. Biodiversity within hot spring microbial mat communities: Molecular monitoring of enrichment cultures. Antonie van Leeuwenhoek 71, 143-150.

Ward, D.M., Ferris, M.J., Nold, S.C., Bateson, M.M., 1998. A natural view of microbial biodiversity within hot spring cyanobacterial mat communities. Microbiology and Molecular Biology Reviews 62, 1353-1370.

White, D.C., Davis, W.M., Nickels, J.S., King, J.D., Bobbie, R.J., 1979. Determination of the sedimentary microbial biomass by extractable lipid phosphate. Oecologia 40, 51-62.

Whittle, G.L., Alsharhan, A.S., Kendall, C.G.S.C., 1998. Petrography of Holocene beachrock and hardgrounds, Abu Dhabi, United Arab Emirates. In: Alsharhan, A.S., Glennie, K.W. Whittle, G.L., Kendall, C.G.S.C. (Eds.), Quaternary Deserts and Climatic Change. Balkema, Rotterdam, pp. 57-68.

Wieland, A., Kühl, M., 2000. Irradiance and temperature regulation of oxygenic photosynthesis and O_2 consumption in a hypersaline cyanobacterial mat (Solar Lake, Egypt). Marine Biology 137, 71-85.

Wieland, A., Kühl, M., McGowan, L., Fourçans, A., Duran, R., Caumette, P., García de Oteyza, T., Grimalt, J.O., Solé, A., Diestra, E., Esteve, I., Herbert, R.A., 2003. Microbial mats on the Orkney Islands revisited: Microenvironment and microbial community composition. Microbial Ecology 46, 371-390.

www.brot-fuer-die-welt.de/images/laender/weltkarte_vorderasien_aktuelle-projekte.gif, Stand September 2008.

Zelles, L., 1999. Fatty acid patterns of phospholipids and lipopolysaccharides in the characterisation of microbial communities in soil: A review. Biology and Fertility of Soils 29, 111-129.

Zeng, Y.B., Ward, D.M., Brassell, S.C., Eglinton, G., 1992a. Biogeochemistry of hot spring environments: 2. Lipid compositions of Yellowstone (Wyoming, U.S.A.) cyanobacterial and *Chloroflexus* mats. Chemical Geology 95, 327-345.

Zeng, Y.B., Ward, D.M., Brassell, S.C., Eglinton, G., 1992b. Biogeochemistry of hot spring environments, 3. Apolar and polar lipids in the biologically active layers of a cyanobacterial mat. Chemical Geology 95, 347-360.

Zhang, C.L., 2002. Stable carbon isotopes of lipid biomarkers: Analysis of metabolites and metabolic fates of environmental microorganisms. Current Opinion in Biotechnology 13, 25-30.

Zhang, C.L., Fouke, B.W., Bonheyo, G.T., Peacock, A.D., White, D.C., Huang, Y., Romanek, C.S., 2004. Lipid biomarkers and carbon-isotopes of modern travertine deposits (Yellowstone National Park, USA): Implications for biogeochemical dynamics in hot-spring systems. Geochimica et Cosmochimica Acta 58, 3157-3169.

Zhang, Y.-M., Rock, C.O., 2008. Membrane lipid homeostasis in bacteria. Nature Reviews 6, 222-233.

Zink, K.-G., Mangelsdorf, K., 2004. Efficient and rapid method for extraction of intact phospholipids from sediments combined with molecular structure elucidation using LC-ESI-MS-MS analysis. Analytical and Bioanalytical Chemistry 380, 798-812.

8 Anhang

8.1 Zusätzliche Daten

Tabelle 8.1: Konzentrationen der *n*-Alkane, Methylalkane, *n*-Alkene und Isoprenoide in µg/g organischer Gesamtextrakt in den Mikrobenmatten und der Oberflächenschicht der Roten Matte

	Rote	**OF Rote**	**Olive**	**Pinke**	**Pinnacle**	**Gelatinöse**
n-15:0	0	5644	0	310	600	33
n-16:0	137	1371	31	281	308	798
Me-16:0	0	0	0	203	24	849
Σ *n*-17:1	3731	18458	1089	4784	8782	1666
n-17:0	7784	22706	3196	6170	9994	2446
8-Me-17:0	0	708	0	196	1938	96
7-Me-17:0	0	143	0	255	1739	65
6-Me-17:0	0	62	0	0	291	0
Σ *n*-18:1	1046	2970	516	1302	525	4834
verzw. 19:0	20	0	0	175	0	56
n-18:0	124	163	163	546	132	1529
Phytan	509	531	193	370	95	49
Σ Phytene	615	5863	943	3308	842	1755
Phytadiene	1038	25	1569	51	31	35
10-Me-18:0	121	252	174	113	62	145
Σ verzw. 20:2	568	2096	303	272	924	125
Verzw. 20:0	0	0	534	150	0	0
n-19:1	147	674	143	176	2290	65
n-19:0	235	190	208	189	141	150
n-20:1	0	65	0	231	51	0
n-20:0	50	41	81	98	69	50
n-21:3	0	84	0	0	0	0
n-21:2	280	4500	145	451	261	302
n-21:2	14	131	0	44	0	13
n-21:1	72	295	24	0	0	7
n-21:0	47	85	94	60	87	37
n-22:0	40	32	74	86	52	19
n-23:3	0	94	0	53	0	0
n-23:2	0	87	0	0	0	0
n-23:1	0	110	0	20	0	0
n-23:1	13	11	0	10	17	0
n-23:0	63	40	135	79	67	19
n-24:0	63	33	102	56	44	20
n-25:3	0	38	0	0	0	0
n-25:2	0	30	0	0	0	0

	Rote	**OF Rote**	**Olive**	**Pinke**	**Pinnacle**	**Gelatinöse**
n-25:1	58	51	0	0	0	0
n-25:0	86	62	179	109	85	30
Me-27:1	0	0	0	0	0	4
n-26:0	62	39	128	74	45	22
n-27:2	103	100	0	0	0	0
n-27:1	62	23	0	0	0	8
n-27:1	92	87	0	0	0	67
ΣC_{30} HBIs	545	234	0	41	183	544
n-27:0	163	138	371	257	180	84
n-28:0	94	62	210	118	92	38
Squalene	623	2332	650	1308	1476	444
n-29:0	220	193	610	264	273	101
n-30:0	73	40	218	79	40	16
n-31:0	236	114	550	256	219	68
n-32:0	0	0	292	152	0	13
n-33:0	0	0	352	120	0	20

Tabelle 8.2: Konzentrationen der *n*-Alkane, Methylalkane, *n*-Alkene und Isoprenoide in µg/g organischer Gesamtextrakt in den Schichten der Gelatinösen Matte

	Schicht 1	**Schicht 2**	**Schicht 3**	**Schicht 4**	**Schicht 5**	**Schicht 6**
n-15:0	650	52	-	-	-	-
n-16:0	2308	2166	280	143	-	62
Me-16:0	353	2435	819	261	-	21
Σ *n*-17:1	2832	6740	1688	501	24	144
n-17:0	3260	2737	1741	1250	230	576
8-Me-17:0	32	-	-	17	-	-
7-Me-17:0	21	337	184	20	-	-
6-Me-17:0	-	461	241	54	-	-
Σ *n*-18:1	1536	1984	1606	1841	1770	263
verzw. 19:0	68	827	504	249		
n-18:0	1104	3607	2291	1437	77	123
Phytan	19	-	36	36	-	-
Σ Phytene	2079	5563	3657	2909	53	301
Phytadiene	94	-	19	-	-	547
10-Me-18:0	131	418	249	213	87	-
Σ verzw. 20:2	326	174	182	200	-	263
verzw. 20:0	-	497	409	211	-	65
n-19:1	784	474	323	189	-	50
n-19:0	74	298	168	138	62	82
n-20:1	87	-	21	18	-	-
n-20:0	42	170	95	91	77	31
n-21:2	6695	1553	641	301	-	104
n-21:2	331	99	38	17	72	15
n-21:1	330	44	19	9	-	19
n-21:0	48	75	14	42	19	45
n-22:0	24	12	14	36	16	29
n-23:3	59	6	-	-	-	-
n-23:2	67	7	-	-	-	-
n-23:1	36	6	-	-	-	-
n-23:1	6	4	-	-	-	-
n-23:0	18	9	12	26	18	27
n-24:0	15	11	22	36	39	24
n-25:3	6	-	-	-	-	-
n-25:1	3	-	-	-	-	-
n-25:0	18	12	17	33	31	46
Me-27:1	-	5	28	34	-	-
n-26:0	10	8	15	23	22	34
n-27:1	3	2	-	-	-	-
n-27:1	-	1	4	4	-	-

	Schicht 1	Schicht 2	Schicht 3	Schicht 4	Schicht 5	Schicht 6
Σ C_{30} HBIs	64	331	641	902	124	724
n-27:0	18	17	25	33	43	85
n-28:0	14	14	23	43	28	46
Squalene	117	-	395	1153	212	292
n-29:0	27	21	48	64	60	267
n-30:0	8	9	25	21	8	19
n-31:0	14	15	28	29	36	202
n-32:0	-	24	9	5	5	-
n-33:0	-	9	13	12	7	-

Tabelle 8.3: Relative Anteile aller Phospholipidfettsäuremethylester in % in den Mikrobenmatten und der Oberflächenschicht der Roten Matte

	Rote	**OF Rote**	**Olive**	**Pinke**	**Pinnacle**	**Gelatinöse**
n-9:0	1,3	4,9	3,1	7,5	2,2	9,3
n-10:0	0,5	2,1	1,2	2,7	0,8	4,9
n-11:0	0,03	0,1	0,1	0,2	0,04	0,4
n-12:0	0,2	0,3	0,4	0,5	0,2	1,5
n-13:0	0,1	-	0,1	0,1	0,03	0,4
Me-12:0 a	-	-	-	0,4	-	0,4
Me-12:0 b	0,2	0,1	0,3	0,2	0,1	-
Me-12:0 c	-	-	-	0,1	0,1	-
n-14:1	-	-	-	-	-	-
n-14:0	1,1	1,4	2,2	2,1	1	10,6
Me-13:1	0,1	-	-	0,4	0,2	-
Me-13:0 a	0,1	-	-	0,4	0,3	-
Me-13:0 b	-	-	-	-	0,2	0,1
Me-13:0 c	0,2	-	0,1	1	0,3	0,4
Me-13:0 d	-	-	-	-	-	-
i-15:0	3,1	2,6	5,3	6,1	2	4,5
ai-15:0	2	0,8	2,9	1,8	1,1	2,4
n-15:0	0,6	0,7	0,9	0,9	0,5	3,9
Me-15:0 a	0,1	-	0,03	0,1	-	-
Me-15:0 b	0,1	-	-	-	-	-
i-16:0	1,1	0,5	1,7	1,7	1,1	1
n-16:1 a	0,4	0,7	0,5	0,8	1,6	-
n-16:1 b	-	-	0,5	0,8	1,3	-
n-16:1w9	3,8	3,7	6,7	4,9	5,3	1,4
n-16:1 c	0,6	3,1	-	-	1,1	1
n-16:1 d	0,9	1,5	0,6	-	1	0,3
n-16:0	18,9	24,5	23,8	24,2	25,2	21,4
Me-16:0 a	5,1	0,7	3,9	1,3	1,2	0,3
Me-16:0 b	-	-	-	0,1	0,1	-
Me-16:0 c	0,3	-	0,3	0,2	0,3	-
i-17:0	0,9	0,4	1,1	1,8	1	0,7
ai-17:0	0,9	0,4	1,3	0,8	0,9	0,6
cy-17:0	4	-	1,6	0,3	0,4	-
n-17:0	1,2	0,5	0,7	0,7	0,6	0,5
Me-17:0 a	0,8	5,2	1,3	2	1	0,1
Me-17:0 b	0,3	0,1	-	0,1	0,3	1
n-18:2	1,9	0,8	1,2	1,2	3,5	0,2
cis -18:1ω9	7,9	10,4	6,7	9,6	9,1	4,9
trans -18:1ω9	9,8	11,6	10,4	6,4	8,7	2,8

	Rote	**OF Rote**	**Olive**	**Pinke**	**Pinnacle**	**Gelatinöse**
n-18:1 a	2,5	3,6	1,8	4,9	3,4	0,2
n-18:1 b	0,6	0,2	0,3	-	0,4	0,1
n-18:0	6,5	8	7,7	7,8	12	11,9
Me-18:1	2,1	0,4	1	0,6	0,6	0,6
i-19:0	0,9	0,1	0,3	0,2	0,4	0,04
ai-19:0	0,2	-	0,1	0,2	0,1	0,2
cy-19:0 a	0,3	0,1	0,2	0,1	0,3	0,8
cy-19:0 b	16,6	10,1	9,1	2,5	6,4	7,8
n-19:0	0,3	-	0,1	0,1	0,1	0,1
n-20:2 a	0,1	-	0,1	0,1	0,3	0,1
n-20:2 b	0,1	-	-	-	0,1	-
n-20:1 a	0,3	0,1	0,1	0,5	0,7	0,04
n-20:1 b	0,4	0,5	0,2	0,4	0,8	0,2
n-20:0	0,2	0,1	0,2	0,4	0,2	0,7
n-21:0	0,04	-	-	-	0,1	2
n-22:2 a	0,3	-	0,1	0,4	0,7	-
n-22:2 b	0,03	-	-	0,1	0,2	-
n-22:1	0,1	-	0,15	0,1	0,1	-
n-22:0	0,1	-	0,06	0,1	0,1	0,2
n-23:0	-	-	-	-	-	0,1
n-24:0	0,03	-	0,05	0,1	0,1	-
n-25:0	-	-	-	-	0,01	-
n-27:0	-	-	-	-	0,1	-
n-28:0	-	-	-	-	0,04	-

Tabelle 8.4: Relative Anteile aller Phospholipidfettsäuremethylester in % in den Schichten der Gelatinösen Matte

	Schicht 1	**Schicht 2**	**Schicht 3**	**Schicht 4**	**Schicht 5**	**Schicht 6**
n-9:0	1,3	1,9	0,9	1,9	1,2	4,4
n-10:0	0,6	0,7	0,4	0,8	0,7	1,9
n-11:0	-	-	0,04	-	-	0,2
n-12:0	0,3	0,5	0,3	0,4	1,6	0,5
n-13:0	0,1	0,5	0,4	0,2	0,1	0,1
Me-12:0 a	0,2	3,9	2,9	0,8	-	-
Me-12:0 b	0,1	0,2	0,4	0,4	-	0,3
Me-12:0 c	-	0,1	-	0,0	-	0,04
n-14:1 a	0,2	0,2	0,2	0,0	-	-
n-14:1 b	-	0,1	0,03	0,0	-	-
n-14:0	2,4	3,9	2,7	2,5	2,8	1,9
Me-13:1	0,1	-	-	-	-	-
Me-13:0 a	-	-	0,03	-	-	-
Me-13:0 b	-	-	0,1	-	-	-
Me-13:0 c	-	-	0,1	-	-	-
Me-13:0 d	0,2	2,9	2,2	0,9	-	-
Me-13:0 e	-	-	0,4	-	-	-
i-15:0	3,9	4,8	10,7	11,3	2,3	5,4
ai-15:0	1,3	1,6	3	3,5	1,5	3,9
n-15:0	2	1,4	0,9	0,9	1,1	0,8
Me-15:0 a	-	0,2	0,2	-	-	-
Me-15:0 b	-	0,04	0,3	-	-	-
i-16:0	1,6	0,9	2,6	2,7	0,7	2,3
n-16:1	0,5	0,2	0,5	0,2	-	-
n-16:1	-	0,3	0,2	0,3	0,9	0,5
n-16:1ω9	7,3	1,4	1,2	1,2	1,3	0,7
n-16:1	0,4	0,3	0,2	-	-	0,1
n-16:1	1,3	0,3	0,4	0,2	-	-
n-16:0	20,1	22,4	14,7	16,3	25,9	14,1
Me-16:0 a	0,5	0,3	0,8	0,9	0,7	0,5
Me-16:0 b	-	0,1	0,1	0,1	0,1	0,3
Me-16:0 c	-	0,1	0,2	0,2	0,1	-
Me-16:0 d	-	-	0,2	0,1	-	-
i-17:0	1,4	0,8	2	1,6	0,4	0,9
ai-17:0	1,2	0,7	1,1	1,2	0,7	1,2
cy-17:0	0,3	0,2	0,5	0,4	-	-
n-17:0	0,9	0,9	1	0,8	0,6	1,2
Me-17:0	1,1	-	-	-	-	-
Me-17:0	-	-	-	-	-	-

	Schicht 1	Schicht 2	Schicht 3	Schicht 4	Schicht 5	Schicht 6
n-18:2	1,7	0,7	0,6	0,6	4,8	0,7
cis -18:1ω9	18,9	14	5,5	3,9	5,1	1,5
trans -18:1ω9	10,6	5,7	4,6	5,4	1,8	3,1
n-18:1 a	3,6	-	3,6	4,1	0,6	2,7
n-18:1 b	0,3	-	0,7	0,5	-	1
n-18:0	6,1	8,7	8,4	11,3	36,9	17,9
Me-18:1	0,9	1,3	2,2	1,5	0,4	1,9
i-19:0	0,1	0,1	0,3	0,2	0,2	0,1
ai-19:0	0,2	0,6	0,8	0,6	0,3	0,2
n-19:1	-	2	1,2	1,2	0,8	0,3
cy-19:0 a	2,4	13,8	6	20,1	3,8	28,8
cy-19:0 b	4,1	0,2	12,2	-	-	-
n-19:0	0,1	0,4	0,5	0,2	0,2	0,2
n-20:2 a	0,3	0,1	0,1	-	-	-
n-20:2 b	0,1	-	0,1	-	-	-
n-20:1 a	0,5	0,3	0,3	-	-	-
n-20:1 b	0,4	0,6	0,8	0,4	-	0,3
n-20:0	0,1	0,1	0,2	0,2	0,9	0,3
n-21:0	-	-	-	-	-	-
n-22:2 a	0,1	-	-	-	-	-
n-22:2 b	0,2	-	-	-	-	-
n-22:1	0,1	-	-	-	0,6	-
n-22:0	0,02	0,1	0,1	0,1	0,4	0,1
n-23:0	-	-	-	-	0,1	-
n-24:0	0,01	0,02	0,02	0,04	0,2	0,1
n-27:0	-	-	-	-	0,1	-

Tabelle 8.5: Doppelbestimmungen der Kohlenstoffisotopenverhältnisse des organischen Gesamtextraktes der Proben aus dem Inkubationsexperiment

Zeit der Probennahme [h nach Start]	Unmarkiertes Bicarbonat		+ 1% ^{13}C-Bicarbonat		+ 10% ^{13}C-Bicarbonat		+ 30% ^{13}C-Bicarbonat	
Schicht 1								
0	-11,23	-11,23	-12,33	-12,36	-11,53	-11,65	-11,84	-11,90
0,5	-11,35	-11,43	-13,36	-13,44	-11,03	-11,08	-10,14	-10,08
1	-12,97	-12,97	-12,95	-13,07	-9,61	-9,61	-3,63	-3,60
3	-10,55	-10,54	-13,64	-13,64	-7,52	-7,64	-1,67	-1,58
5,5	-13,68	-13,59	-12,84	-12,75	-10,27	-10,35	-2,53	-2,70
10,5	-9,83	-9,99	-12,55	-12,57	-6,16	-6,14	0,15	0,03
21,5	-12,88	-12,65	-10,4	-10,29	-5,21	-5,22	3,90	3,96
25,5	-13,26	-13,3	-10,53	-10,77	-3,72	-3,67	26,13	26,11
Schicht 2								
0	-13,76	-14	-12,48	-12,37	-13,35	-13,36	-13,89	-13,95
0,5	-13,37	-13,39	-12,51	-12,4	-14,04	-14,04	-13,38	-13,48
1	-14,06	-14,05	-13,09	-13,31	-14,44	-14,51	-13,74	-13,68
3	-13,5	-13,7	-11,89	-11,7	-13,71	-13,65	-12,42	-12,40
5,5	-12,67	-12,81	-13,72	-13,59	-13,92	-13,98	-13,44	-13,59
10,5	-13,12	-13,13	-13,95	-13,82	-14,33	-14,13	-12,91	-12,84
21,5	-13,54	-13,49	-14,19	-14,25	-13,65	-13,80	-11,82	-11,74
25,5	-13,66	-13,41	-13,25	-13,38	-12,89	-12,99	-11,23	-11,03
Schicht 3								
0	-11,57	-11,6	-12,14	-12,03	-12,37	-12,38	-12,13	-12,16
0,5	-11,42	-11,4	-12,95	-12,94	-11,87	-12,05	-13,14	-13,12
1	-12,15	-12,12	-12,13	-12,09	-13,35	-13,34	-12,35	-12,32
3	-11,34	-11,54	-12,22	-12,28	-12,32	-12,30	-11,80	-11,86
5,5	-11,65	-11,52	-11,85	-11,97	-12,22	-12,33	-12,75	-12,93
10,5	-12,93	-12,76	-11,91	-11,8	-12,11	-12,11	-11,95	-11,99
21,5	-11,67	-11,72	-11,96	-12,17	-12,73	-12,71	-12,00	-11,86
25,5	-11,78	-11,92	-11,81	-11,58	-11,81	-11,78	-11,47	-11,45

Tabelle 8.6: Doppelbestimmungen der Kohlenstoffisotopenverhältnisse ausgewählter Kohlenwasserstoffe in Schicht 1 aus dem Inkubationsexperiment

Zeit der Probennahme [h nach Start]	Unmarkiertes Bicarbonat		+10% 13C-Bicarbonat		+30% 13C-Bicarbonat	
n-Heptadecen						
0	-15,33	-16,51	-	-23,91	-14,91	-15,98
0,5	-13,42	-13,44	-19,09	-21,14	-15,43	-16,41
1	-15,5	-15,47	-19,43	-19,62	-	-
3	-14,16	-13,69	-24,12	-22,71	-13,82	-13,84
5,5	-15,04	-	-19,46	-17,34	-15,63	-15,65
10,5	-23,93	-22,56	-18,25	-18,09	-16,75	-17,55
21,5	-16,64	-15,04	-	-	-16,01	-16,52
25,5	-17,63	-16,71	-24,96	-21,99	-15,21	-14,4
n-Heptadecan						
0	-13,99	-14,2	-14,87	-16,26	-14,54	-13,64
0,5	-14,02	-13,50	-13,97	-15,8	-14,06	-13,91
1	-16,26	-15,33	-20,32	-18,7	-	-
3	-12,11	-13,31	-12,51	-15	7,67	8,59
5,5	-14,45	-	-10,76	-8,76	13,97	13,27
10,5	-20,37	-18,46	-13,03	-12,75	8,89	10,63
21,5	-14,94	-14,93	-	-	12,9	12,23
25,5	-15,34	-16,84	-8,25	-9,27	42,07	42,21
n-Heneicosadien (a)						
0	-14,50	-15,23	-16	-17,56	-14,59	-14,41
0,5	-16,92	-17,08	-16,72	-17,36	-12,58	-13,67
1	-15,65	-16,67	-17,36	-16,54	-	-
3	-13,61	-13,47	-13,28	-13,88	1,59	2,15
5,5	-18,48	-	-14,92	-14,09	4,48	5,7
10,5	-14,83	-14,65	-10,12	-9,47	1,85	1,26
21,5	-15,93	-16,03	-10,71	-9,66	5,9	5,97
25,5	-16,51	-15,01	-20,31	-21,72	29,63	30,05
n-Heneicosadien (b)						
0	-9,14	-8,75	-6,8	-8,66	-7,2	-7,20
0,5	-8,26	-7,88	-9,64	-9,18	-5,46	-6,20
1	-7,82	-7,57	-7,02	-7,70	-	-
3	-3,52	-4,24	-5,43	-6,04	-5,17	-4,82
5,5	-17,08	-	-8,76	-7,44	-1,05	-0,99
10,5	-10,55	-10,33	-6,17	-4,38	2,65	0,73
21,5	-7,31	-7,73	-7,08	-5,95	2,44	3,13
25,5	-9,02	-7,51	-18,40	-18,36	14,51	12,5

Tabelle 8.7: Doppelbestimmungen der Kohlenstoffisotopenverhältnisse ausgewählter Kohlenwasserstoffe in Schicht 2 aus dem Inkubationsexperiment

Zeit der Probennahme [h nach Start]	Unmarkiertes Bicarbonat		+10% 13C-Bicarbonat	
n-Heptadecan				
0	-23,19	-14,81	-15,75	-18,12
0,5	-16,94	-16,79	-15,67	-16,53
1	-14,29	-13,99	-16,75	-16,19
3	-13,61	-15,17	-23,46	-27,40
5,5	-22,50	-22,25	-30,56	-27,20
10,5	-	-	-29,52	-25,16
21,5	-	-	-23,65	-19,49
25,5	-15,49	-14,79	-27,61	-28,38
n-Heneicosadien (a)				
0	-17,40	-17,03	-17,61	-8,87
0,5	-16,35	-16,99	-19,25	-20,53
1	-16,22	-16,68	-23,73	-22,90
3	-14,62	-15,69	-23,10	-25,04
5,5	-14,14	-18,78	-28,44	-27,27
10,5	-	-	-30,78	-25,64
21,5	-18,03	-18,35	-21,43	-21,08
25,5	-19,94	-18,10	-27,26	-23,52
n-Heneicosadien (b)				
0	-9,26	-8,80	-7,80	-16,15
0,5	-5,55	-5,64	-7,52	-6,77
1	-7,78	-8,36	-8,65	-7,36
3	-5,11	-4,43	-13,98	-17,05
5,5	-	-	-22,73	-21,60
10,5	-	-	-25,23	-21,93
21,5	-	-	-11,25	-9,58
25,5	-11,04	-10,47	-12,35	-12,25

Tabelle 8.8: Doppelbestimmungen der Kohlenstoffisotopenverhältnisse ausgewählter PLFAs in Schicht 1 aus dem Inkubationsexperiment

Zeit der Probennahme [h nach Start]	Unmarkiertes Bicarbonat		+10% 13C-Bicarbonat	
n-Hexadecansäure				
0	-16,35	-17,83	-14,93	-15,17
0,5	-15,87	-15,97	-14,51	-13,93
1	-16,24	-16,10	-14,96	-14,64
3	-13,16	-14,02	-9,32	-10,01
5,5	-17,92	-17,88	-13,28	-13,84
10,5	-15,42	-15,90	-8,94	-10,07
21,5	-15,65	-15,36	-12,08	-11,49
25,5	-15,94	-15,84	-19,03	-19,67
n-Octadecensäure (a)				
0	-14,90	-14,98	-12,84	-
0,5	-16,93	-17,41	-	-12,81
1	-17,75	-17,45	-17,69	-17,56
3	-14,18	-	-15,33	-13,54
5,5	-18,23	-18,37	-13,63	-14,98
10,5	-15,34	-	-	-6,32
21,5	-15,43	-15,63	-16,20	-15,61
25,5	-13,23	-13,31	-11,21	-10,51
n-Octadecensäure (b)				
0	-15,40	-16,40	-14,39	-
0,5	-16,84	-16,32	-	-14,83
1	-16,91	-16,98	-13,27	-13,03
3	-14,09	-14,16	-9,97	-9,23
5,5	-17,52	-18,20	-13,60	-14,66
10,5	-14,48	-14,89	-9,91	-10,70
21,5	-17,12	-17,57	-13,54	-12,71
25,5	-16,75	-17,06	-8,14	-9,34
n-Octadecansäure				
0	-18,80	-20,56	-14,37	-
0,5	-18,02	-17,19	-15,40	-15,45
1	-17,16	-20,28	-16,75	-15,57
3	-14,56	-14,38	-1,40	-0,93
5,5	-16,04	-17,07	-10,57	-10,24
10,5	-13,50	-13,81	-9,38	-9,58
21,5	-15,25	-16,09	-17,83	-17,39
25,5	-13,90	-14,45	-25,61	-26,41

Tabelle 8.9: Doppelbestimmungen der Kohlenstoffisotopenverhältnisse ausgewählter PLFAs in Schicht 2 aus dem Inkubationsexperiment

Zeit der Probennahme [h nach Start]	Unmarkiertes Bicarbonat		+10% 13C-Bicarbonat	
n-Hecadecansäure				
0	-14,01	-14,85	-17,61	-17,76
0,5	-15,73	-15,74	-17,69	-17,76
1	-16,95	-17,16	-16,77	-17,72
3	-16,89	-16,11	-18,29	-19,48
5,5	-16,30	-17,21	-22,91	-
10,5	-16,85	-16,41	-21,38	-22,53
21,5	-16,84	-16,94	-20,8	-20,89
25,5	-17,06	-16,72	-18,04	-17,89
n-Octadecensäure (a)				
0	-14,13	-14,75	-22,03	-21,55
0,5	-17,49	-15,58	-14,41	-13,84
1	-18,91	-19,13	-14,3	-14,16
3	-12,76	-	-	-15,58
5,5	-12,99	-	-20,89	-
10,5	-16,58	-18,47	-	-24,94
21,5	-16,52	-18,45	-22,34	-22,3
25,5	-14,70	-15,73	-17,52	-17,12
n-Octadecensäure (b)				
0	-14,29	-14,37	-20,6	-22,07
0,5	-16,73	-16,93	-17,56	-17,3
1	-15,97	-16,07	-19,66	-20,17
3	-17,23	-17,2	-17,83	-17,62
5,5	-15,84	-15,56	-17,89	-
10,5	-17,39	-17,28	-21,75	-22,7
21,5	-18,83	-19,45	-18,88	-18,46
25,5	-12,91	-13,51	-15,54	-15,02
n-Octadecansäure				
0	-17,44	-	-17,19	-18,33
0,5	-19,22	-18,71	-20,62	-20,2
1	-21,87	-22,28	-17,81	-17,35
3	-17,39	-	-	-20,03
5,5	-17,77	-	-25,12	-
10,5	-	-18,57	-26,21	-27,8
21,5	-19,00	-18,04	-20,71	-20,16
25,5	-18,40	-18,71	-22,8	-23,35

Tabelle 8.9: Fortsetzung

cy-Nonadecansäure				
0	-18,53	-19,68	-16,57	-16,8
0,5	-17,26	-17,34	-18,31	-18,75
1	-18,71	-19,07	-15,37	-15,17
3	-19,38	-19,32	-19,1	-19,74
5,5	-21,87	-21,74	-21,81	-
10,5	-22,2	-22	-22,09	-22,66
21,5	-18,52	-18,89	-19,89	-20,18
25,5	-16,04	-17,58	-18,00	-17,66

8.2 Photographische Dokumentation

Abb. 8.1: Oberfläche und Seitenansicht der Roten Matte.

Abb. 8.2: Nahaufnahme der „Pinnacles“.

Abb. 8.3: Großflächig ausgebreitet die Pinnacle Matte (schwarz) und von Wasser überflutet die Gelatinöse Matte.

Abb. 8.4: Ohne die Reflektion des Lichtes gut erkennbar: Die rote Oberfläche der Gelatinösen Matte.

Abb. 8.5: Seitenansicht der Gelatinösen Matte.

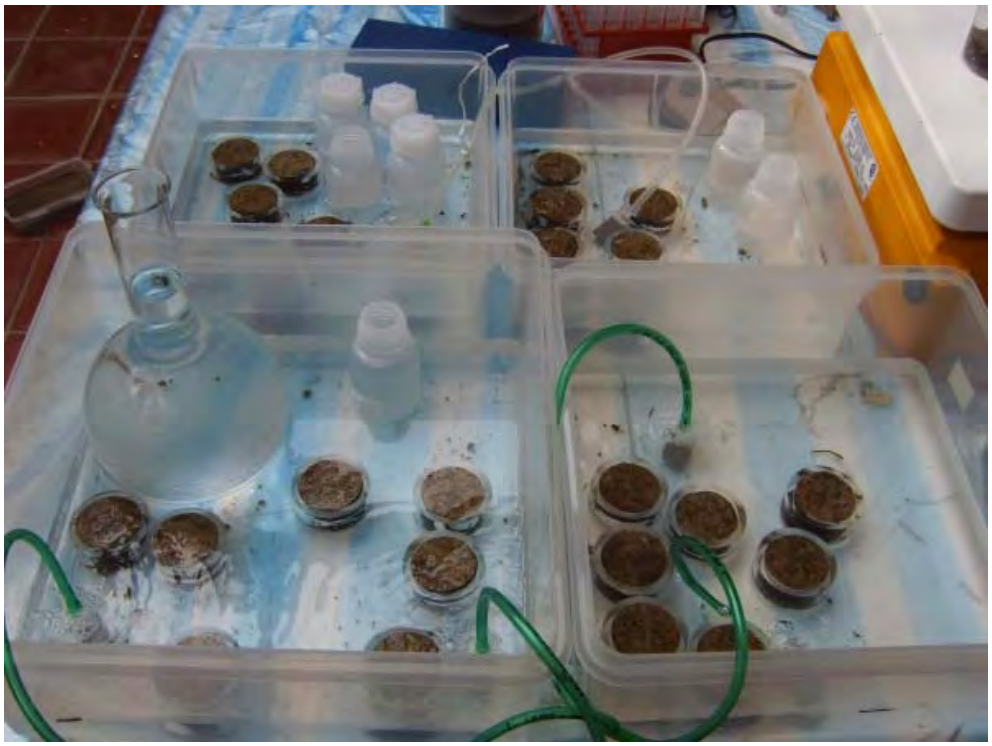

Abb. 8.6: Aufbau des Inkubationsexperimentes.

Lebenslauf

Name:	Ann-Kathrin Scherf
geboren:	23.04.1981 in Perleberg

Berufserfahrung

Seit 10/2008	Wissenschaftliche Mitarbeiterin am Helmholtz-Zentrum Potsdam Deutsches GeoForschungsZentrum - GFZ
12/2004 - 01/2008	Wissenschaftliche Mitarbeiterin am Institut für Chemie und Biologie des Meeres (ICBM) an der Carl-von-Ossietzky Universität Oldenburg
03/2002 - 09/2003	Studentische Hilfskraft am ICBM, Universität Oldenburg (AGs Mikrobiogeochemie und Organische Geochemie)
10/2001 - 02/2002	Studentische Hilfskraft im Institut für Mathematik, Universität Oldenburg
10/2000 - 07/2001	Studentische Hilfskraft am ICBM, Universität Oldenburg

Studium

12/2004-09/2008	Promotionsstudium Chemie an der Carl-von-Ossietzky Universität Oldenburg
11/2004	Diplom in Marine Umweltwissenschaften Thema der Diplomarbeit „Geochemische Charakterisierung und Biodegradationsklassifizierung von Ölproben aus dem West-Shetland-Becken“
10/2003 - 01/2004	Praktikum am GeoForschungsZentrum Potsdam (AG Organische Geochemie)
10/1999 - 11/2004	Studium Marine Umweltwissenschaften an der Universität Oldenburg Hauptfach: Meeres- und Geochemie

Schulabschluss

07/1999	Abitur am mathematisch-naturwissenschaftlichen Spezialschulteil des Albert-Schweitzer-Gymnasiums Erfurt

Eidesstattliche Erklärung

Hiermit versichere ich, dass ich die vorliegende Dissertation selbstständig angefertigt und keine anderen als die angegebenen Quellen verwendet habe. Zusätzlich erkläre ich, dass diese Dissertation weder in ihrer Gesamtheit noch in Teilen einer anderen wissenschaftlichen Hochschule zur Begutachtung in einem Promotionsverfahren vorliegt oder vorgelegen hat.

Oldenburg, den 30. September 2008

Ann-Kathrin Scherf